(54) Title: SYSTEMS AND METHODS OF DETECTING LI DENDRITES
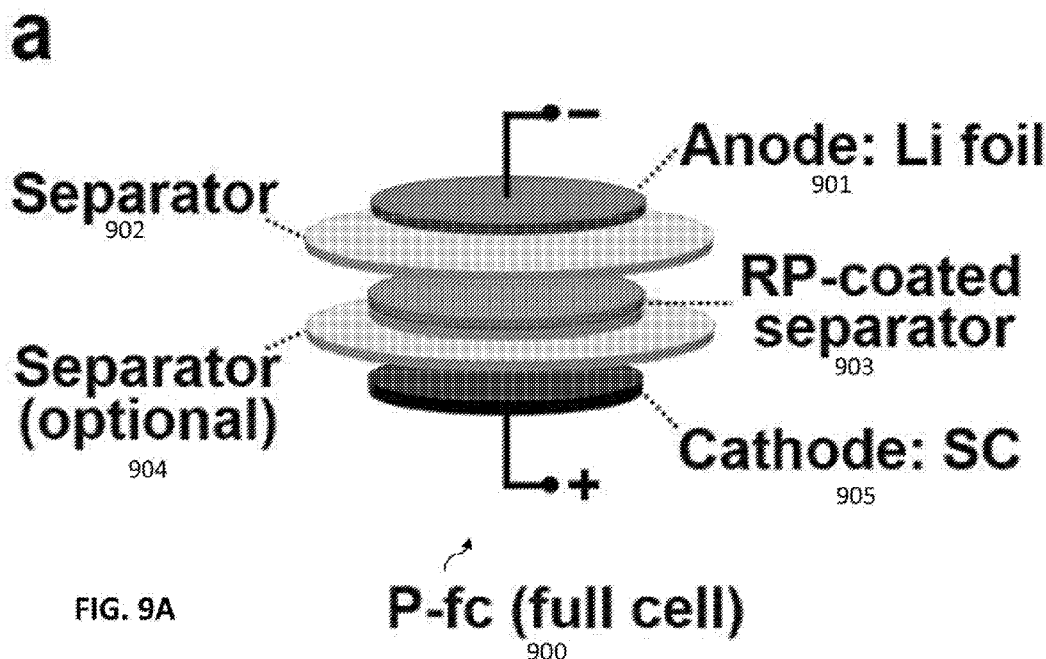
FIG. 9A

(57) Abstract: Systems and methods that utilize a separator coated by particles for Li dendrite detection in an ordinary two-electrode battery system. The particles can be red phosphorus (RP) particles and/or other particles that are poor electronic conductors, are able to react with Li, and will form an insoluble product with Li, such as silicon, germanium, arsenic, metal oxides, metal halides, metal chalcogenides, chalcogenides, and $LiM_xE_yO_z$ (M=metal, E=nonmetal, 0=oxygen, x≥0, y≥0, z≥0). These other particles can be used by themselves or in combination with one another. No additional electrode is needed, and the presence of Li dendrites can be detected simply based on the voltage profile during the charging step.

SC, SD, SE, SG, SK, SL, SM, ST, SV, SY, TH, TJ, TM, TN, TR, TT, TZ, UA, UG, US, UZ, VC, VN, ZA, ZM, ZW.

(84) Designated States *(unless otherwise indicated, for every kind of regional protection available)*: ARIPO (BW, GH, GM, KE, LR, LS, MW, MZ, NA, RW, SD, SL, ST, SZ, TZ, UG, ZM, ZW), Eurasian (AM, AZ, BY, KG, KZ, RU, TJ, TM), European (AL, AT, BE, BG, CH, CY, CZ, DE, DK, EE, ES, FI, FR, GB, GR, HR, HU, IE, IS, IT, LT, LU, LV, MC, MK, MT, NL, NO, PL, PT, RO, RS, SE, SI, SK, SM, TR), OAPI (BF, BJ, CF, CG, CI, CM, GA, GN, GQ, GW, KM, ML, MR, NE, SN, TD, TG).

Declarations under Rule 4.17:
— *as to the applicant's entitlement to claim the priority of the earlier application (Rule 4.17(iii))*

Published:
— *with international search report (Art. 21(3))*
— *before the expiration of the time limit for amending the claims and to be republished in the event of receipt of amendments (Rule 48.2(h))*

SYSTEMS AND METHODS OF DETECTING LI DENDRITES

CROSS-REFERENCE TO RELATED PATENT APPLICATIONS

[0001] This application claims priority to U.S. Patent Appl. Serial No. 62/683,158, entitled "Systems and Methods Of Detecting Li Dendrites," filed June 11, 2018, and to U.S. Patent Appl. Serial No. 62/720,033, entitled "Systems and Methods Of Detecting Li Dendrites," filed August 20, 2018, which patent applications ire commonly owned by the owner of the present invention. These patent applications are incorporated herein in their entirety.

TECHNICAL FIELD

[0002] The present invention relates to systems and methods for detecting Li dendrites, and more particularly, systems and methods for detecting Li dendrites in a two-electrode system.

GOVERNMENT INTEREST

[0003] This invention was made with government support under Grant Nos. FA9550-14-1-0111 awarded by the Air Force Office of Scientific Research. The United States government has certain rights in the invention.

BACKGROUND

[0004] Lithium-ion batteries are today's energy storage device technology of choice for electronic devices and electric vehicles. Since its commercialization in 1991, the lithium-ion battery (LIB) enabled wireless electronic devices, revolutionizing global communications. Almost three decades later, the LIB is expected to facilitate the integration of renewable energy into the electrical grid, as well as to allow affordable electric transportation. [*Goodenough 2013; Noorden 2014; Dunn 2011; Zhang 2017*]. However, these applications demand energy storage capabilities that the LIBs will be unable to meet, even if the theoretical energy density is reached. Therefore, new battery chemistries with higher energy densities have attracted the attention of the scientific community. There are new efforts to develop new battery chemistries with higher energy densities, such as lithium-air ($Li-O_2$) and lithium-sulfur (Li-S), while also

resolving the current limitations with pure lithium, commonly called lithium metal anodes. Li-air ($Li-O_2$) and Li-sulfur (Li-S) systems have shown great promise as the energy densities are almost one order of magnitude higher than that of the LIB. [*Noorden 2014*; *Bruce 2011*; *Girishkumar 2010*; *Manthiram 2015*; *Armand 2008*].

[0005] The use of high-energy density Li metal anodes in rechargeable batteries is prohibited because of dendrite formation that could potentially result in a battery fire. Although so-called dendrite-free Li metal anodes are reported in many recent publications, Li dendrite growth is still kinetically favorable and it remains a severe safety concern upon mass production. We report here a detection system capable of alerting for Li dendrite formation in a two-electrode battery with no additional electrodes required. When dendrites contact a red phosphorous-coated separator, dendrite growth is revealed by a significant voltage change. This could activate a signal through the battery management system, warning of the presence of Li dendrites and leading to shutdown of the battery before the dendrites become dangerous.

[0006] Li metal batteries are considered the next-generation technology because of their high energy density and power density. [*Cano 2018*; *Liu 2018*]. But commercially, Li metal has only been employed in non-rechargeable primary batteries due to the safety issues associated with dendrite growth upon charging [*Liu 2018*; *Shen 2018*] that can penetrate separators and lead to runaways, fires and explosions.[*Xu 2014*; *Orsini 1999*]. There have been very few studies on Li dendrite detection, and the only known method is to use a Cu film in the separator connected to a third electrode to detect short circuits. [*Wu 2014*; *Lin 2016*]. The added manufacturing complexity of three-electrode batteries retards such a consideration for large-scale use.

[0007] But, commercially, Li metal has only been employed in primary batteries that cannot be recharged due to the safety issue associated with "dendrite" growth. When Li metal is regenerated in the charging step, it tends to form whisker and needle-like dendritic structures, often called "dendrites." These dendrites can penetrate separators and eventually short the

batteries, which could lead to fires or explosions. This is a main challenge for Li metal batteries.

[0008] Accordingly, tremendous efforts have been made to develop dendrite-free Li metal anodes by using host materials or constructing artificial solid-electrolyte interface (SEI) layers to suppress dendrite growth. But those materials were only studied on the bench scale, and the number of batteries that have been tested was very limited. When it comes to the mass production of batteries on the industrial level, the number of batteries could reach a billion or even more, and it is nearly impossible to ensure that every single one of them is dendrite-free. However, if an insurance system can be developed in combination with dendrite-free Li metal anodes where the chance of growing dendrite is exceedingly low already, then the practical application of Li metal batteries may become reality. That insurance system would act as a sensor and be able to detect Li dendrite formation when the battery is being used, such that it can send a signal to the battery management system, warning of the presence of Li dendrites, which leads to shutdown of the battery before the dendrites have progressed to the cathode causing an internal short circuit with a possible battery fire resulting.

[0009] Dendrite-free Li metal anodes were developed by adding host materials, constructing supplemental solid-electrolyte interphase (SEI) layers, and modifying the electrolytes or separators to suppress dendrite growth.[*Liu 2018*; *Cheng 2017*; *Wang 2017*; *Raji 2017*; *Lin II 2016*; *Liu 2017*] These studies were conducted on the bench scale with a limited number of batteries tested. Since mass production of batteries on the industrial level could reach billions, it is nearly impossible to ensure that all would operate dendrite-free. However, if a detection system could be deployed in combination with so-called dendrite-free Li metal anodes where the chance of growing dendrites is already low, the large-scale production of safe, rechargeable Li metal batteries can become a reality.

[0010] Accordingly, there is a need for an improved method for detecting Li dendrites.

SUMMARY OF THE INVENTION

[0011] The present invention is directed to systems and methods that utilize a separator coated by particles for Li dendrite detection in an ordinary two-electrode battery system. The particles can be red phosphorus (RP) particles and/or other particles that are poor electronic conductors, are able to react with Li, and will form an insoluble product with Li, such as silicon, germanium, arsenic, metal oxides, metal halides, metal chalcogenides, chalcogenides, and $LiM_xE_yO_z$ (M=metal, E=nonmetal, O=oxygen, $x\geq0$, $y\geq0$, $z\geq0$). These other particles can be used by themselves or in combination with one another. No additional electrode is needed, and the presence of Li dendrites can be detected simply based on the voltage profile during the charging step. For embodiments that utilize RP as the main ingredient, RP is inexpensive and the preparation of the RP-coated separators is facile and scalable. The present invention makes it much more convenient to produce and safely operate Li metal batteries.

[0012] In general, in one embodiment, the invention features a structure in a metal-anode-based battery that includes an anode that includes a metal, a cathode, and an electrodeless separator positioned between the anode and the cathode. A detectable electrical response signal will result during a charging or discharging of the battery when the metal from the metal anode contacts the electrodeless separator.

[0013] Implementations of the invention can include one or more of the following features:

[0014] The metal that contacts the electrodeless separator can extend from the anode.

[0015] The metal can be selected from a group consisting of lithium, sodium, potassium, magnesium, calcium, aluminum, zinc, cesium, mixtures thereof, and composites therefrom.

[0016] The electrodeless separator can have a resistance of at most 10^{-5} S/cm.

[0017] The electrodeless separator can include red phosphorous.

[0018] The electrodeless separator can include a material selected from a group consisting of red phosphorous, silicon, germanium, arsenic, metal oxides, metal halides, metal

chalcogenides, chalcogenides, LiMxEyOz with M=metal, E=nonmetal, O=oxygen, x≥0, y≥0, and z≥0, MXenes, 2D materials, polymers, organic polymers, inorganic polymers, and mixtures thereof or composites therefrom.

[0019] The material can be a poor electronic conductor, is able to react with Li, and will form an insoluble product with Li when reacted with Li.

[0020] The electrodeless separator can be independent of all other films.

[0021] The electrodeless separator can be deposited upon or within another film or matrix host material.

[0022] In general, in another embodiment, the invention features an electronic system that includes a battery management system having the above-described structure. The electronic system is operable to signal a turnoff or cessation of battery use in response to the detectable electrical response signal resulting from the metal from the metal anode contacting the electrodeless separator in the above-described structure.

[0023] Implementations of the invention can include one or more of the following features:

[0024] The detectable electrical response signal generated can be a change in voltage with respect to time during the charging of the battery.

[0025] The change in voltage can be least 0.25 V.

[0026] In the structure, the voltage will decrease by at most 0.1 V if the battery rests for at least 1 hour after the voltage increases at least 1 V.

[0027] The change in voltage can be least 1 V.

[0028] In general, in another embodiment, the invention features an energy-storage device that includes an anode including a metal. The energy-storage device further includes a cathode. The energy-storage device further includes an electrolyte containing cations of the metal. The electrolyte is disposed between the anode and the cathode. The energy-storage device further includes an electrodeless reagent partition in the electrolyte between the anode and the cathode.

The electrodeless reagent partition includes a reagent that can react chemically with the metal.

[0029] Implementations of the invention can include one or more of the following features:

[0030] The reagent can react with a morphological feature of the metal extending from the anode.

[0031] The metal can include lithium.

[0032] The reagent can include phosphorous.

[0033] The reagent can include red phosphorous.

[0034] The reagent can include particles.

[0035] The reagent can include at least one material selected from a group consisting of silicon, germanium, arsenic, metal oxides, metal fluorides, and LiMxEyOz with M=metal, E=nonmetal, O=oxygen, and x$\geq$0, y$\geq$0, and z$\geq$0.

[0036] The energy-storage device can further include a separator extending through the electrolyte between the reagent partition and the anode.

[0037] The reagent partition can be disposed on the separator.

[0038] The energy-storage device can further include a separator extending through the electrolyte between the reagent partition and the cathode.

[0039] The reagent can be an electrical insulator.

[0040] The reagent can have a resistance of less than 10^{-5} S/cm.

[0041] The electrolyte can be a liquid.

[0042] The cathode can include a conductive reagent that reacts chemically with the cations of the metal.

[0043] The electrodeless reagent partition can be of a thickness less than one millimeter.

[0044] The electrodeless reagent partition can include multiple separator layers.

[0045] The electrodeless reagent partition can be essentially red phosphorus.

[0046] The electrodeless reagent partition can include a separator layer coated with the reagent.

[0047] The reagent can be prepared by a process that includes coating the separator with a slurry.

[0048] The reagent can be applied to the separator layer by a process that includes coating the separator by vacuum filtration.

[0049] In general, in another embodiment, the invention features a test method for dendrite detection in an energy-storage device having a first electrode and a second electrode. The test method includes measuring charge timing of the energy-storage device. The test method further includes storing a charging model of the measured charge timing of the energy-storage device, the charging model providing an expected charge timing. The test method further includes charging the energy-storage device while monitoring a charging time and a charging voltage between the first electrode and the second electrode. The test method further includes issuing a dendrite-detection signal if the charging voltage reaches a threshold voltage before the expected charge timing.

[0050] Implementations of the invention can include one or more of the following features:

[0051] The expected charge timing can include an expected full-charge timing.

[0052] The dendrite-detection signal can be a tentative signal. The method can further include adjusting a charging current responsive to the dendrite-detection signal to limit the charging voltage.

[0053] The adjusting of the charging current can limit the charging voltage.

[0054] The test method can further include issuing an affirmative dendrite-detection signal if the charging current falls while the device is charged at the charging voltage.

[0055] The test method can further include issuing the affirmative dendrite-detection signal if the charging current falls for at least ten seconds while the device is charged at the charging voltage.

[0056] The energy-storage device can include a lithium-metal battery.

[0057] The charging the energy-storage device can include maintaining the charging current at at least 2.5 mA/cm^2.

[0058] The dendrite-detection signal can be a tentative signal. The method can further include continuing to charge the energy-storage device after the issuing of the tentative signal for a dendrite-verification period.

[0059] The test method can further include disabling the energy-storage device if the energy-storage device is charged at at least the threshold voltage after the dendrite-verification period.

[0060] The dendrite-verification period can be at least ten seconds.

[0061] The expected charge timing and the measured charge timing can be equal.

[0062] In general, in another embodiment, the invention features

[0063] Implementations of the invention can include one or more of the following features:

[0064] In general, in another embodiment, the invention features a battery-management system that executes one or more of the above-described methods to test a battery. The battery includes an anode that includes a metal. The battery further includes a cathode. The battery further includes an electrolyte containing cations of the metal. The electrolyte is disposed between the anode and the cathode. The battery further includes an electrodeless reagent partition in the electrolyte between the anode and the cathode. The electrodeless reagent partition includes a reagent that can react chemically with the metal.

[0065] In general, in another embodiment, the invention features a test method for dendrite detection in an energy-storage device having a first electrode and a second electrode. The test method includes storing a charging model of the energy-storage device with the charging model providing an expected charge voltage. The test method further includes charging the energy-storage device while monitoring a charging voltage between the first electrode and the second electrode. The test method further includes issuing a dendrite-detection signal if the charging voltage exceeds the expected charge voltage.

[0066] Implementations of the invention can include one or more of the following features:

[0067] The test method can further include issuing the dendrite-detection signal if the charging voltage exceeds the expected charge voltage by at least 0.25 V.

[0068] The test method can further include issuing the dendrite-detection signal if the charging voltage exceeds the expected charge voltage by at least 1.0 V.

[0069] The test method can further include allowing the charging voltage to exceed the expected charge voltage by a voltage margin. The test method can further include storing a measure of the charging voltage. The test method can further include allowing the device to rest for a rest period. The test method can further include measuring a test voltage between the first electrode and the second electrode after the rest period. The test method can further include affirming the dendrite-detection signal if the test voltage falls below a detection level during the rest period.

[0070] The voltage margin can be at least one volt.

[0071] The rest period can be at least one hour.

[0072] The detection level can be at least 0.1 V below the measured charging voltage.

DESCRIPTION OF DRAWINGS

[0073] **FIGS. 1A-1J** show half-cell tests with red P (RP) coating on a separator (P-hc). **FIG. 1A** is a configuration of the half-cell with RP coating (P-hc). **FIG. 1B** is a testing protocol showing the current density versus time. (The discharge steps were time-control (20/10/5/2/1 min at ~0.083 mAh/cm^2 and 12 min at ~1 mAh/cm^2); the charge steps were voltage-control (2 V) and are thus shown as dashed lines because the areal capacities (<0.083 mAh/cm^2) varied. The discharge steps were time-control (20/10/5/2/1 min at ~0.083 mAh/cm2 and 12 min at ~1 mAh/cm2); the charge steps were voltage-control (2 V) and are thus shown as dashed lines because the areal capacities (<0.083 mAh/cm2) varied.) **FIG. 1C** is the voltage profile at low areal capacity (~0.083 mAh/cm^2). **FIG. 1D** is the voltage profile at 5 mA/cm^2 and high areal

capacity (~1 mAh/cm^2). The voltage decrease indicated by the arrow in **FIG. 1D** is the electrochemical response generated when Li dendrite contacts the RP coating. **FIGS. 1E-1G** are photographs of the RP-coated separator at different stages showing (in **FIG. 1E**) no silver-colored Li metal and (in **FIGS. 1F-1G**) Li metal on the RP. **FIG. 1H** is the XRD spectrum of the silver-colored spots in **FIG. 1G**. **FIGS. 1I-1J** are SEM images of the silver-colored spots in **FIG. 1G** showing the dendritic morphology of Li. Scale bars for **FIGS. 1I-1J** are 100 μm and 2 μm, respectively.

[0074] **FIG. 2** is an SEM image of a cross-section of a RP-coated separator. The scale bar is 10 μm.

[0075] **FIGS 3A-3D** shows dendrite growth visualized while monitoring the cell voltage. **FIG. 3A** shows a configuration of the transparent half-cell with a RP-coated separator. **FIG. 3B** is a graph that shows voltage and current profiles of transparent half-cells with and without the RP-coated separator when discharging the Li metal wrapped by the separator. **FIG. 3C** are a series of photographs (top view) of the discharged Li metal surface taken over time. **FIG. 3D** is an enlarged photographic image of the area indicated in the photograph taken at 15 minutes. The scale bars for **FIGS. 3C-3D** are 1 mm and 0.2 mm, respectively.

[0076] **FIGS. 4A-4F** show half-cell tests without the RP coating on the middle separator (ctrl-1 and ctrl-2). **FIG. 4A** is the configuration of ctrl-1. **FIG. 4B** is the voltage profile of ctrl-1 at low areal capacity (~0.083 mAh/cm^2). **FIG. 4C** is the voltage profile of ctrl-1 at 5 mA/cm^2 and high areal capacity (~1 mAh/cm^2). **FIG. 4D** is the configuration of ctrl-2. **FIG. 4E** is the voltage profile of ctrl-2 at low areal capacity (~0.083 mAh/cm^2). **FIG. 4F** is the voltage profile of ctrl-2 at 5 mA/cm^2 and high areal capacity (~1 mAh/cm^2).

[0077] **FIGS. 5A-5B** are photographs (top view) showing dendrite growth at different stages in a transparent half-cell without a RP-coated separator. The scale bars for **FIGS. 5A-5B** are 1 mm and 0.2 mm, respectively.

[0078] **FIG. 6A** is an SEM image of the RP-coated separator shown in **FIG. 3A** (after the last discharge step at ~0.083 mAh/cm2).

[0079] **FIGS. 6B-6D** are energy-dispersive X-ray spectroscopy (EDS) mapping of P, O and F for the SEM of **FIG. 6A**. The scale bars for **FIGS. 6A-6D** is 200 μm.

[0080] **FIG. 7A-7B** are SEM images of the silver-colored spots on the RP-coated separator shown in **FIG. 1F** (after the first discharge step at ~1 mAh/cm^2).

[0081] **FIGS. 7C-7D** are the EDS mapping of P and O for **FIG. 7B**.

[0082] **FIGS. 7E-7F** are SEM images of Li metal deposited on the Cu foil at the same stage as in **FIG. 1F**. The scale bars for **FIGS. 7A, 7B-7E**, and **7F** are 500 μm, 50 μm, and 5 μm, respectively.

[0083] **FIGS. 8A-8E** are SEM images of the silver-colored spots shown in **FIG. 1G**. FIGS. **8B-8C** show the dendritic morphology of Li in **FIG. 8A**. **FIGS. 8D-8E** show the RP particles around the Li dendrites in **FIG. 8A**.

[0084] **FIG. 8F** shows the same aggregate of dendrites in the center of **FIG. 8A**.

[0085] **FIGS. 8G-8I** are the EDS mapping of P, O and F for **FIG. 8F**. The scale bars for (i) **FIG. 8A**, (ii) **FIGS. 8B** and **8D**, (iii) **FIGS. 8C** and **8E**, and (iv) **FIGS. 8F-8I** are (i) 100 μm, (ii) 20 μm, (iii) 2 μm, and (iv) 50 μm, respectively.

[0086] **FIGS. 9A-9D** show full-cell tests with and without a separator having an RP layer. **FIG. 9A** shows a configuration of the full-cell with a RP coating (P-fc). **FIG. 9B** is a graph showing a voltage profile of P-fc shown in **FIG. 9A** at 5 mA/cm^2 and ~0.8 mAh/cm^2. **FIG. 9C** shows the configuration of ctrl-3, which includes all separators without any RP coating. **FIG. 9D** is a graph showing the voltage profile of ctrl-3 shown in **FIG. 9C** at 5 mA/cm^2 and ~1 mAh/cm^2.

[0087] **FIGS. 10A** and **10B-10C** are, respectively, a photograph and SEM images of the middle separator on the bottom side (facing the Cu foil) from ctrl-1 shown in **FIG. 4A** after the

first discharge step at ~1 mAh/cm^2. The scale bars for **FIGS. 10A-10C** are 5 mm, 20 μm, and 2 μm, respectively.

[0088] **FIGS. 11A-11C** are photographs for the RP-coated separators in full-cells at different stages, namely 0.083 mAh/cm^2 (last cycle), 1 mAh/cm^2 (first cycle), and 1 mAh/cm^2 (tenth cycle). The scale bars for **FIGS. 11A-11C** are each 5 mm.

[0089] **FIG. 11D-11F** are SEM images of the RP-coated separators shown in **FIGS. 11A-11C**, respectively. The scale bars for **FIGS. 11D-11E** and **FIG. 11F** are 200 μm and 50 μm, respectively.

[0090] **FIG. 11G-11I** are the EDS mapping for P of **FIG. 11D-11F**, respectively. The scale bars for **FIGS. 11G-11H** and **FIG. 11I** are 200 μm and 50 μm, respectively.

[0091] **FIG. 11J-11L** are the EDS mapping for O of **FIG. 11D-11F**, respectively. The scale bars for **FIGS. 11J-11K** and **FIG. 11L** are 200 μm and 50 μm, respectively.

[0092] **FIG. 11M-11N** are SEM images of the RP-coated separators shown in **FIGS. 11B-11C**, respectively. The scale bars for **FIG. 11M** and **FIG. 11N** are 20 μm and 2 μm, respectively.

[0093] **FIGS. 12A** and **12B-12C** are, respectively, a photograph and SEM images of the middle separator on the bottom side (facing the Cu foil) from ctrl-3 shown in **FIG. 9C** after the tenth discharge step at ~1 mAh/cm^2. The scale bars for **FIGS. 12A-12C** are 5 mm, 20 μm, and 2 μm, respectively.

[0094] **FIG. 13A** shows the configuration of ctrl-4, which includes a separator without an RP coating.

[0095] **FIGS. 13B-13D** are graphs showing normalized charge and discharge profiles of ctrl-4 (shown in **FIG. 13**), ctrl-3 (shown in **FIG. 9C**) and P-fc (shown in **FIG. 9A**) at 0.4C, 0.7C and 1.3 C, respectively.

[0096] **FIGS. 14A-14E** show a mechanistic study of voltage change upon dendrite contact.

FIG. 14A is a graph showing a voltage profile of P-hc (shown in **FIG. 1A**) tested at 5 mA/cm^2.

FIG. 14B is a graph showing a voltage profile of ctrl-1 (shown in **FIG. 4A**) tested at 5 mA/cm^2.

FIG. 14C is a graph showing a comparison of the charge transfer resistance of P-hc and ctrl-

1. **FIG. 14D** is a graph showing P-hc tested at different current densities (unit: mA/cm^2). **FIG.**

14E shows the mechanism of dendrite detection: schematic illustration of Li dendrite growth

at 5 mA/cm^2 under low and high capacities in P-hc.

[0097] **FIGS. 15A-15D** shows a study on electrolyte resistance in half-cells (P-hc). **FIG. 15A**

is a graph showing the testing. **FIG. 15B** is a graph showing the electrolyte resistance of the P-

hc. **FIGS. 15C-15D** are graphs showing particular voltage profiles.

[0098] **FIGS. 16A-16B** are graphs showing the voltage of P-hc discharged at various voltages.

DETAILED DESCRIPTION

[0099] Described are systems and methods that utilize a separator coated by particles for Li

dendrite detection in an ordinary two-electrode battery system. A reagent that reacts with Li

metal is layered on the separator of a Li cell to form a reagent partition between the Li anode

and the cathode. The reagent is of a material that is inert to Li cations in the electrolyte but

reacts chemically with metallic Li. Suitable reagent materials in some embodiments are poor

electronic conductors, are able to react with Li, and will form an insoluble product with Li,

such as red phosphorus (RP) particles and/or other particles, such as silicon, germanium,

arsenic, metal oxides, metal halides, metal chalcogenides, chalcogenides, and LiMxEyOz

(M=metal, E=nonmetal, O=oxygen, x≥0, y≥0, z≥0). Physical isolation prevents the reagent

from reacting with Li metal during normal operation. Such reaction does occur, however, if Li

dendrites extend to the reagent partition. Dendrites combine with the reagent partition to create

dendritic structures that change a cell's voltage response to charging current. Cells equipped

with reagent partitions can thus be stimulated to produce a dendrite-detection signal without

the need for a third electrode. Electrodeless reagent partitions thus facilitate dendrite detection

in two-terminal cells.

[0100] The particle-coated separator can be an RP-coated separator, which will be used herein for exemplary purposes. Other materials as discussed above can be utilized in addition and/or in lieu of RP.

[0101] The separator, such as the RP-coated separator, is used to detect the growth of morphological features, such as dendrites, in accordance with one embodiment. The coating can be 90 wt% RP and 10 wt% polyvinyl difluoride (PVDF) as the binder that ensures the uniformity of the coating. The mass loading of RP can be around 2 mg/cm^2 or greater. The RP-coated separator can be physically separated from the anode and the cathode, as side reactions could occur between RP and the anode/cathode materials. If not separated, RP could be directly lithiated. When Li dendrites grow long enough to reach the RP coating, there will be a noticeable electrochemical response in the voltage profile with respect to time. The voltage decreases in half-cells or increases in full-cells when Li dendrites reach the RP separator. Changes in cell voltage can thus alert the user (or battery management system) of Li dendrite formation.

RP-Coated Separators In Half-Cells

[0102] The configuration of a half-cell (P-hc) **100** is shown in **FIG. 1A**. Li foils were used as the anode **105** and Cu foils were used as the current collector for the cathode **101** where Li metal was electrochemically deposited in the discharge process. An RP-coated separator **103** is located between the cathode **101** and anode. Additional separators **102** and **104** can also be positioned between the RP-coated separator and the cathode **101** and anode **105**, respectively. Separator **104** is optional since the separator that RP was coated on was enough to isolate the RP layer from the anode. However, separator **104** can be added to ensure that the RP on the edge did not contact anode **105**.

[0103] The RP-coated separator can be prepared by adding RP (MilliporeSigma) or a mixture

of RP and graphene nanoplatelets (GNP) (xGnP® C-300 from XG Sciences) to a mortar and adding polyvinyl difluoride (PVDF) (Alfa Aesar) as a binder. Generally, the coating can be around 90 wt% RP (or RP-GNP) and around 10 wt% of the binder to ensure uniformity of the coating. For instance, the RP (or RP/GNP mixture) can be around 32 mg and the binder is around 3.5 mg. The slurry can then be prepared by adding NMP (MilliporeSigma) (such as 0.5-0.8 mL of NMP), and the mixture was ground (such as for 5 min) to form a slurry that was then coated on the separators using a spatula. Such separators can be, for example, Celgard 2500 polypropylene separators (20 μm thick, around 2 cm^2 each) or Targray SW312D separators (which are 12 μm-thick polyethylene membranes). The separators can then be dried, such as by drying under vacuum (~1 Torr) at 60 °C overnight. A similar slurry process can be utilized to make separators coated with GNP. By the above amounts, the mass loading of RP, GNP or RP/GNP was about 2 mg/cm^2.

[0104] Such coated separators can also be made using alternative methods, such as a vacuum filtration method that coats the RP, RP/GNP, or GNP on the non-electrode side of the separators.

Dendrite Detection Using RP-Coated Separators In Half-Cells

[0105] Half-cell tests were performed to demonstrate the operation of the RP-coated separator. The RP-coated separator was prepared utizing the slurry method described above. The RP-coated separator was around 20 μm thick with around 2 mg/cm^2 of RP (*see* **FIG. 2**), while the RP layer of the RP-coated separator **103** was physically isolated from the anode **105** and the cathode **101**, with the separator **104** again being optional). (For the testing, the two separators used in half-cells (and for the full-cells) were each 12 μm thick, thereby reducing the thickness of the entire separator/RP/separator stack to ~45 μm). LiPF$_6$ was selected as the electrolyte in testing since it is known to produce dendrites faster than other common electrolytes. [*Ding 2013*]. In **FIG. 2**, layer **201** is around 20 μm thick RP layer on a separator **202** that is around

20 μm.

[0106] A special testing protocol was developed (shown in **FIG. 1B**) to induce dendrite growth and demonstrate the dendrite-detection response. The half-cell was first cycled at 0.25 mA/cm^2 under a low capacity (~0.083 mAh/cm^2) until the coulombic efficiency (CE) stabilized to minimize the effects of irreversible side reactions. [*Wang 2017*; *Raji* 2017]. The discharge rate was increased progressively to 0.50/1.0/2.5/5.0 mA/cm^2. The above steps accelerate the aging of the cathode that benefits dendrite growth. The charge rate remained at 0.25 mA/cm^2 to ensure complete removal of Li from the cathode and negligible dendrite growth on the anode, which simplified the analysis. In the initial 70 cycles at low capacity (0.083 mAh/cm^2), the stable charge and discharge plateaus in **FIG. 1C** verified that the half-cell was functioning normally. Higher discharge rates led to lower CE and hence more SEI or dendrite formation (**FIG. 1C**), but the low capacity ensured that the dendrites did not extend to the RP-coated separator and stable discharge plateaus were always present.

[0107] The dendrite-detection alert signal was observed when the discharge capacity was raised to 1 mAh/cm^2 while maintaining the high rate (5 mA/cm^2). The high capacity was intended to increase the thickness of the dendrite layer so that the dendrites would extend to the RP coating. A striking decrease of voltage ($|\Delta V|$ >2 V) was observed (**FIG. 1D**) in the first discharge step. The RP-coated separator remained red and clean with no visible impurities at ~0.083 mAh/cm^2, and only RP particles were observed (**FIG. 1E** and **FIG. 4SA-4SD**). Two control samples were tested using the same protocol, and the voltage change was not present in either sample. **FIG. 4A** shows the half-cell **400** ctrl-1 that is similar to P-hc **100**, except that its separators **403** are without any RP layer. **FIG. 4D** shows the half-cell **410** ctrl-2 that is similar to half-cell **400** ctrl-1, except that it only has one separator **413** (which is without any RP layer) between cathode **101** and anode **105**. **FIG. 4B** is the voltage profile of ctrl-1 at low areal capacity (~0.083 mAh/cm^2). **FIG. 4C** is the voltage profile of ctrl-1 at 5 mA/cm^2 and

high areal capacity (~1 mAh/cm^2). **FIG. 4E** is the voltage profile of ctrl-2 at low areal capacity (~0.083 mAh/cm^2). **FIG. 4F** is the voltage profile of ctrl-2 at 5 mA/cm^2 and high areal capacity (~1 mAh/cm^2).

[0108] Referring back to **FIGS. 1F-1G**, at ~1 mAh/cm^2, silver-colored spots with metallic appearance were apparent on the RP (**FIG. 1F**), which grew larger after another 9 cycles (**FIG. 1G**). The presence of Li metal in **FIG. 1G** was confirmed by the X-ray diffraction (XRD) spectrum (**FIG. 1H**), scanning electron microscopy (SEM) and energy-dispersive X-ray spectroscopy (EDS) mapping (**FIGS. 1I-1J** and **FIGS. 8A-8I**). [*Li 2018*].

[0109] Although Li is not active in EDS, we found large amounts of oxygen (**FIGS. 7D and 8H**) distributed in the area suspected to be Li metal, likely resulting from Li$_2$O that formed when the sample was exposed to air during the transfer from an Ar-filled box to the SEM chamber. The surrounding particles were confirmed to be RP (**FIGS. 6B, 7C,** and **8G**). The control cell ctrl-1 was also opened after discharging at 5 mA/cm^2 to ~1 mAh/cm^2 for 10 cycles, and Li dendrite formation was revealed by the visual appearance and the SEM images (**FIGS. 10A-10C**), meaning that dendrite growth reached the same level without the RP coating, but no significant voltage change was detected. This indicates that the RP coating was indeed responsible for the dramatic voltage change in **FIG. 1D**. It is also found that the initial cycling at low capacity had facilitated dendrite growth presumably by increasing the thickness of the dendrite layer.

[0110] The dendrite growth was visualized using a homemade transparent cell **300** shown in **FIG. 3A**. Transparent cell **300** includes glass substrates **301a** and **301b** (such as 75 x 25 x 1 mm^3, Corning), with each glass slide having, respectively, copper **302a** and **302b** (such as 25 μm copper ribbons, Alfa Aesar) and lithium metal **303a** and **303b** (such as 300 μm Li metal foil). A separator **304** having a RP layer **305** is positioned between the glass substrates **301a** and **301b**. Epoxy (extra fast setting, Hardman) was used to adhere the Li metal surface to the

glass substrates and prevent leakage. The copper ribbons were used to electrically connect the Li metal electrodes to a battery testing station. The cell was filled with electrolyte (around 200 μL).

[0111] The cell voltage and the morphology of the discharged Li metal were monitored simultaneously. [*Li 2018*; *Wood 2016*]. As shown in **FIG. 3B**, a voltage drop to around 6 V was observed when Li dendrites contacted the RP-coated separator at 5 mA/cm^2 and, as shown in **FIGS. 3C-3D**, started growing along the RP. Times **311-316** correspond to different states of dendrite growth at 0, 4, 8, 12, 15, and 22 minutes, respectively. Photographs **306a-306f** correspond to photograph taken at times **311-316**, respectively. Box **307** in photograph **306e** is enlarged and shown in **FIG. 3D**. The areas indicated by the arrows show signs of dendrite formation.

[0112] As shown in **FIGS. 5A-5B**, when an ordinary separator was used instead, no voltage change was observed when dendrites had contacted and penetrated the separator. Photographs **501a-501f** correspond to photograph taken at 0, 5, 10, 15, 20, and 25 minutes, respectively. The photograph in **FIG. 5B** was taken at 1 hour. Again, the areas indicated by the arrows show signs of dendrite formation.

RP-Coated Separators In Full-Cells

[0113] The configuration of a full-cell (P-fc) **900** is shown in **FIG. 9A**. The arrangement is similar to that of half-cell **100** shown in **FIG. 1A**, in that it has an anode **901**, separator **902**, RP-coated separator **903**, separator **904** (which again is optional), and a cathode **905**. In full-cell **900**, cathode **905** contains a sulfurized carbon cathode. Sulfurized carbon was selected as the cathode material because of its high specific capacity and low charging voltage. This provides a 3 V window for the voltage to increase, with the voltage limit of the battery test equipment being 5 V. If conventional cathode materials are used, the voltage could only increase by 1-1.5 V.

Dendrite Detection Using RP-Coated Separators In Full-Cells

[0114] To demonstrate that the RP-coated separator could practically work in full Li metal batteries, it was tested in a full Li-S cell that, as shown in **FIG. 9A**, contained a sulfurized carbon cathode. The testing protocol for full-cells was the same as used for half-cells, except that the charge rate was tuned while the discharge rate was fixed.

[0115] A dramatic voltage increase ($|\Delta V|$ >2 V) was observed at ~0.8 mAh/cm^2 (**FIG. 9B**), which is consistent with the voltage decrease in half-cells, while the control sample **906** (ctrl-3) in **FIG. 9D** had a normal charge plateau at ~2.5 V. (**FIG. 9D**). (As shown in **FIG. 9C**, control sample **906** includes anode **901**, cathode **905** and separators **906**, none of which separators having an RP coating). The voltage increase indicated by the arrow in **FIG. 9B** is the electrochemical response generated when the Li dendrites contact the RP coating.

[0116] The fact that the voltage stayed >5 V for more than 6 min in the P-fc revealed another advantage of using an overpotential instead of detecting short circuits with a conductive interlayer. Voltage is monitored in both cases, and voltage fluctuation could happen occasionally. When a voltage change occurs, it is necessary to determine whether it is a valid dendrite-detection signal or merely noise. For the method involving a non-conductive interlayer, one can simply wait for 1 min and see if the voltage remains at that level. But for methods involving conductive interlayers, it is more difficult to further analyze the signal since the charging process cannot be allowed to continue, because if it is indeed a dendrite-detection signal, there will be a short-circuit current that might cause a runaway within seconds.

[0117] SEM analysis and EDS mapping were conducted at different stages of dendrite growth in full-cells (**FIGS. 11A-11N** and **FIGS. 12A-12C**), which displayed the dendritic structures of the Li metal attached to the RP in both P-fc and ctrl-3. As shown in **FIGS. 13A-13D** and **TABLE 1**, the RP did not lower the specific capacity of the sulfurized carbon or bring in significant overpotential when full-cells are cycled normally. (**FIG. 13A** shows control sample

1300 (ctrl-4), which is similar to control sample **906** (ctrl-3) but has only one separator **907**)

Additionally, it was found that 12 μm-thick polyethylene separators (in place of Celgard 2500 separators) worked equally well. The mass loading of sulfurized carbon was ~8 mg/cm^2.

Table 1
The specific capacity of the full-cells (ctrl-4, ctrl-3 and P-fc) based on the mass of sulfurized carbon at 0.4C, 0.7C and 1.3C

	0.4C	0.7C	1.3C
ctrl-4	502 mAh/g	401 mAh/g	322 mAh/g
ctrl-3	489 mAh/g	415 mAh/g	305 mAh/g
P-fc	496 mAh/g	411 mAh/g	315 mAh/g

Mechanism Of Dendrite Detection In Half-Cells

[0118] High resistance is often an obvious reason for having an overpotential in batteries. Therefore, the mechanism was studied in half-cells where the impact of the cathode can be avoided. Electrolyte resistance and charge transfer resistance of P-hc were analyzed by electrochemical impedance spectroscopy (EIS) analyses (**FIGS. 14A-14B**) [*Zhang 2004; Liu 2008*], because the anode might have consumed a significant amount of electrolyte for SEI formation.

[0119] **FIG. 15A** shows the testing protocol where the times of electrolyte resistance measurement are marked at the 10th, 70th, and 71st cycles. **FIG. 15B** shows the electrolyte resistance of the P-hc. **FIG. 15C** shows the voltage profile at 1 mAh/cm^2 and 5 mA/cm^2 (the 71st cycle in **FIG. 15A**). **FIG. 15D** shows the voltage profile for the cycle at 1 mAh/cm^2 and 1 mA/cm^2 (after 71st cycle in **FIG. 15A**). The electrolyte resistance only increased by ~3 Ω over cycling at low capacity (**FIG. 15A-15B**). As shown in **FIG. 14C**, the difference of charge-transfer resistance between P-hc and ctrl-1 was also <5 Ω (peak-3 and end in **FIG. 14C**). [*Zhang 2004; Liu 2008*]. Moreover, as shown in **FIGS. 15C-15D**, the voltage decrease disappeared when the discharge rate was reduced to 1 mA/cm^2. These reflect that the voltage change was not generated by large resistance.

[0120] The high rate was found important: lower discharge rates (0.50/1.0/2.5 mA/cm^2) could

not generate the voltage decrease. *See* **FIG. 14D**. The insulating property of the dendrite-detection interlayer was also essential. Graphene nanoplatelets (GNPs) was added in the RP coating using different P/GNP ratios. With a GNP content of >50 wt%, the voltage change was not observed.

[0121] FIGS. 16A-16B show, respectively, the voltage profile of P-hc discharged above (a) -1.5 V and (b) -5 V (lower voltage limit of the instrument) at 5 mA/cm^2 and charged at 0.25 mA/cm^2. These show that when the discharge voltage was limited to above (*i.e.*, less than) -1.5 V, this yielded a higher CE than discharging to -5 V. This reveals that a significant amount of irreversible side-products may be formed in the low voltage region, which could be non-rechargeable Li, *e.g.* the silver-colored spots on the RP shown in **FIGS. 1F-1G**.

[0122] Based these results, it is believed that the following mechanism is responsible for the voltage change. When a small capacity was applied, the dendrites did not reach the RP coating **(FIG. 14E**, stage **410(I))**. The ends of dendrites were fully exposed to electrolyte solution and were accessible for the charge transfer that resulted in Li plating. (Numbers I to III represent different stages (namely stages **1410(I)-1410(III)**) of dendrite growth.

[0123] When the capacity was increased to around 1 mAh/cm^2, the dendrites penetrated the bottom separator and reached the RP layer **(FIG. 14E**, stage **1410(II))**. The dendrites developed electrical contact with RP by forming Li$_3$P at the interface. [*Mayo 2016*]. Note that RP has a very low electronic conductivity of around 10^{-14} S cm^{-1} and the local current density was exceedingly high on the dendrites under high bulk current density. [*Li 2016; Harry 2016*]. Consequently, it is believed, electrons were blocked at the interface between the dendrites and RP, and thus the electrons accumulated on the dendrite tips, lowering the electrode potential. Under these conditions, the reaction between Li$^+$ and electrons became the rate-determining step of the entire discharge process due to the limited access of Li$^+$ in the electrolyte solution to the dendrite tips and the electrons that had to inevitably flow through them.

[0124] As dendrites continued to grow, albeit slower, they bypassed the RP particles or extended their surface underneath the RP particles to become exposed to the electrolyte again (**FIG. 14E**, stage **1410(III)**). This explains why the voltage eventually returned to its near-original level. [*See* **FIG. 1D**]. The Li dendrites that irreversibly transferred onto the RP interlayer created additional electron pathways for Li plating through the RP interlayer; the RP was no longer an effective barrier to electrons and Li^+ ions after several cycles, and the voltage decrease eventually disappeared.

[0125] This mechanism can also be interpreted in another way that the cathode is treated as a supercapacitor. The cathode has both double-layer capacitance (C_1) that is responsible for the electrostatic charge storage (e.g. negatively charged Cu-Li and physically absorbed Li ions) and pseudocapacitance that is responsible for the electrochemical charge storage (e.g. thin layer of Li plating). The total capacitance $C = C_1 + C_2$. When Li dendrites contacted RP, a thin layer of Li_3P was generated at the interface which served as a dielectric that increased C_1. Meanwhile, the Li_3P layer blocked the incoming Li ions from the electrolyte and impeded further Li plating, which significantly reduced C_2. Note that C_2 was much larger than C_1. Thus, the change in C was dominated by the sharp decrease in C_2, meaning that the total capacitance C would sharply decline. This resulted in a much smaller $|dQ/dV|$ ($C = Q/V$), which displayed in the voltage profile as a sudden increase in $|dV/dt|$, given the constant current in the discharge process ($Q = It$).

[0126] It may therefore be important to stop charging and halt cell use at the first or second indication of significant voltage change.

[0127] In practice, different charge modes can be developed based on this dendrite-detection system if high charge voltage or high charge rate is not applicable. When dendrites form and reach the RP-coated separator layer in full-cells, the charging voltage will reach the upper limit much sooner than expected, triggering another detection protocol to rule out the possibility of

random voltage fluctuation. For instance, the charge mode can be switched from voltage-control constant-current (*e.g.*, 5 mA/cm^2 corresponding to ~2C for commercial pouch cells) charging to voltage-control charging. If the voltage remains at the upper limit with a current density no higher than the constant value used right before (5 mA/cm^2) for a significant amount of time such as 1 min, it is likely that severe dendrite formation is present. This also reduces the dendrite growth rate and thus the damage to the cell, because the total current becomes lower.

[0128] Another option is to let the cell rest for a certain amount of time to have the accumulated electrons dissipated, so that the voltage might drop back to the normal range and rise to the upper limit rapidly again, which would confirm the presence of dendrite formation.

[0129] When high charge rate (5 mA/cm^2) is not always applicable, it could be applied periodically (*e.g.*, every 30 cycles) in the charge steps to reveal possible dendrite formation before it is too late. It is upon such algorithms that the battery management system can be programmed. For example, suppose a battery management system charges a multi-cell battery module at an average cell rate optimized for the module or charging environment but below what is required or optimal for dendrite detection. The battery management system can periodically subject subsets of the cells, in turn, to a higher charge rate suitable for dendrite detection.

Method Of Dendrite Detection Using RP-Coated Separators

[0130] Embodiments of the present invention can be applied in batteries with metal electrodes for consumer electronics and electric/hybrid vehicles.

[0131] The reagent partition detects dendrite formation before the dendrites short the cell, and therefore ensures safe operation of Li metal cells such that dendrite formation is no longer a major concern when using Li metal anodes.

[0132] The reagent partition can be electrically isolated within the cell absent dendrite contact,

and thus does not require an electrode for dendrite detection. Electrodeless reagent partitions thus facilitate dendrite detection in two-terminal cells. Only a thin RP coating between the cathode and the anode is added in the current battery configuration during the making of the battery.

[0133] The formation of dendrite is detected by simply monitoring the charge voltage during the use of the battery beyond a certain charge rate.

[0134] In embodiments of the present invention, the method can include one or more of the following steps: preparation of the RP-coated separators, performing electrochemical tests (battery tests and EIS analysis); and instructions on its practical use.

[0135] For example with regard to preparation of the RP-coated separators, RP and PVDF (binder) can be mixed in a mortar at a mass ratio of 9:1. NMP was added to form a slurry after grinding for 5 min. The slurry was coated on a Celgard 2500 separator and dried in a vacuum oven (~1 Torr) at 60 °C overnight. The mass loading of RP was ~2 mg/cm^2.

[0136] Further, for example with regard to electrochemical tests (battery tests and EIS analysis), the half-cells and full-cells were assembled using $LiPF_6$ in EC/DEC (v/v=1/1) as the electrolyte solution.

[0137] Further, for example with regard to instructions on its practical use, in practical applications, when a user wants to check if there is severe dendrite formation in the battery, a specific testing program can be activated to start charging the battery (such as at ≥ 5 mA/cm^2) while the voltage is monitored by the battery management system. Once the charge voltage reaches 2 V higher than the maximum charge voltage used in normal charge steps and stays ≥ 2 V higher for a predetermined period (such as 30 seconds), the battery system can *e.g.* disconnect the errant cell or sells or warn the user of the hazardous condition of the battery and recommend shutting it down instantly.

Battery Management Systems

[0138] Battery-management systems can use signals generated by electrodeless regent partitions to detect dendrites before they present an imminent threat of failure. Effected cells, batteries, or modules can thus be physically or electrically removed, and harm averted.

[0139] The battery-management system can test for dendrites in a cell, battery, or module by periodically measuring full-charge timing of the device. The full-charge timing is a function of charging current and a full-charge voltage applied between the anode and cathode. Full-charge timing changes over the life of a device so the system periodically updates and stores a full-charging model for a given device. The model can be simple, such as a measure of the time required to reach a full-charge voltage. More complex models can estimate full-charge timing based on e.g. current state of charge, charging voltage, charging current, and temperature. The full-charging model, derived from measure and/or simulation, can provide the system with expected full-charge timing for a device under a range of charging scenarios.

[0140] In some embodiments the system monitors charging time and voltage, issuing a tentative dendrite-detection signal if the charging voltage reaches the full-charge voltage, or some other threshold, sooner than expected based on the full-charging model. In one embodiment, for example, the management system issues a tentative dendrite-detection signal if a device under charge reaches the full-charge voltage within 80% of the full-charge timing predicted by the device-specific full-charging model.

[0141] Voltage readings over short periods can be inaccurate. The management system can thus continue to monitor a suspect cell, battery, or module before affirming the tentative dendrite detection. In one embodiment, the system adjusts the charging current responsive to the tentative dendrite-detection signal to limit the charging voltage to e.g. the full-charge voltage. The system can then issue an affirmative dendrite-detection signal if the charging current responsive to that constant charging voltage falls below a threshold. For example, the system may affirm dendrite detection if the charging falls for, *e.g.*, 10 seconds while the battery

is being charged at the full-charge voltage.

[0142] The battery-management system may periodically subject each battery to a charge current that is sufficiently high to ensure a robust dendrite-detection. In one embodiment in which the energy-storage device is a lithium-metal battery, for example, the system subjects the battery to a charging current of at least 2.5 mA/cm^2. Systems with many devices under management and insufficient power to provide all devices with the requisite level of current can test the devices in turn.

[0143] When dendrites are detected by periodic tests, the battery-management system may compare the full-charge time of a dendrite-detection step to the last cycle that used the same charge current. This allows the system to recognize the differences coming from the dendrite formation. For periodic tests, the last cycle that used the same current may have been many cycles ago, so the stored full-charge time may no longer be comparable. The system is therefore adapted to simulate the full-charging model at the high current needed for dendrite detection based on the normal charge curve at a lower current before performing a dendrite-detection process.

[0144] In one embodiment, a RP-coated separator was used for dendrite detection and was prepared by the slurry method using N-methyl-2-pyrrolidone (NMP) as the solvent and poly(vinylidene difluoride) (PVDF) as the binder. The RP layer had a thickness of ~20 μm with a mass loading of ~2 mg/cm^2. The RP layer was physically isolated from the electrodes. The bottom separator was optional because the separator upon which RP was coated is enough to isolate the RP layer from the anode.

[0145] When Li dendrites extended to the RP coating, there was a noticeable and dramatic electrochemical response in the voltage profile (voltage vs capacity or time). The voltage decreased in half cells or increased in full cells when Li dendrites contact the RP. These voltage changes can activate a signal of Li dendrite formation through the battery management system

that is installed on all recharging devices.

Additional Variations

[0146] In some embodiments, the loading of the RP can be modified (such as the loading is reduced).

[0147] In some embodiments, the preparation method can include one or more of the following:

[0148] The RP coating can be formed using various techniques, including but not restricted to spray coating, filtration, and physical/chemical deposition and doctor blade methods.

[0149] The RP coating can be impregnated in the middle of the separator when the separator is produced.

[0150] The RP can be in the form of a free-standing film.

[0151] The method of preparation can include (a) the RP coating can be formed using various techniques, including but not restricted to spray coating, filtration, and physical/chemical deposition and doctor blade methods, (b) the RP coating can be impregnated in the middle of separator when the separator is produced, and (c) the RP can be in the form of a free-standing film.

[0152] In some embodiments, the use of the RP coating can include one or more of the following:

[0153] The type of batteries includes but is not restricted to coin cells, cylindrical cells, prismatic cells, and pouch cells.

[0154] The type of batteries includes but is not restricted to Li, Na, K, Mg, Ca, Al, and Zn metal batteries.

[0155] The type of separator that RP is coated on can be any separator that works for a battery.

[0156] Battery electrolyte is not necessarily $LiPF_6$. The RP coating can work for any kind of battery electrolyte, as long as the active material in the anode or cathode includes metals.

[0157] Embodiments of the present invention can be applied in batteries with metal electrodes for consumer electronics and electric/hybrid vehicles.

[0158] In some embodiments, the use of the RP coating can include (a) the type of batteries including, but is not restricted to, coin cells, cylindrical cells, prismatic cells, and pouch cells, (b) the type of batteries, including, but is not restricted to, Li, Na, K, Mg, Ca, Al, and Zn metal batteries, (c) the type of separator that RP is coated on can be any separator that works for a battery, and (d) battery electrolyte is not necessarily $LiPF_6$. The RP coating can work for any kind of battery electrolyte, as long as the active material in the anode or cathode includes metals.

[0159] In some embodiments, the composition of the coating need not be RP only. The coating can be made from anything that is a poor electronic conductor, able to react with Li, and forms an insoluble or slightly soluble product with Li. This includes but is not restricted to Si, Ge, As, metal oxides, metal fluorides, $LiM_xE_yO^z$ (M=metal, E=nonmetal, O=oxygen, $x \geq 0$, $y \geq 0$, $z \geq 0$), and any combination of the above

[0160] In some embodiments, the separator that contains the RP coating can be situated in the middle.

REFERENCES

[0161] Armand, M. *et al.*, Building Better Batteries. *Nature* **2008**, *451* (7179), 652–657 ("*Armand 2008*").

[0162] Bruce, P. G. *et al.*, Li–O2 and Li–S Batteries with High Energy Storage. *Nat. Mater.* **2011**, *11* (2), 172–172 ("*Bruce 2011*").

[0163] Cano, Z. P. *et al.*, Batteries and fuel cells for emerging electric vehicle markets *Nat. Energy.* **2018**, *3*, 279-289 ("*Cano 2018*").

[0164] Cheng, X. B. *et al.*, Toward Safe Lithium Metal Anode in Rechargeable Batteries: A Review. *Chem. Rev.* **2017**, *117*, 10403-10473 ("*Cheng 2018*").

[0165] Ding, F. *et al.*, Dendrite-free lithium deposition via self-healing electrostatic shield mechanism. *J. Am. Chem. Soc.* **2013**, *135*, 4450-4456 (*"Ding 2013"*).

[0166] Dunn, B.; Kamath, H. *et al.*, Electrical Energy Storage for the Grid: A Battery of Choices. *Science (80).* **2011**, *334* (6058), 928–935 (*"Dunn 2011"*).

[0167] Goodenough, J. B. *et al.*, The Li-Ion Rechargeable Battery: A Perspective. *J. Am. Chem. Soc.* **2013**, *135* (4), 1167–1176 (*"Goodenough 2013"*).

[0168] Girishkumar, G. *et al.*, Lithium-Air Battery: Promise and Challenges. *J. Phys. Chem. Lett.* **2010**, *1* (14), 2193–2203 (*"Girishkumar 2010"*).

[0169] Harry, K. J. *et al.*, Influence of Electrolyte Modulus on the Local Current Density at a Dendrite Tip on a Lithium Metal Electrode. *J. Electrochem. Soc.* **2016**, *163*, A2216-A2224 (*"Harry 2016"*).

[0170] Li, L. *et al.*, Self-heating-induced healing of lithium dendrites. *Science* **2018**, 359, 1513-1516 (*"Li 2018"*).

[0171] Li, W. *et al.*, Amorphous Red Phosphorus Embedded in Highly Ordered Mesoporous Carbon with Superior Lithium and Sodium Storage Capacity. *Nano Lett.* **2016**, 16, 1546-1553 (*"Li 2016"*).

[0172] Lin, D. *et al.*, All-Integrated Bifunctional Separator for Li Dendrite Detection via Novel Solution Synthesis of a Thermostable Polyimide Separator. *J. Am. Chem. Soc.* **2016**, 138, 11044-11050 (*"Lin I 2016"*).

[0173] Lin, D. *et al.*, Layered reduced graphene oxide with nanoscale interlayer gaps as a stable host for lithium metal anodes. *Nat. Nanotechnol.* **2016**, *11*, 626-632 (*"Lin II 2016"*).

[0174] Liu, B. *et al.*, Advancing Lithium Metal Batteries. *Joule* **2018**, 2, 833-845 (*"Liu 2018"*).

[0175] Liu, K. *et al.*, Extending the Life of Lithium-Based Rechargeable Batteries by Reaction of Lithium Dendrites with a Novel Silica Nanoparticle Sandwiched Separator. *Adv. Mater.* **2017**, *29*, 1603987 (*"Liu 2017"*).

[0176] Liu, S.-Q. *et al.*, Kinetic study on $Li_{2.8}(V_{0.9}Ge_{0.1})_2(PO_4)_3$ by EIS measurement. *J. Alloys Compd.* **2008**, *450*, 499-504 (*"Liu 2008"*).

[0177] Manthiram, A. *et al.*, Lithium-Sulfur Batteries: Progress and Prospects. *Adv. Mater.* **2015**, *27* (12), 1980–2006 (*"Manthiram 2015"*).

[0178] Mayo, M. *et al.*, Ab Initio Study of Phosphorus Anodes for Lithium- and Sodium-Ion Batteries. *Chem. Mater.* **2016**, *28*, 2011-2021 (*"Mayo 2016"*).

[0179] Noorden, R. Van, The Rechargeable Revolution: A Better Battery. *Nature* **2014**, *507*, 26–28 (*"Noorden 2014"*).

[0180] Orsini, F. *et al.*, In situ SEM study of the interfaces in plastic lithium cells, *J. Power Sources.* **1999**, *81–82*, 918-921 (*"Orsini 1999"*).

[0181] Qian, J. *et al.*, High rate and stable cycling of lithium metal anode *Nat. Commun.* **2015**, *6*, 6362 (*"Quia 2015"*)

[0182] Raji, A. O. *et al.*, Lithium Batteries with Nearly Maximum Metal Storage *ACS Nano* **2017**, *11*, 6362-6369 (*"Raji 2017"*).

[0183] Shen, X. *et al.*, Beyond lithium ion batteries: Higher energy density battery systems based on lithium metal anodes. *Energy Storage Mater.* **2018**, *12*, 161-175 (*"Shen 2018"*).

[0184] Wang, T. *et al.*, Ultrafast Charging High Capacity Asphalt–Lithium Metal Batteries. *ACS Nano* **2017**, 11, 10761-10767 (*"Wang 2017"*).

[0185] Wood, K.N. *et al.*, Dendrites and Pits: Untangling the Complex Behavior of Lithium Metal Anodes through Operando Video Microscopy. *ACS Cent. Sci.* **2016**, *2*, 790-801 (*"Wood 2016"*).

[0186] Wu, H. *et al.*, Improving Battery Safety By Early Detection Of Internal Shorting With A Bifunctional Separator. *Nat. Commun.* **2014**, *5*, 5193-5198 (*"Wu 2016"*).

[0187] Xu, W. *et al.*, Lithium Metal Anodes for Rechargeable Batteries. *Energy Environ. Sci.* **2014**, *7* (2), 513–537 (*"Xu 2014"*).

[0188] Zhang, J.-G. *et al.*, *Lithium Metal Anodes and Rechargeable Lithium Metal Batteries*, 1st ed.; Hull, R. *et al.*, Eds.; Springer International Publishing, 2017 ("*Zhang 2017*").

[0189] Zhang, S. S. *et al.*, Electrochemical impedance study on the low temperature of Li-ion batteries. *Electrochimi. Acta* **2004**, *49*, 1057-1061 ("*Zhang 2004*").

[0190] While embodiments of the invention have been shown and described, modifications thereof can be made by one skilled in the art without departing from the spirit and teachings of the invention. The embodiments described and the examples provided herein are exemplary only, and are not intended to be limiting. Many variations and modifications of the invention disclosed herein are possible and are within the scope of the invention. The scope of protection is not limited by the description set out above, but is only limited by the claims which follow, that scope including all equivalents of the subject matter of the claims.

[0191] The disclosures of all patents, patent applications, and publications cited herein are hereby incorporated herein by reference in their entirety, to the extent that they provide exemplary, procedural, or other details supplementary to those set forth herein. This writing takes precedence over the incorporated materials for purposes of claim construction.

[0192] Amounts and other numerical data may be presented herein in a range format. It is to be understood that such range format is used merely for convenience and brevity and should be interpreted flexibly to include not only the numerical values explicitly recited as the limits of the range, but also to include all the individual numerical values or sub-ranges encompassed within that range as if each numerical value and sub-range is explicitly recited. For example, a numerical range of approximately 1 to approximately 4.5 should be interpreted to include not only the explicitly recited limits of 1 to approximately 4.5, but also to include individual numerals such as 2, 3, 4, and sub-ranges such as 1 to 3, 2 to 4, etc. The same principle applies to ranges reciting only one numerical value, such as "less than approximately 4.5," which should be interpreted to include all of the above-recited values and ranges. Further, such an

interpretation should apply regardless of the breadth of the range or the characteristic being described.

[0193] Unless defined otherwise, all technical and scientific terms used herein have the same meaning as commonly understood to one of ordinary skill in the art to which the presently disclosed subject matter belongs. Although any methods, devices, and materials similar or equivalent to those described herein can be used in the practice or testing of the presently disclosed subject matter, representative methods, devices, and materials are now described.

[0194] Following long-standing patent law convention, the terms "a" and "an" mean "one or more" when used in this application, including the claims.

[0195] Unless otherwise indicated, all numbers expressing quantities of ingredients, reaction conditions, and so forth used in the specification and claims are to be understood as being modified in all instances by the term "about." Accordingly, unless indicated to the contrary, the numerical parameters set forth in this specification and attached claims are approximations that can vary depending upon the desired properties sought to be obtained by the presently disclosed subject matter.

[0196] As used herein, the term "about" and "substantially" when referring to a value or to an amount of mass, weight, time, volume, concentration or percentage is meant to encompass variations of in some embodiments ±20%, in some embodiments ±10%, in some embodiments ±5%, in some embodiments ±1%, in some embodiments ±0.5%, and in some embodiments ±0.1% from the specified amount, as such variations are appropriate to perform the disclosed method.

[0197] As used herein, the term "and/or" when used in the context of a listing of entities, refers to the entities being present singly or in combination. Thus, for example, the phrase "A, B, C, and/or D" includes A, B, C, and D individually, but also includes any and all combinations and subcombinations of A, B, C, and D.

WHAT IS CLAIMED IS:

1.   A structure in a metal-anode-based battery comprising:

        (a)   an anode that comprises a metal;

        (b)   a cathode; and

        (c)   an electrodeless separator positioned between the anode and the cathode,

                 wherein a detectable electrical response signal will result during a charging or

                 discharging of the battery when the metal from the metal anode contacts the

                 electrodeless separator.

2.   The structure of Claim 1, wherein the metal that contacts the electrodeless separator
extends from the anode.

3.   The structure of Claim 1, wherein the metal is selected from a group consisting of
lithium, sodium, potassium, magnesium, calcium, aluminum, zinc, cesium, mixtures thereof,
and composites therefrom.

4.   The structure of Claim 1, wherein the electrodeless separator has a resistance of at most
10^{-5} S/cm.

5.   The structure of Claim 1, wherein the electrodeless separator comprises red
phosphorous.

6.   The structure of Claim 1, wherein the electrodeless separator comprises a material
selected from a group consisting of red phosphorous, silicon, germanium, arsenic, metal oxides,
metal halides, metal chalcogenides, chalcogenides, $LiM_xE_yO_z$ with M=metal, E=nonmetal,

O=oxygen, x≥0, y≥0, and z≥0, MXenes, 2D materials, polymers, organic polymers, inorganic polymers, and mixtures thereof or composites therefrom.

7.   The structure of Claim 6, wherein the material is a poor electronic conductor, is able to react with Li, and will form an insoluble product with Li when reacted with Li.

8.   The structure according of Claim 1, wherein the electrodeless separator is independent of all other films.

9.   The structure of Claim 1, wherein the electrodeless separator is deposited upon or within another film or matrix host material.

10.   An electronic system comprising a battery management system having the structure of Claim 1, wherein the electronic system is operable to signal a turnoff or cessation of battery use in response to the detectable electrical response signal resulting from the metal from the metal anode contacting the electrodeless separator in the structure of Claim 1.

11.   The electronic system of Claim 10, wherein the detectable electrical response signal generated is a change in voltage with respect to time during the charging of the battery.

12.   The electronic system of Claim 11, wherein the change in voltage is least 0.25 V.

13.   The electronic system of Claim 12, wherein, in the structure, the voltage will decrease by at most 0.1 V if the battery rests for at least 1 hour after the voltage increases at least 1 V.

14.   The electronic system of Claim 11, wherein the change in voltage is least 1 V.

15.   A method comprising using the electronic system of Claim 12 to prevent short circuits or fires in the metal-anode-based battery.

16.   An energy-storage device comprising:

(a)   an anode comprising a metal;

(b)   a cathode;

(c)   an electrolyte containing cations of the metal, wherein the electrolyte is disposed between the anode and the cathode; and

(d)   an electrodeless reagent partition in the electrolyte between the anode and the cathode, wherein the electrodeless reagent partition comprises a reagent that can react chemically with the metal.

17.   The energy-storage device of Claim 16, the reagent can react with a morphological feature of the metal extending from the anode.

18.   The energy-storage device of Claim 16, wherein the metal comprises lithium.

19.   The energy-storage device of Claim 16, wherein the reagent comprises phosphorous.

20.   The energy-storage device of Claim 16, wherein the reagent comprises red phosphorous.

21.   The energy-storage device of Claim 16, wherein the reagent comprises particles.

22.   The energy-storage device of Claim 16, wherein the reagent comprises at least one material selected from a group consisting of silicon, germanium, arsenic, metal oxides, metal fluorides, and LiMxEyOz with M=metal, E=nonmetal, O=oxygen, and x$\geq$0, y$\geq$0, and z$\geq$0.

23.   The energy-storage device of Claim 16 further comprising a separator extending through the electrolyte between the reagent partition and the anode.

24.   The energy-storage device of Claim 23, wherein the reagent partition is disposed on the separator.

25.   The energy-storage device of Claim 16 further comprising a separator extending through the electrolyte between the reagent partition and the cathode.

26.   The energy-storage device of Claim 16, wherein the reagent is an electrical insulator.

27.   The energy-storage device of Claim 16, wherein the reagent has a resistance of less than 10^{-5} S/cm.

28.   The energy-storage device of Claim 16, wherein the electrolyte is a liquid.

29.   The energy-storage device of Claim 16, wherein the cathode comprises a conductive reagent that reacts chemically with the cations of the metal.

30.   The energy-storage device of claim 16, wherein the electrodeless reagent partition is of a thickness less than one millimeter.

31.   The energy-storage device of claim 30, wherein the electrodeless reagent partition comprises multiple separator layers.

32.   The energy-storage device of Claim 16, wherein the electrodeless reagent partition consists essentially of red phosphorus.

33.   The energy-storage device of claim 16, wherein the electrodeless reagent partition comprises a separator layer coated with the reagent.

34.   The energy-storage device of claim 33, wherein the reagent is prepared by a process comprising coating the separator with a slurry.

35.   The energy-storage device of claim 33, wherein the reagent is applied to the separator layer by a process comprising coating the separator by vacuum filtration.

36.   A test method for dendrite detection in an energy-storage device having a first electrode and a second electrode, the test method comprising:

(a)   measuring charge timing of the energy-storage device;

(b)   storing a charging model of the measured charge timing of the energy-storage device, the charging model providing an expected charge timing;

(c)   charging the energy-storage device while monitoring a charging time and a charging voltage between the first electrode and the second electrode; and

(d)   issuing a dendrite-detection signal if the charging voltage reaches a threshold voltage before the expected charge timing.

37.   The test method of claim 36, wherein the expected charge timing comprises an expected full-charge timing.

38.   The test method of claim 36, wherein the dendrite-detection signal is a tentative signal, the method further comprising adjusting a charging current responsive to the dendrite-detection signal to limit the charging voltage.

39.   The test method of claim 38, wherein the adjusting of the charging current limits the charging voltage.

40.   The test method of claim 39 further comprising issuing an affirmative dendrite-detection signal if the charging current falls while the device is charged at the charging voltage.

41.   The test method of claim 40 further comprising issuing the affirmative dendrite-detection signal if the charging current falls for at least ten seconds while the device is charged at the charging voltage.

42.   The test method of claim 36, wherein the energy-storage device comprises a lithium-metal battery.

43.   The test method of claim 42, wherein charging the energy-storage device comprises maintaining the charging current at at least 2.5 mA/cm^2.

44.   The test method of claim 36, wherein the dendrite-detection signal is a tentative signal, the method further comprising continuing to charge the energy-storage device after the issuing of the tentative signal for a dendrite-verification period.

45.   The test method of claim 44 further comprising disabling the energy-storage device if the energy-storage device is charged at at least the threshold voltage after the dendrite-verification period.

46.   The test method of claim 45, wherein the dendrite-verification period is at least ten seconds.

47.   The test method of claim 36, wherein the expected charge timing and the measured charge timing are equal.

48.   A battery-management system that executes the method of claim 36 to test a battery, the battery comprising:

   (a)   an anode comprising a metal;

   (b)   a cathode;

   (c)   an electrolyte containing cations of the metal, wherein the electrolyte is disposed between the anode and the cathode; and

   (d)   an electrodeless reagent partition in the electrolyte between the anode and the cathode, wherein the electrodeless reagent partition comprises a reagent that can react chemically with the metal.

49.   A test method for dendrite detection in an energy-storage device having a first electrode and a second electrode, the test method comprising:

(a)   storing a charging model of the energy-storage device, the charging model providing an expected charge voltage;

(b)   charging the energy-storage device while monitoring a charging voltage between the first electrode and the second electrode; and

(c)   issuing a dendrite-detection signal if the charging voltage exceeds the expected charge voltage.

50.   The test method of Claim 49 further comprising issuing the dendrite-detection signal if the charging voltage exceeds the expected charge voltage by at least 0.25 V.

51.   The test method of claim 49 further comprising issuing the dendrite-detection signal if the charging voltage exceeds the expected charge voltage by at least 1.0 V.

52.   The test method of claim 49 further comprising:

(a)   allowing the charging voltage to exceed the expected charge voltage by a voltage margin;

(b)   storing a measure of the charging voltage;

(c)   allowing the device to rest for a rest period;

(d)   measuring a test voltage between the first electrode and the second electrode after the rest period; and

(e)   affirming the dendrite-detection signal if the test voltage falls below a detection level during the rest period.

53.   The test method of claim 52, wherein the voltage margin is at least one volt.

54.   The test method of claim 52, wherein the rest period is at least one hour.

55.   The test method of claim 52, wherein the detection level is at least 0.1 V below the measured charging voltage.
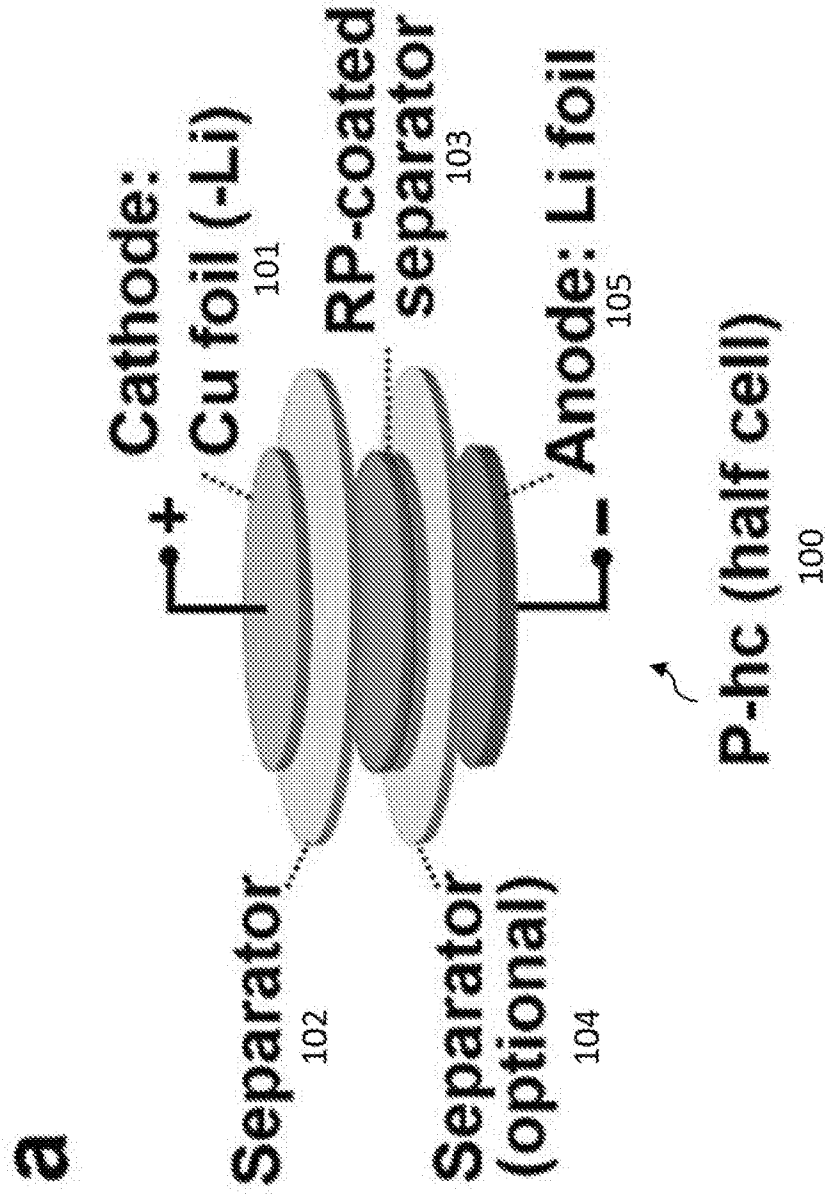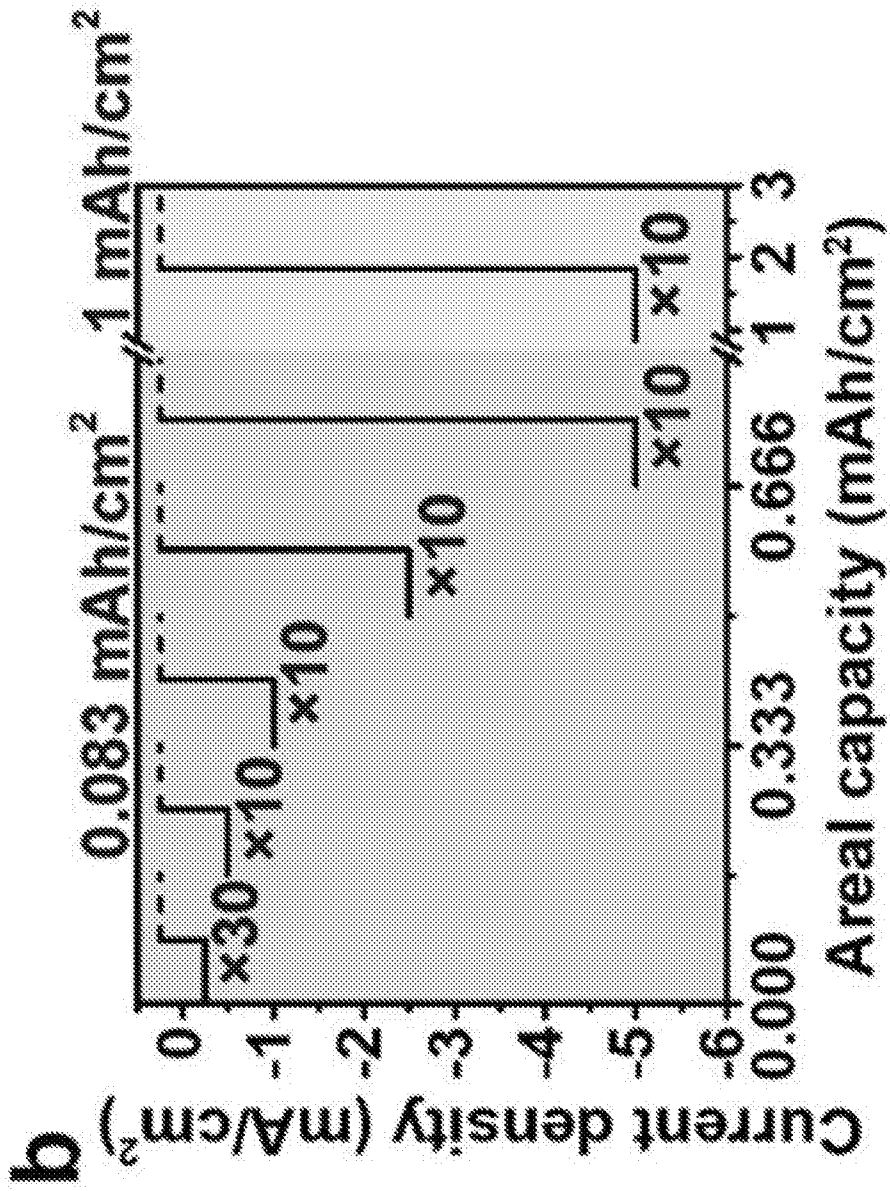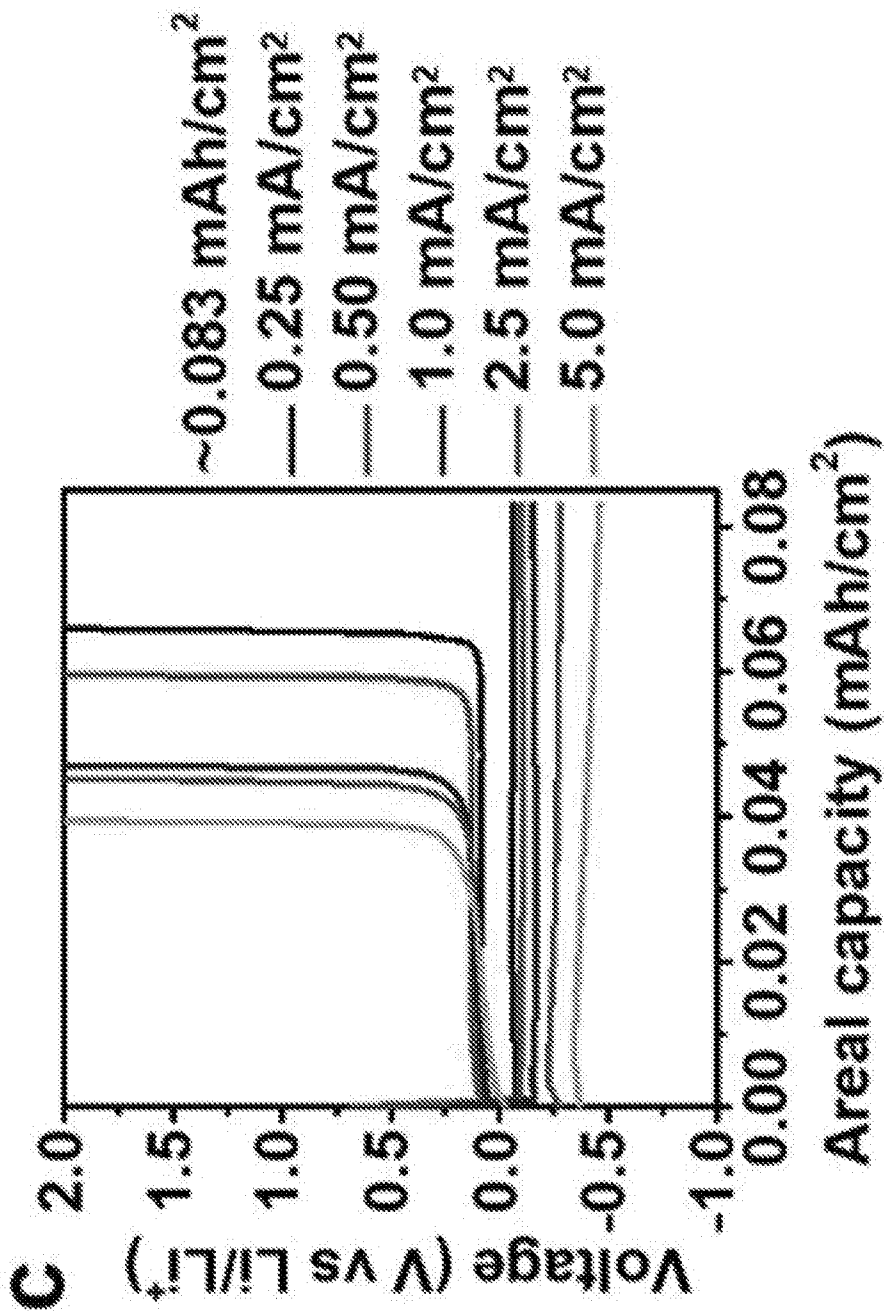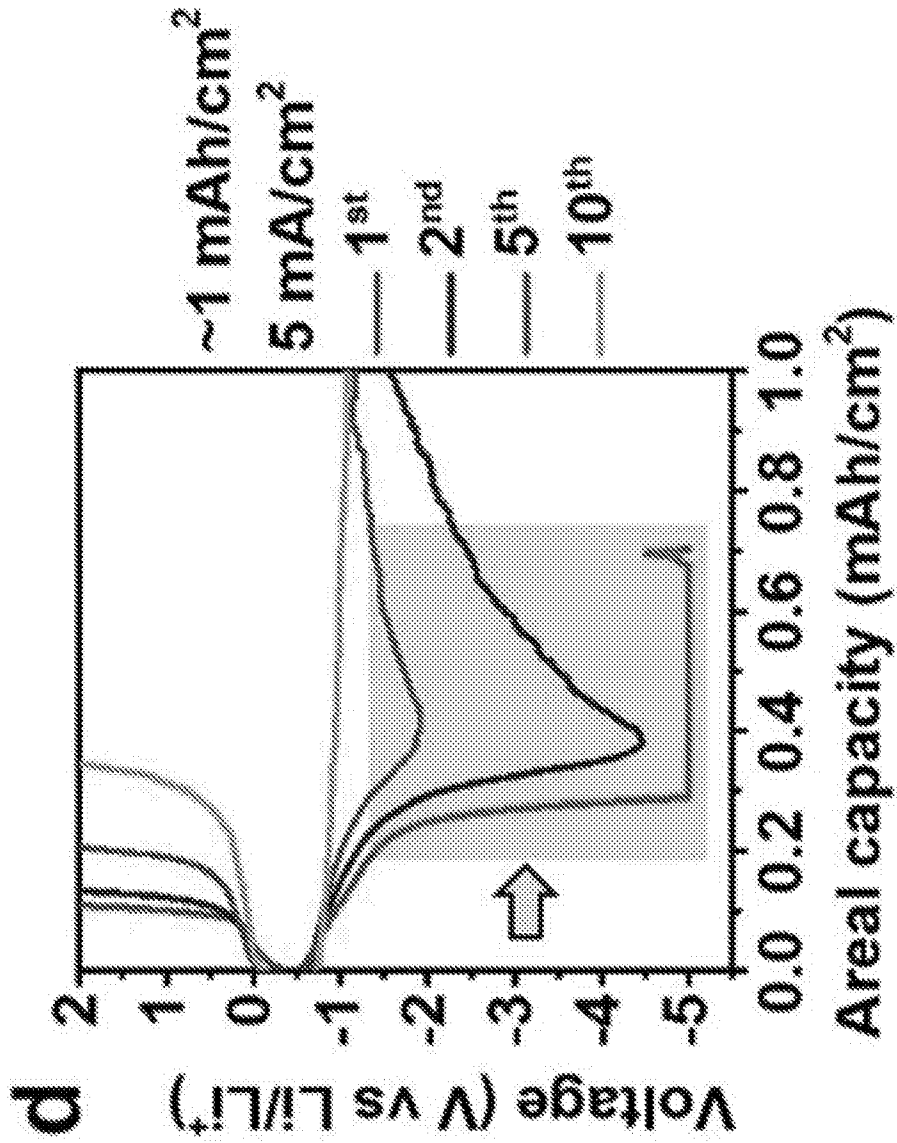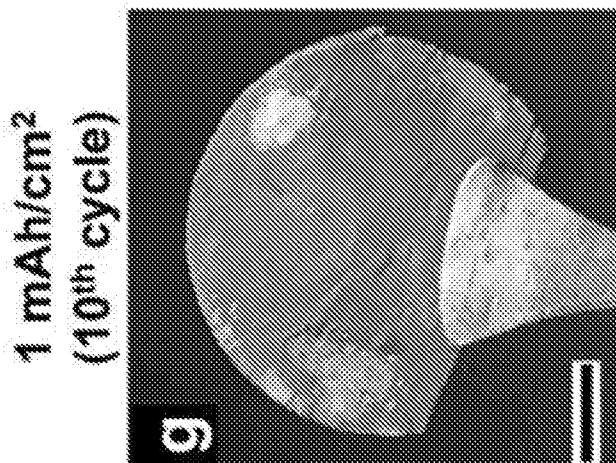
a

Cathode:
Cu foil (-Li)
101

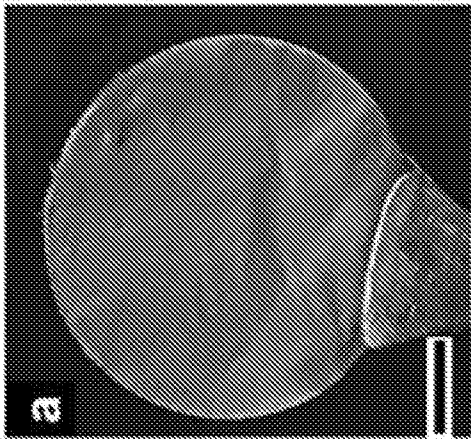RP-coated
separator
103

Anode: Li foil
105

Separator
102

Separator
(optional)
104

P-hc (half cell)
100

FIG. 1A

FIG. 1B

FIG. 1C

FIG. 1D

0.083 mAh/cm² (last cycle)

1 mAh/cm² (first cycle)
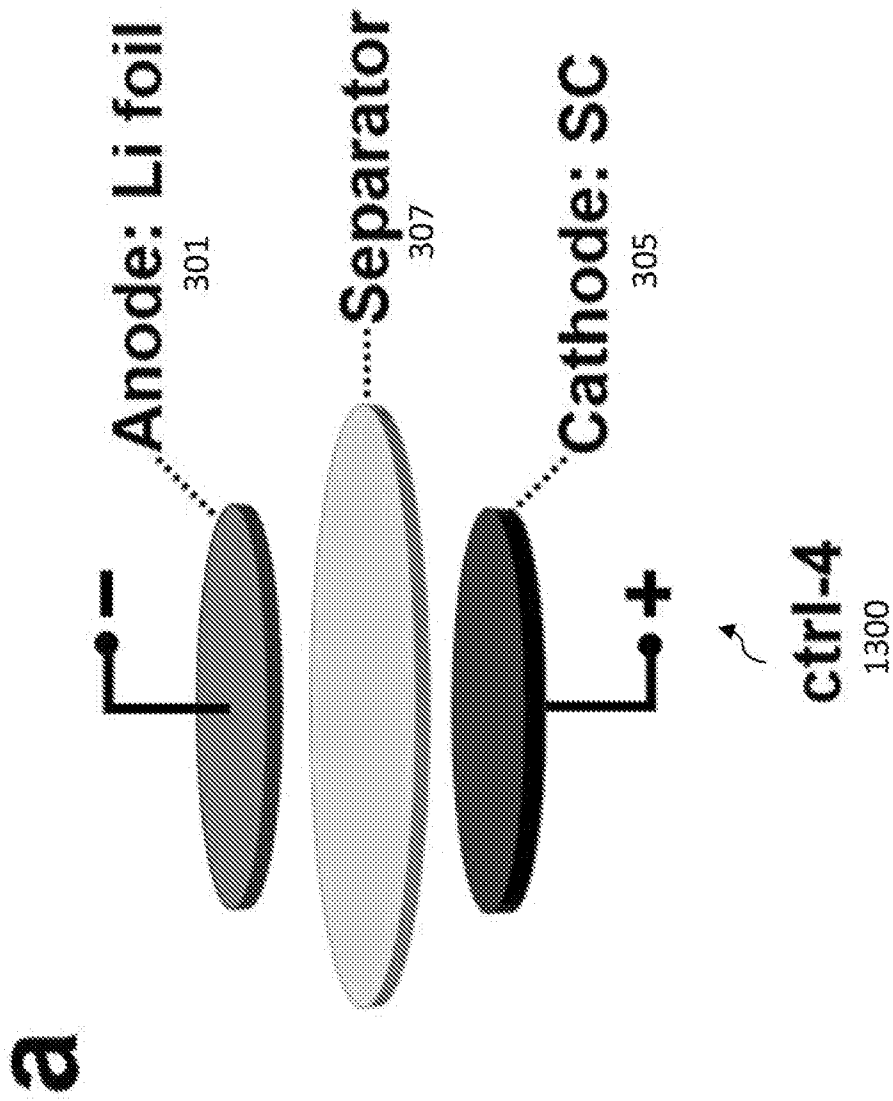
1 mAh/cm² (10th cycle)

FIG. 1E

FIG. 1F

FIG. 1G

FIG. 1H

FIG. 1J

FIG. 1I

FIG. 2

a

FIG. 3A

FIG. 3B

FIG. 3C

FIG. 3D

a

Cathode: Cu foil (-Li)
101

Separator
403

Anode: Li foil
105

ctrl-1
400

FIG. 4A

FIG. 4B

FIG. 4C

Cathode: Cu foil (-Li)
101

Separator
413

Anode: Li foil
105

+

−

d

ctrl-2
410

FIG. 4D

17/44

FIG. 4E

FIG. 4F

FIG. 5A

1 h
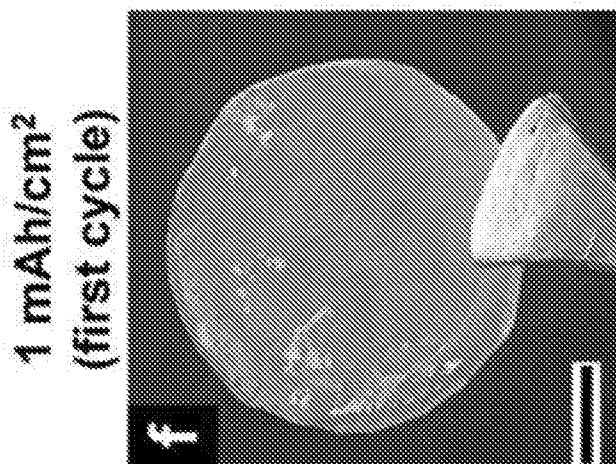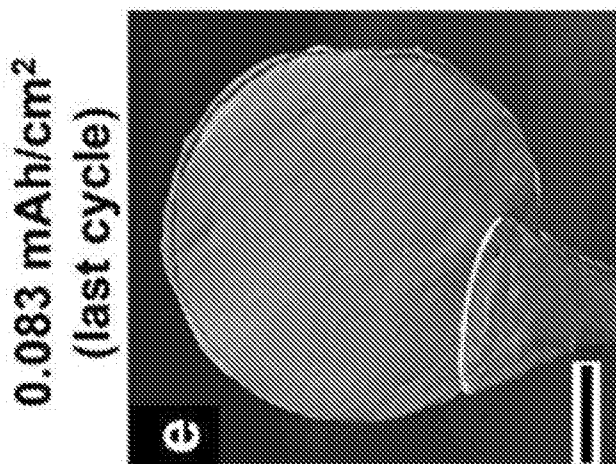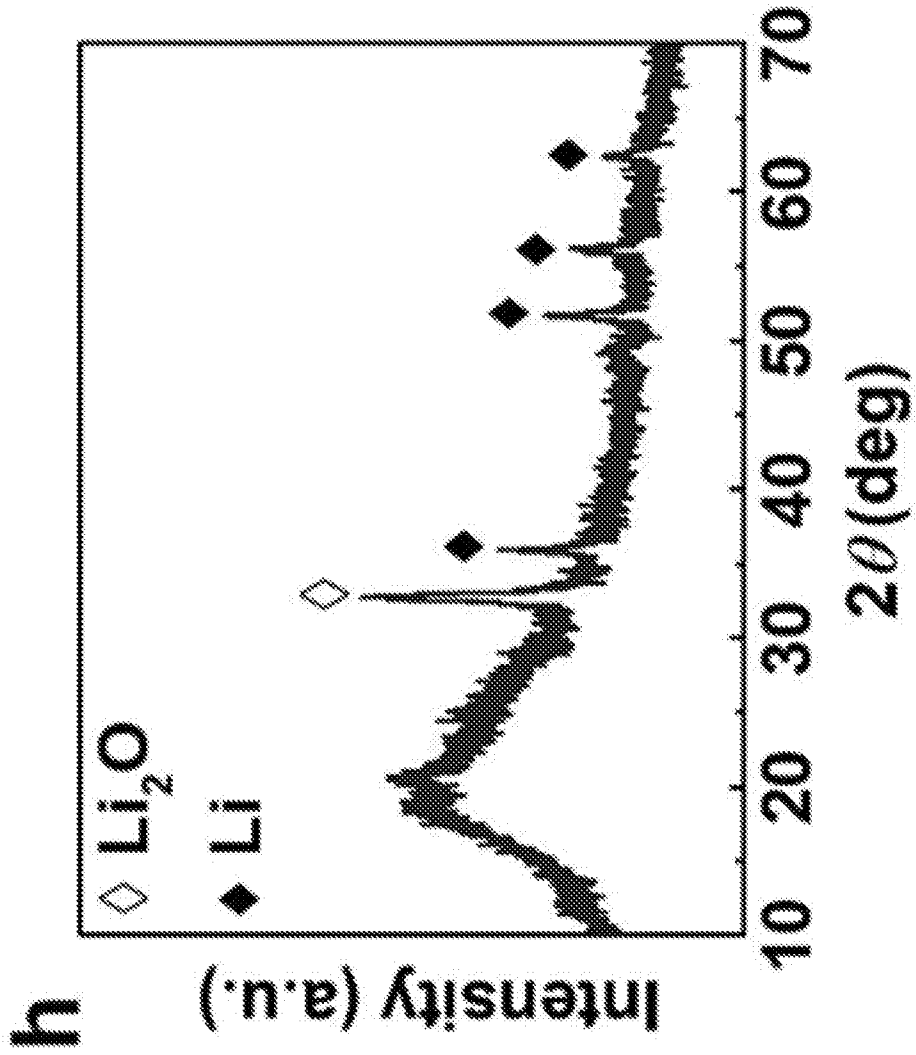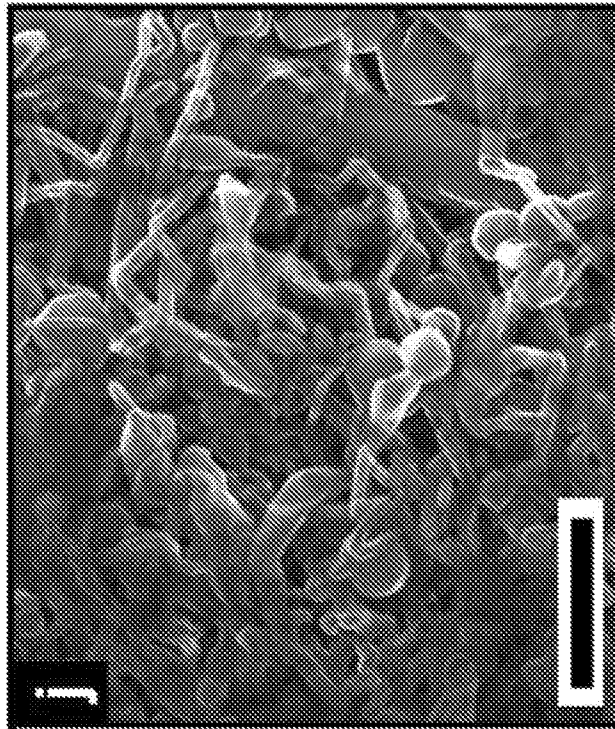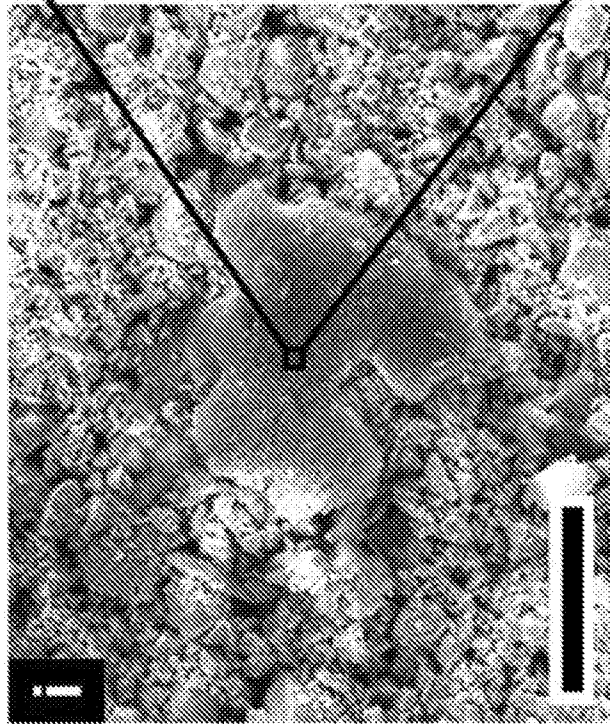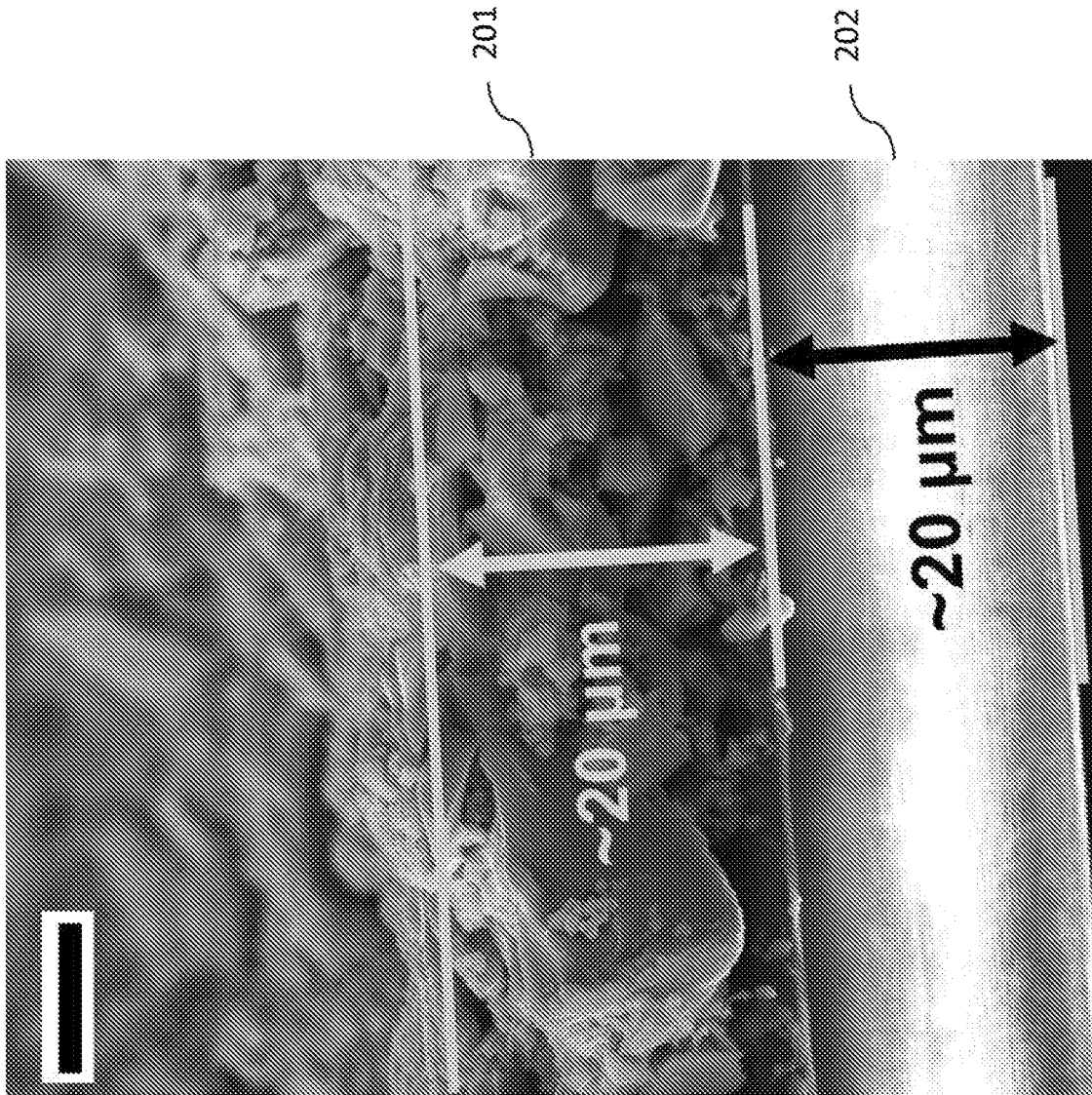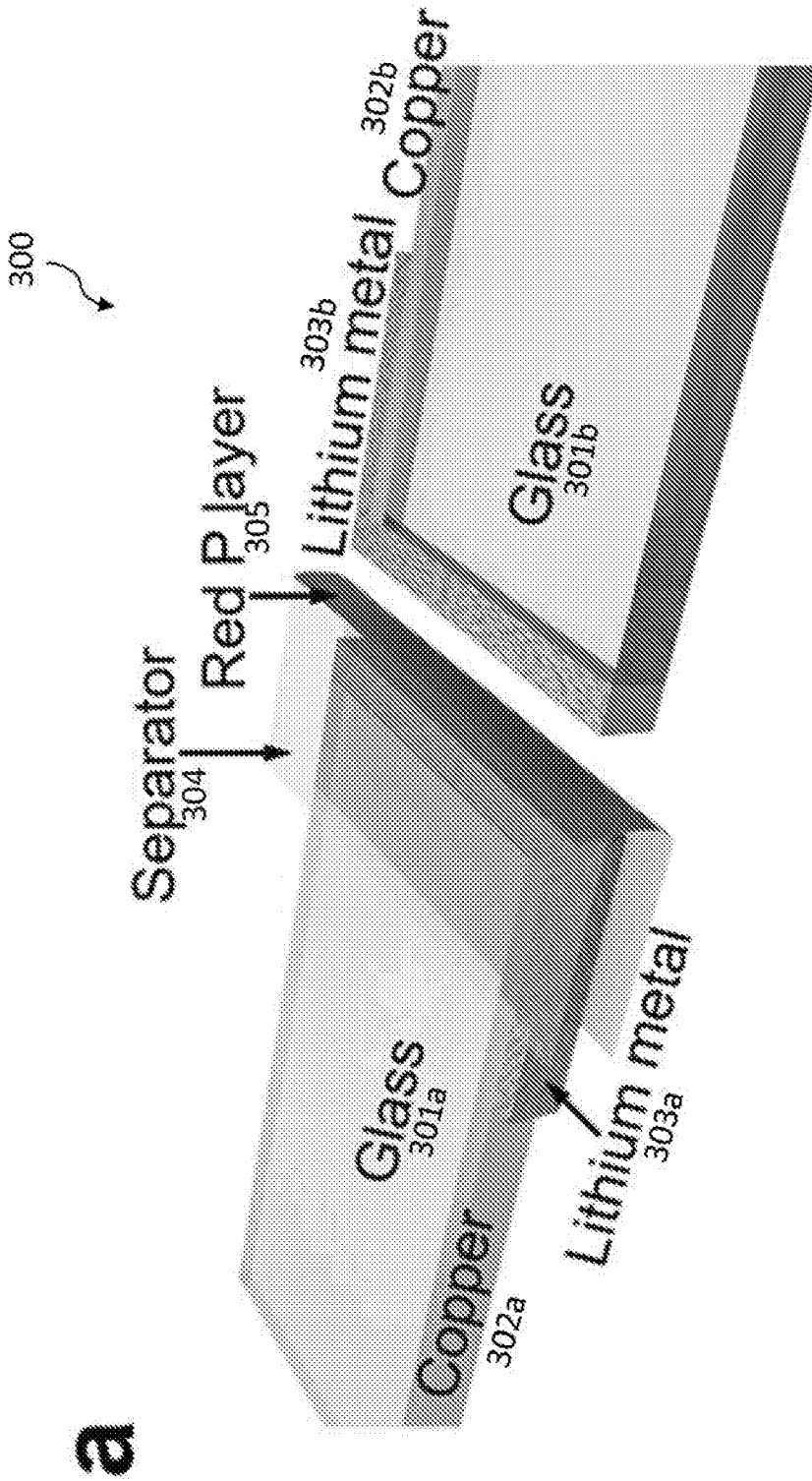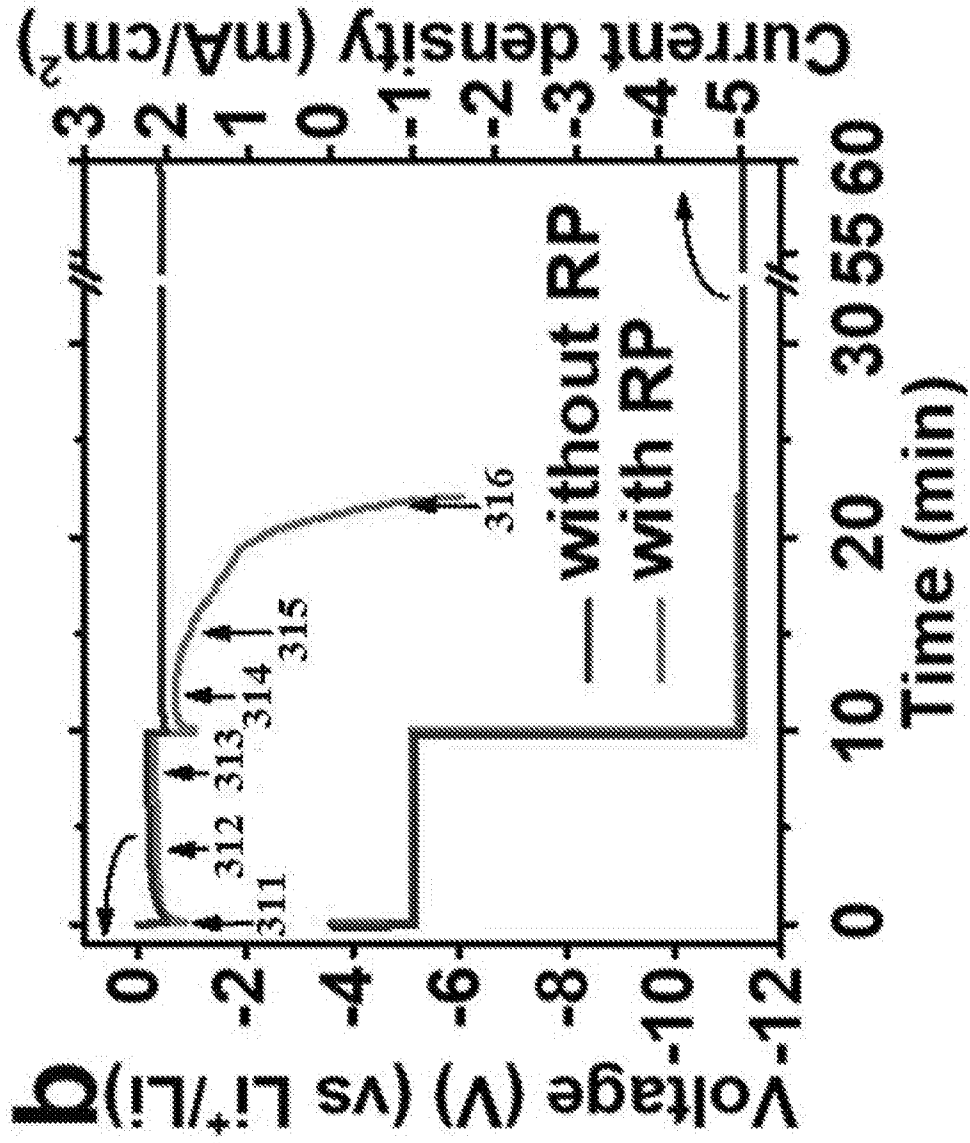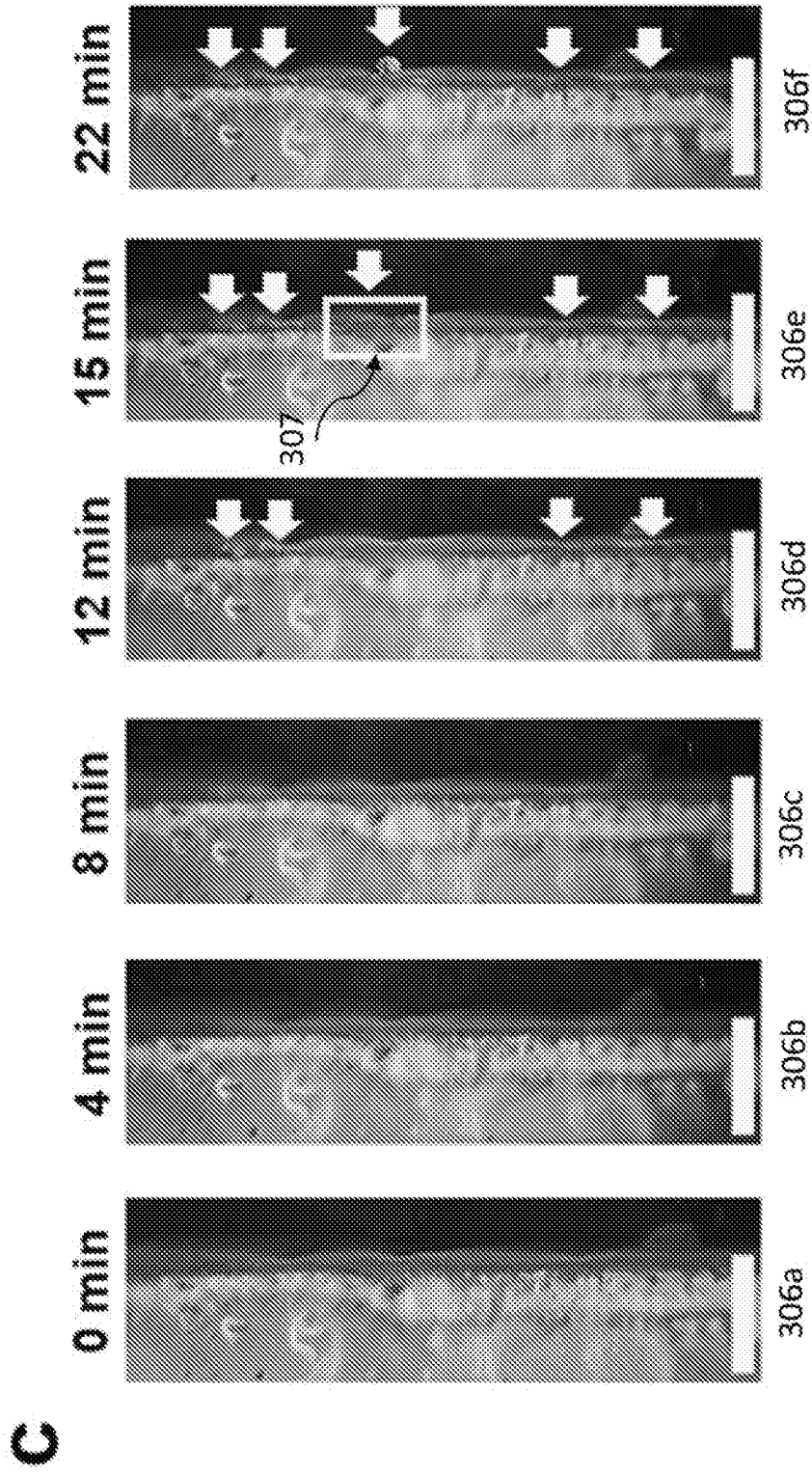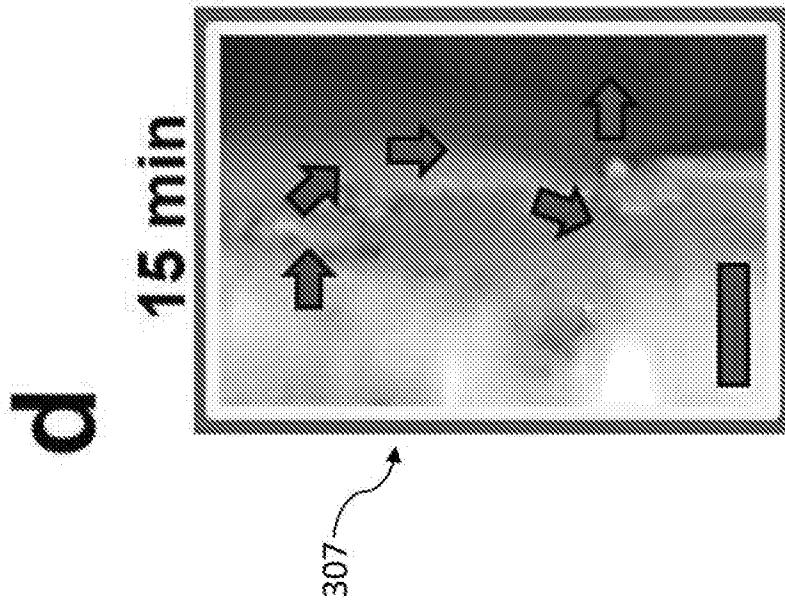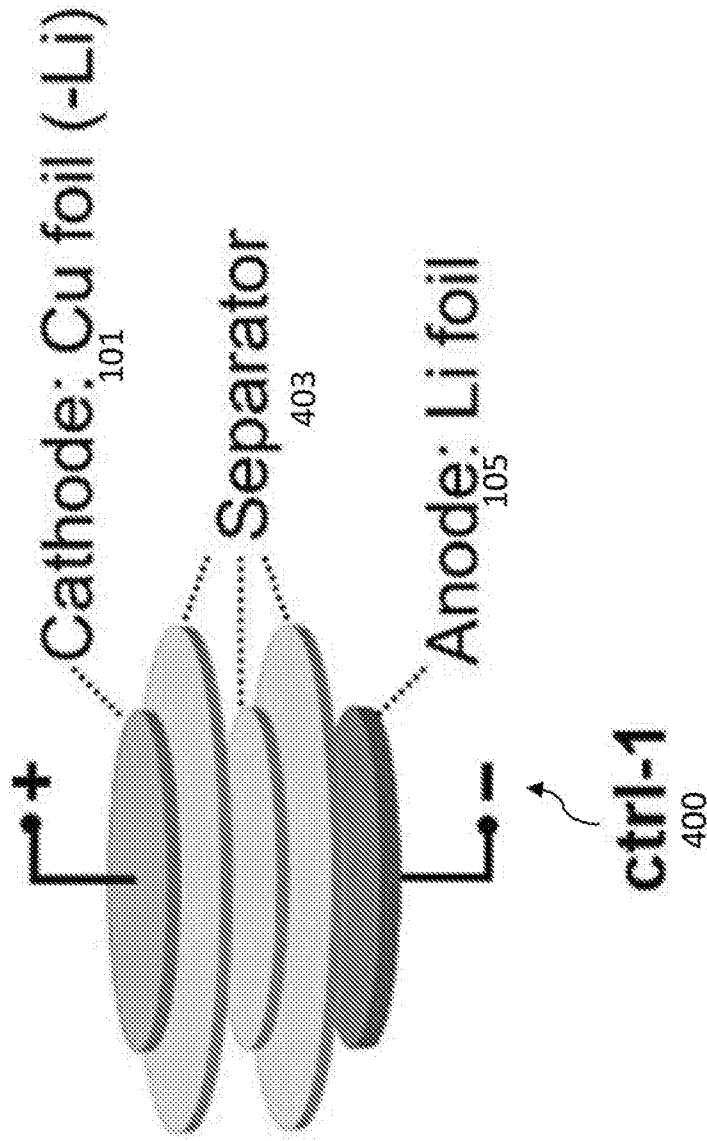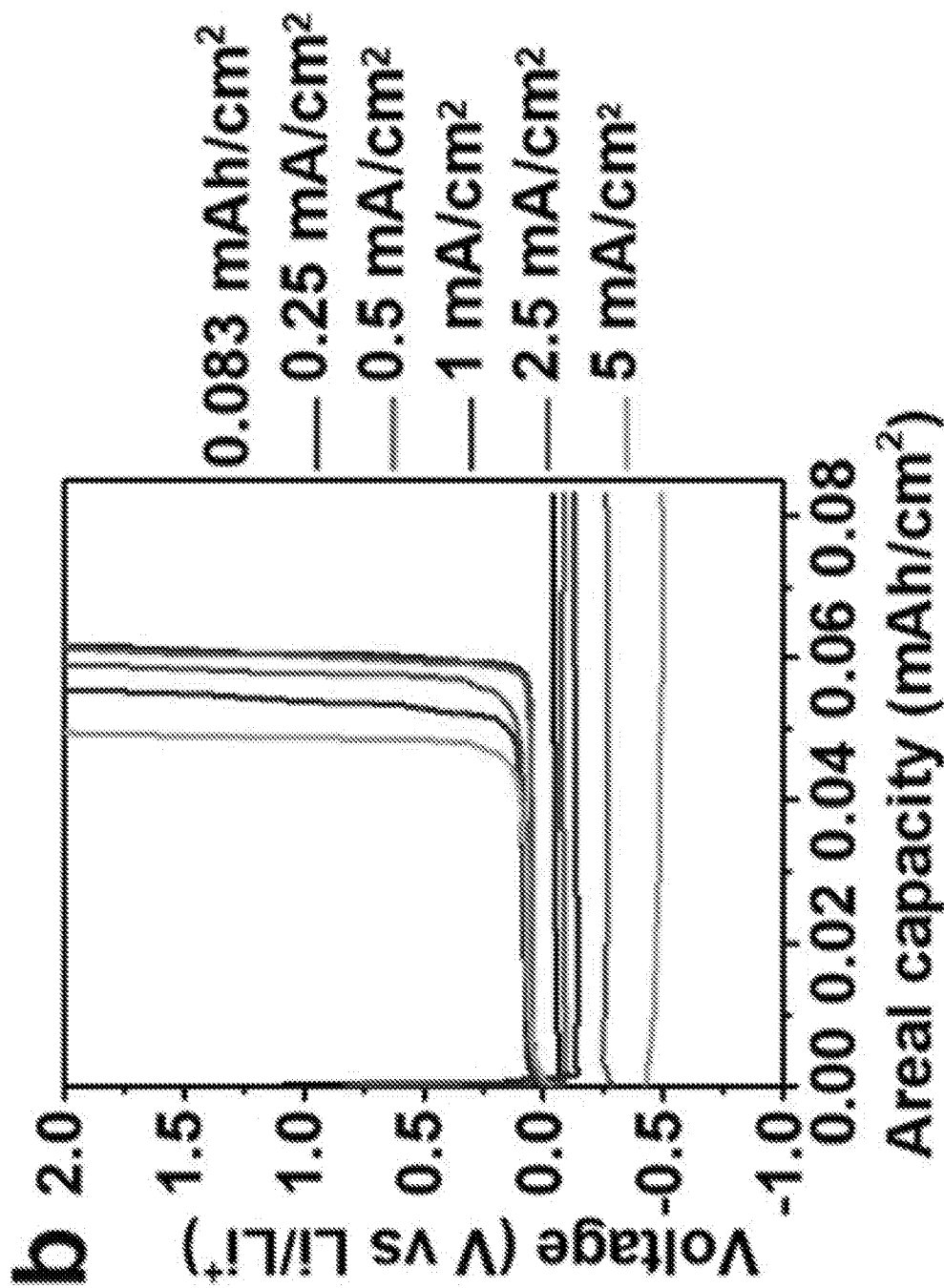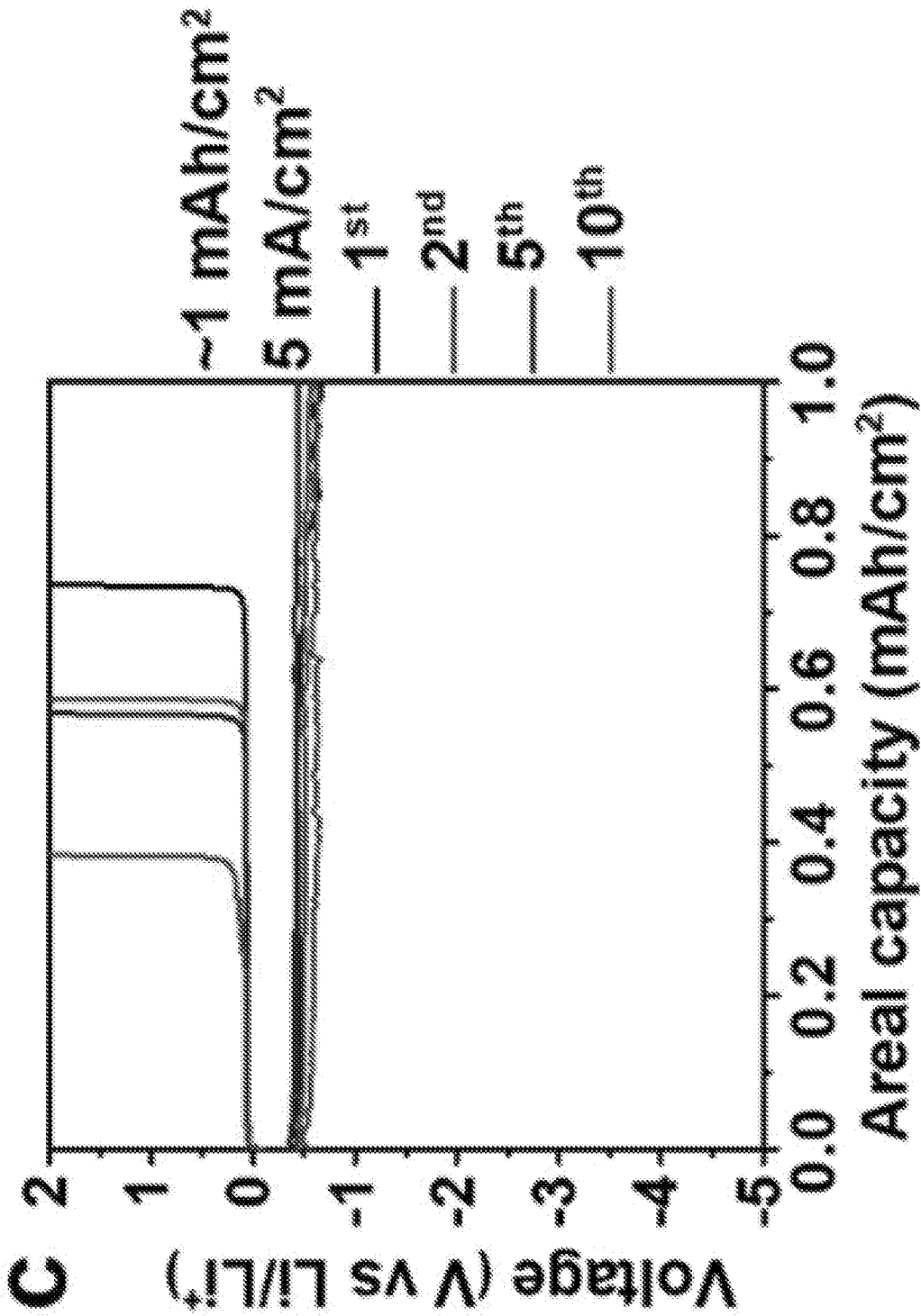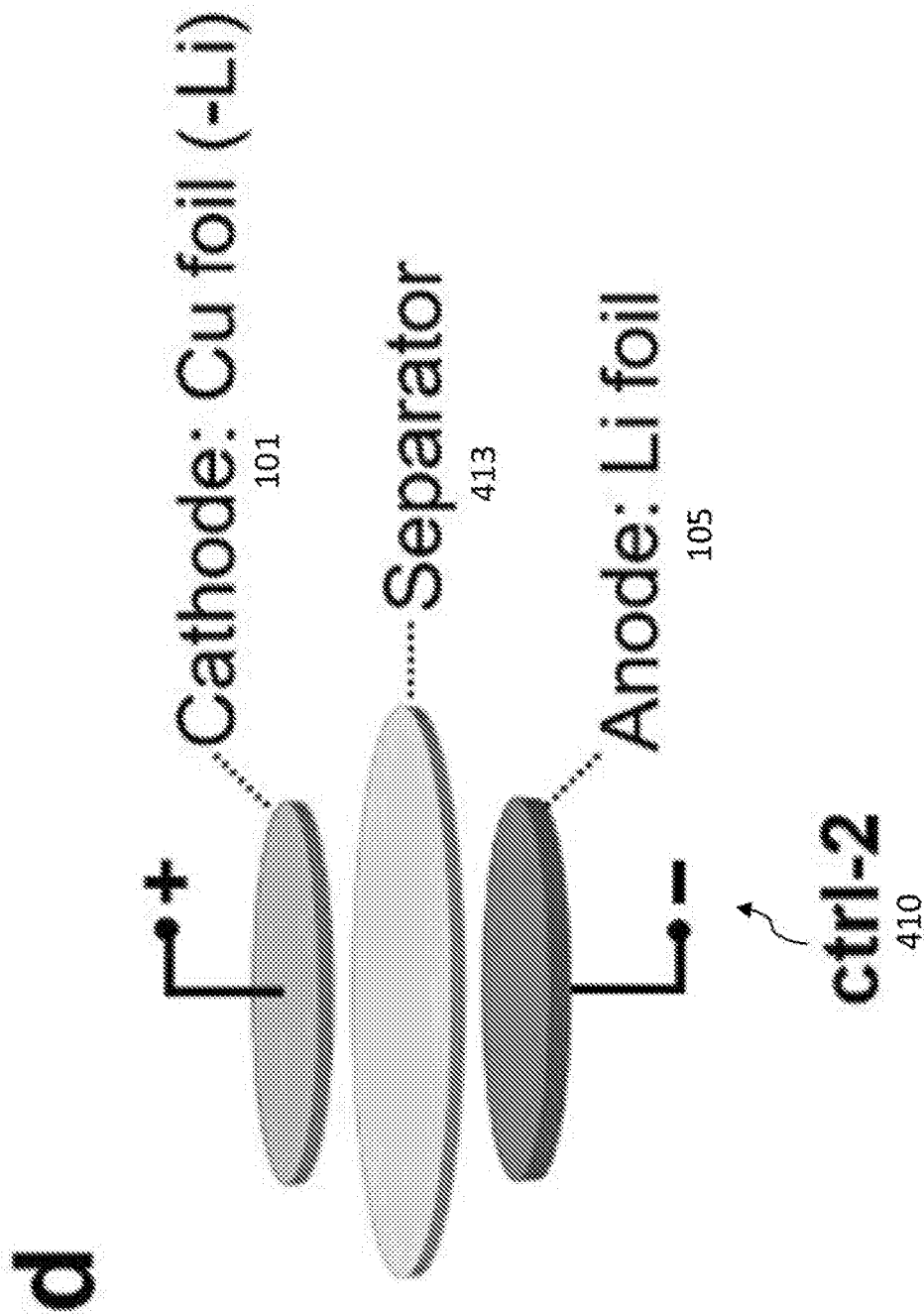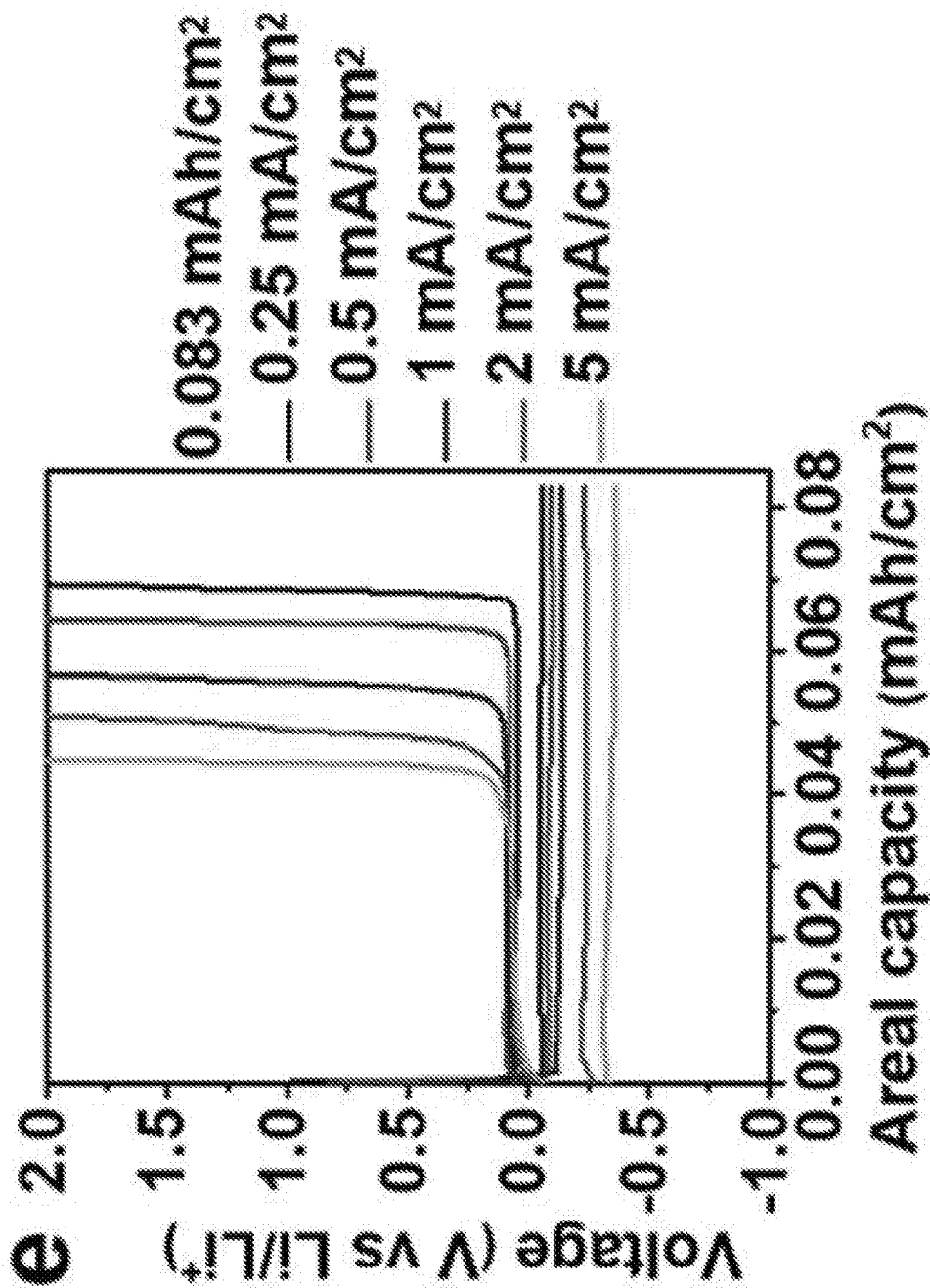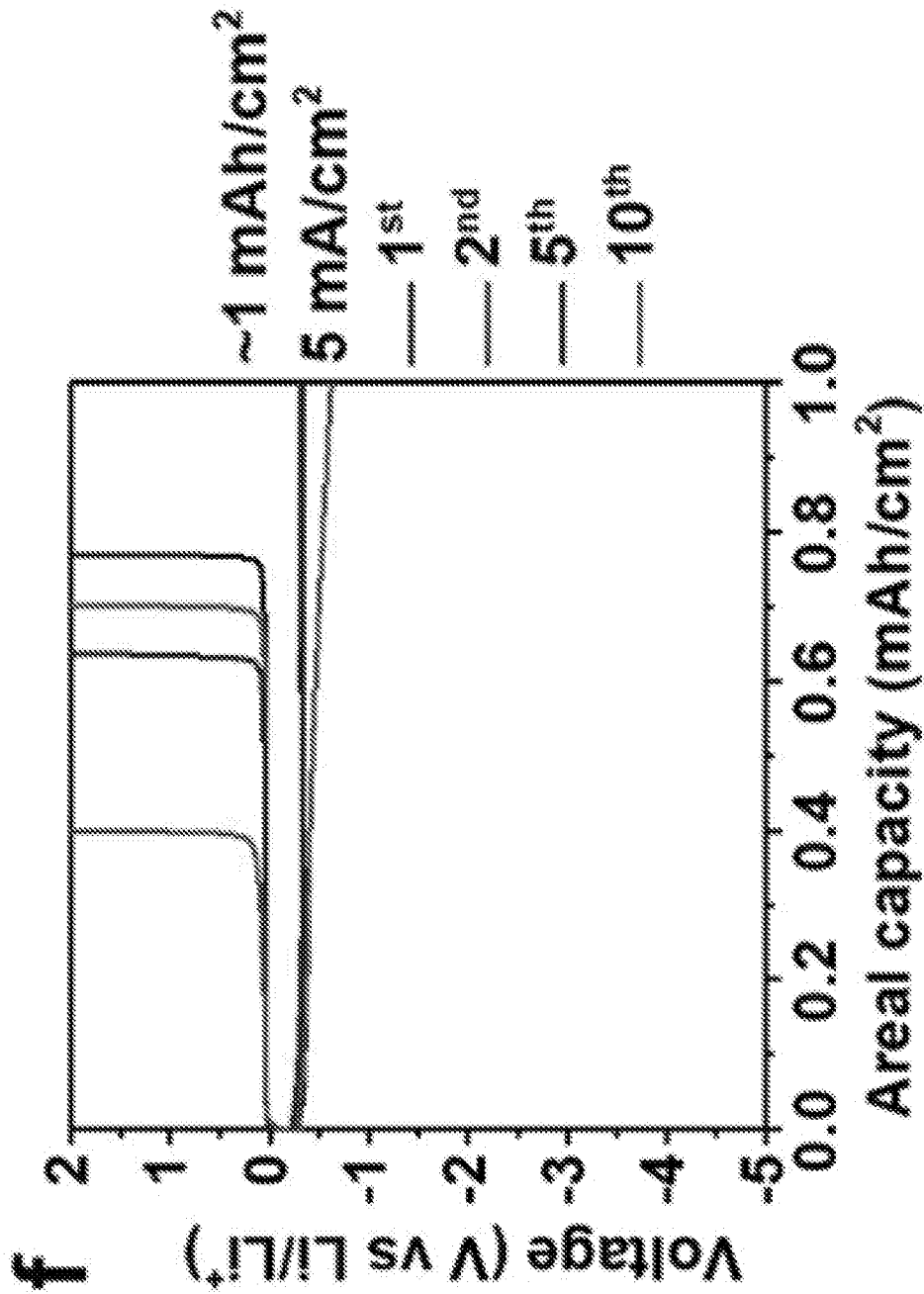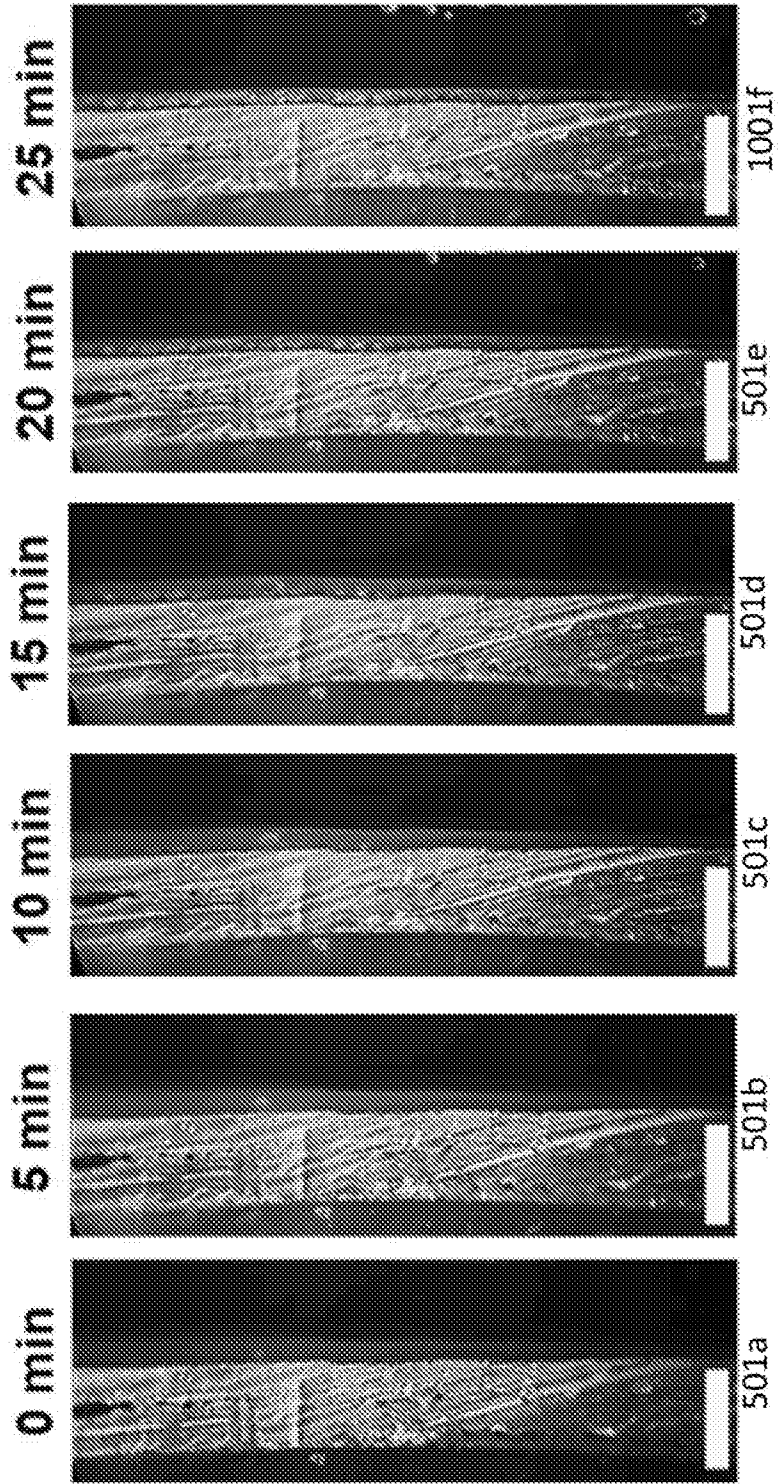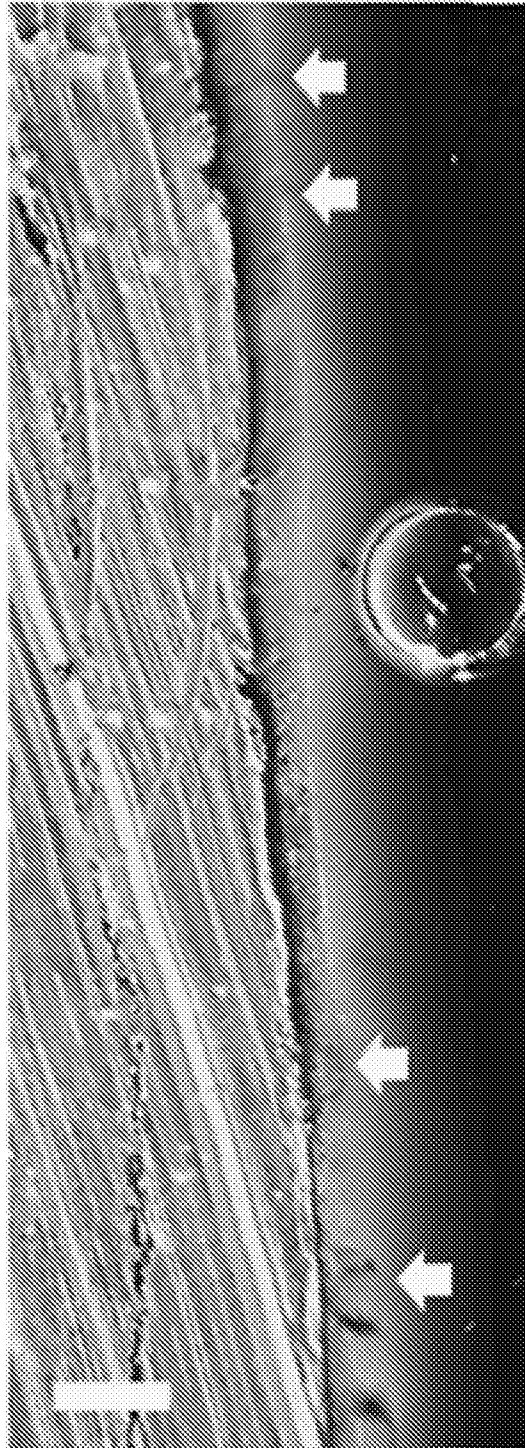
FIG. 5B
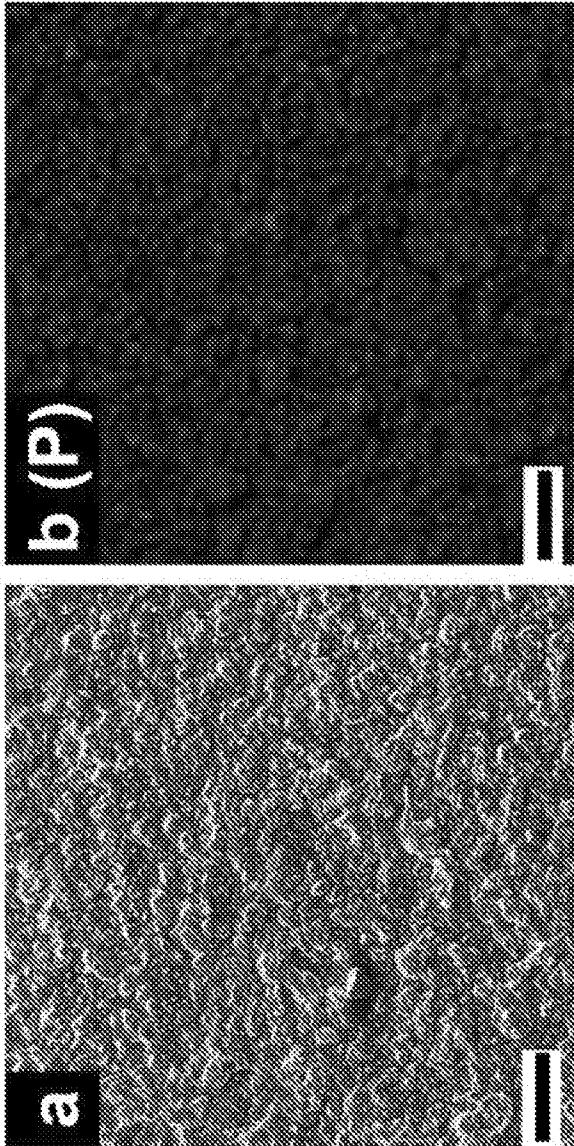
FIG. 6A

FIG. 6B
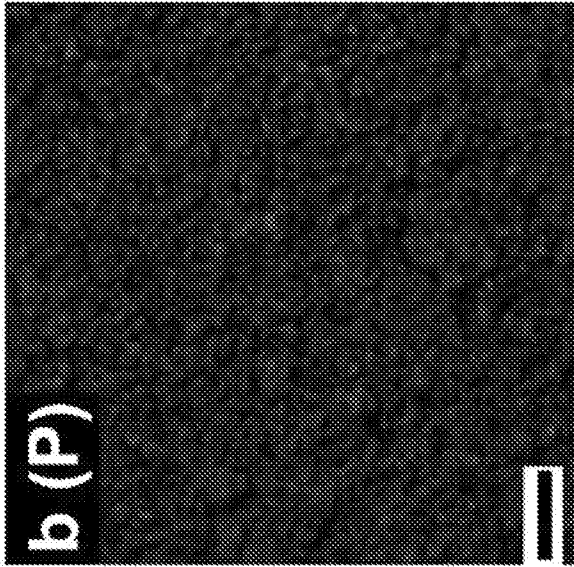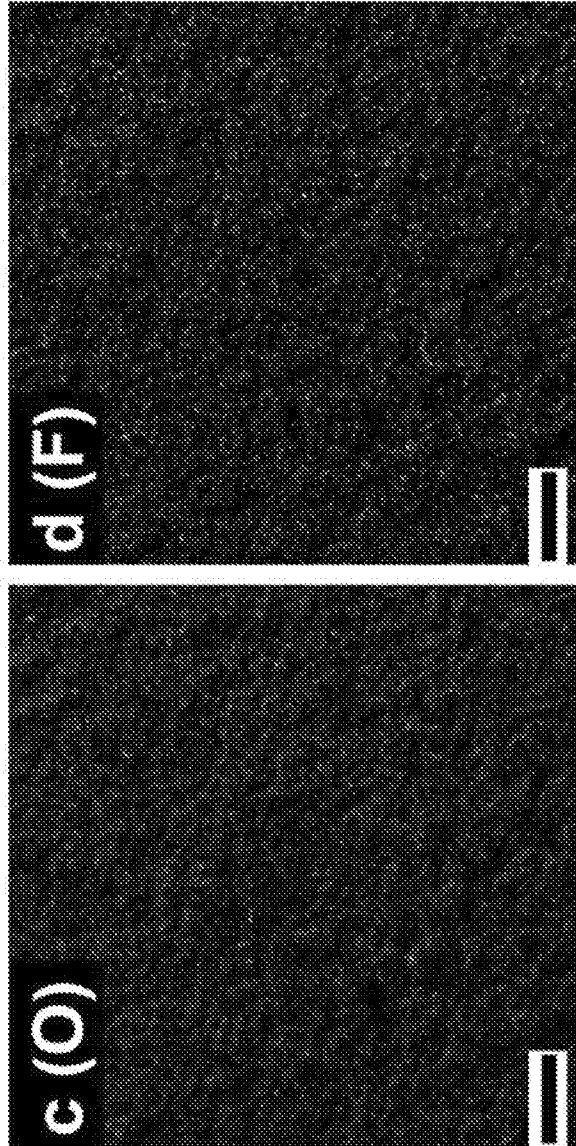
FIG. 6C
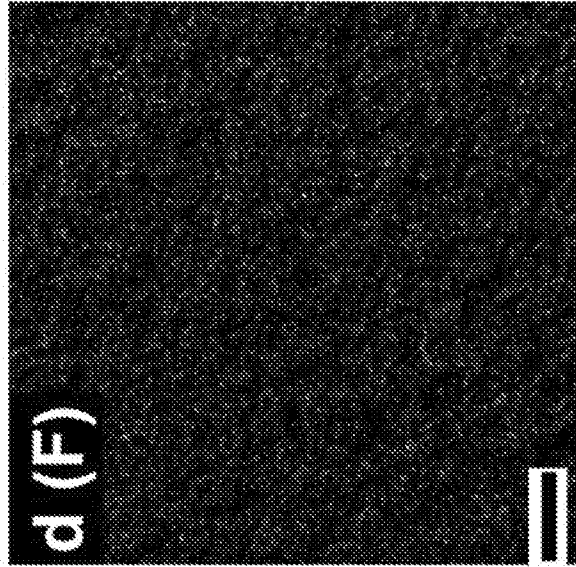
FIG. 6D

FIG. 7A

FIG. 7B

FIG. 7C
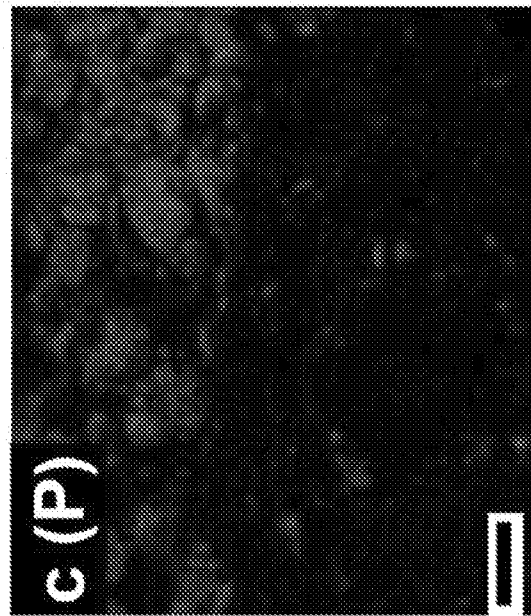
FIG. 7D
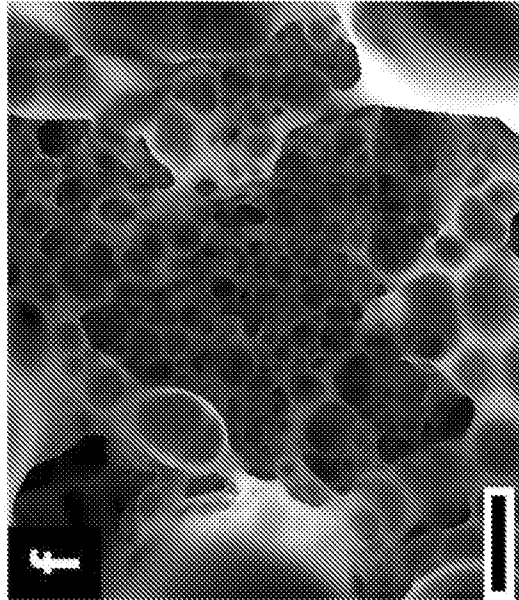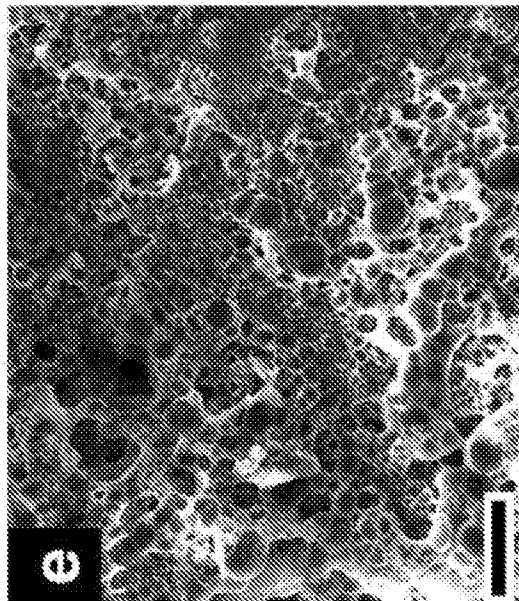
FIG. 7F

FIG. 7E

FIG. 8C

FIG. 8E

FIG. 8B

FIG. 8D

FIG. 8A

g (P)

FIG. 8G

i (F)

FIG. 8I

f

FIG. 8F

h (O)

FIG. 8H

a

Anode: Li foil
901

RP-coated
separator
903

Cathode: SC
905

Separator
902

Separator
(optional)
904

−

+

P-fc (full cell)
900

FIG. 9A

FIG. 9B

C

Anode: Li foil
901

Separator
907

Cathode: SC
905

−

+
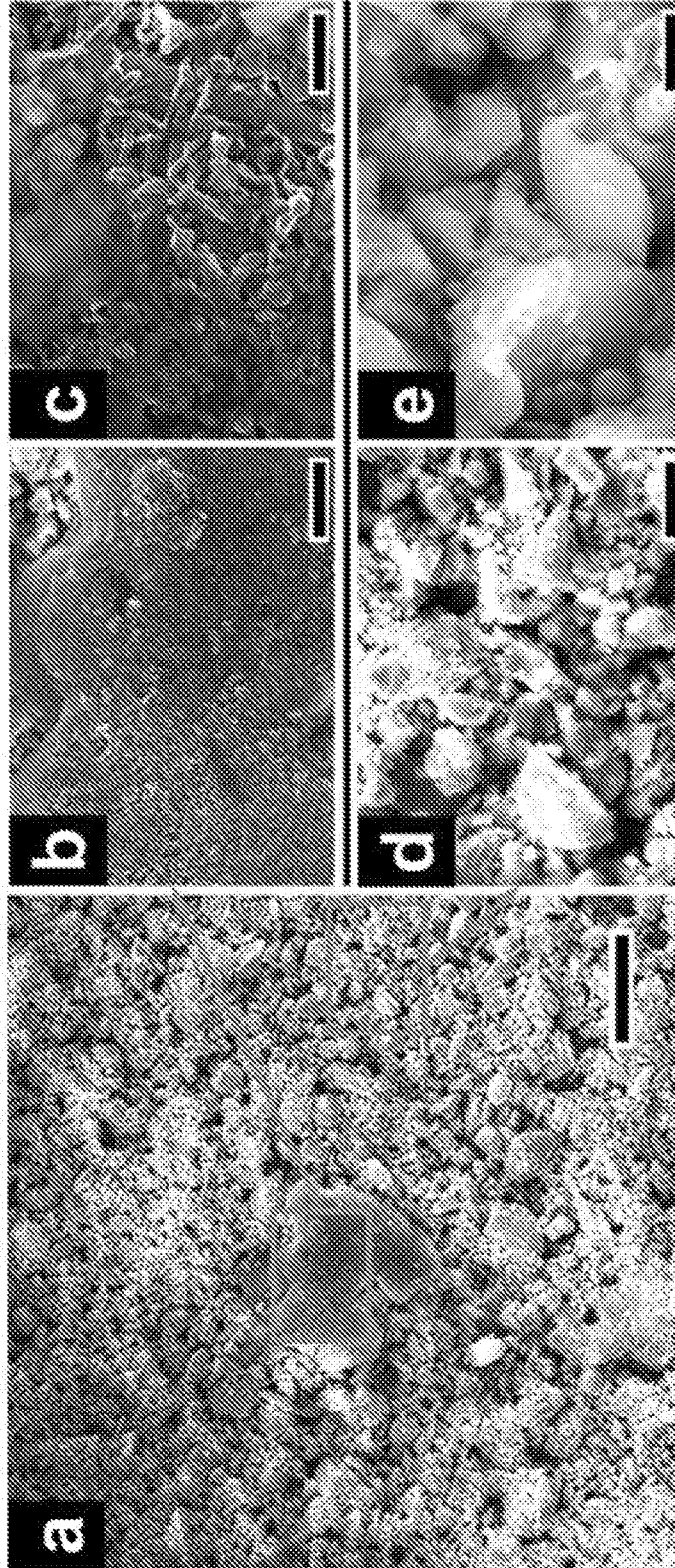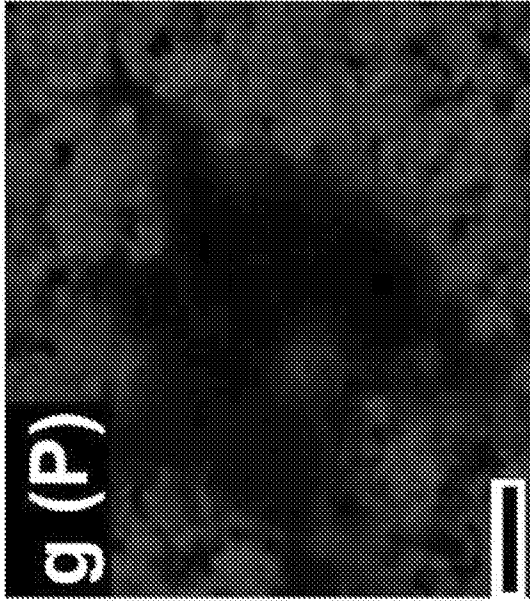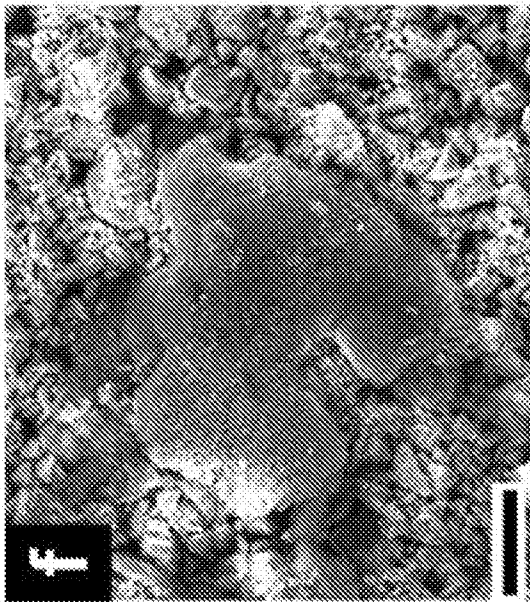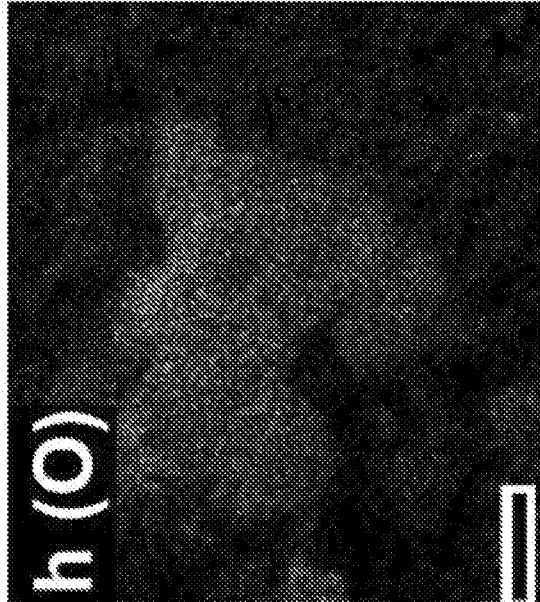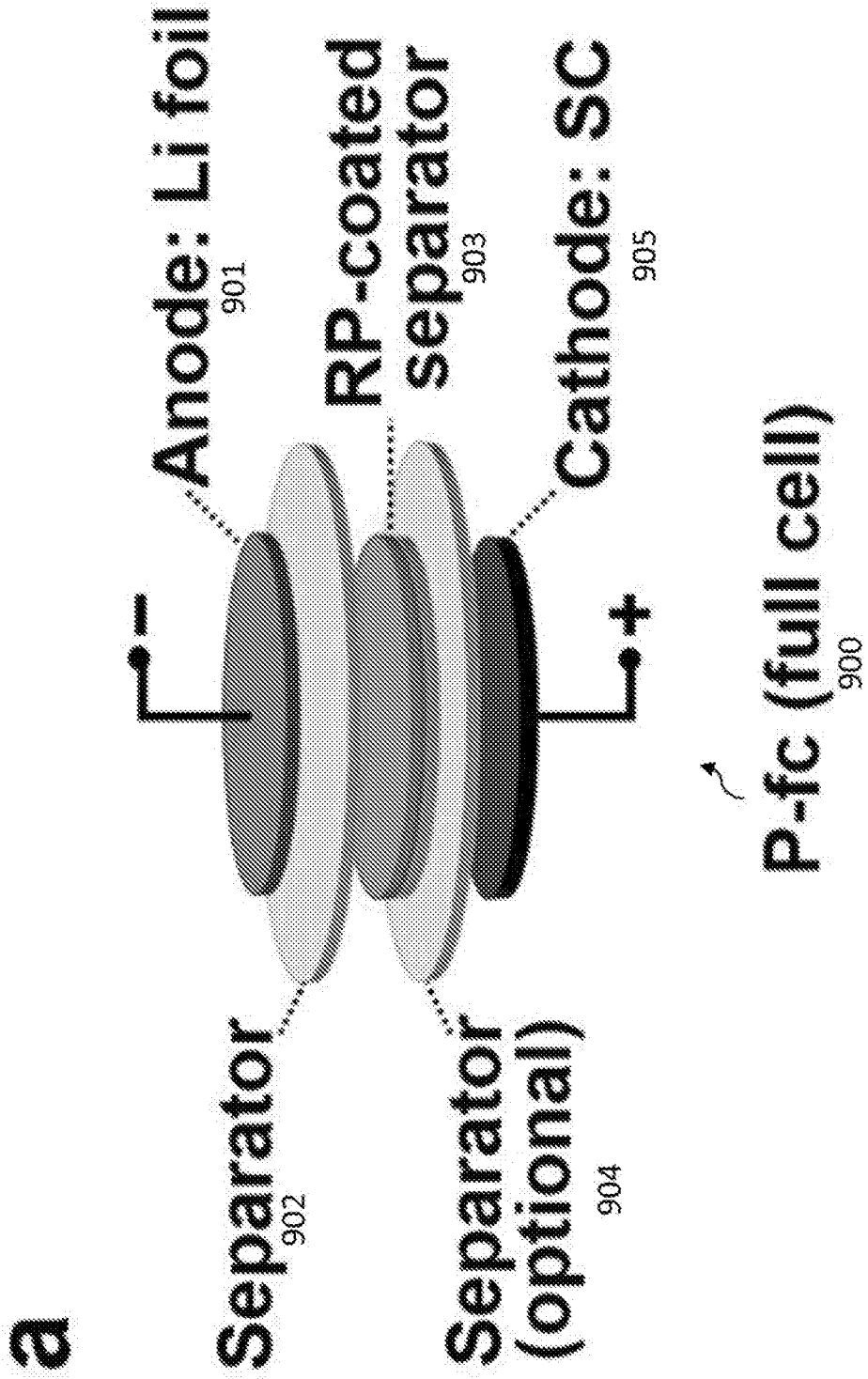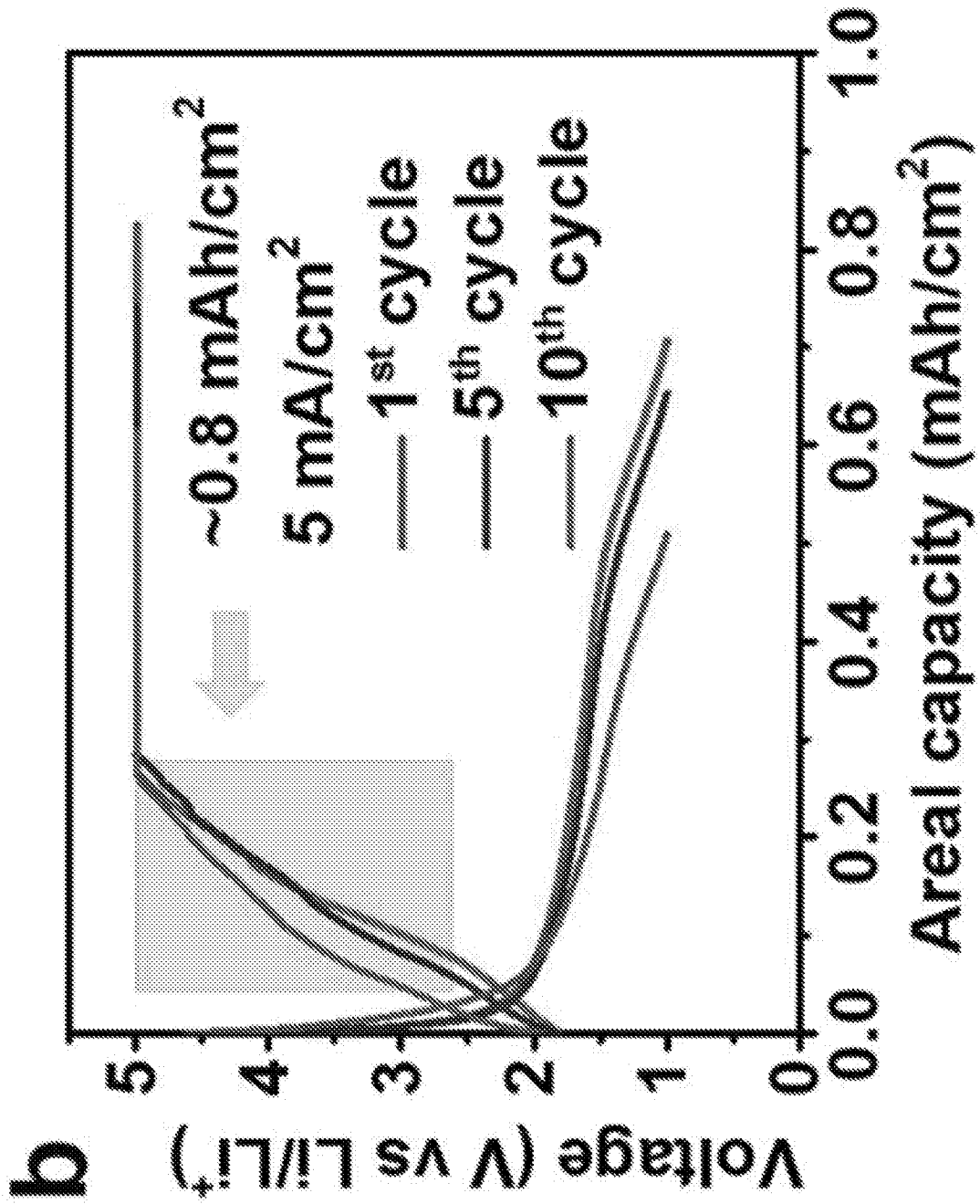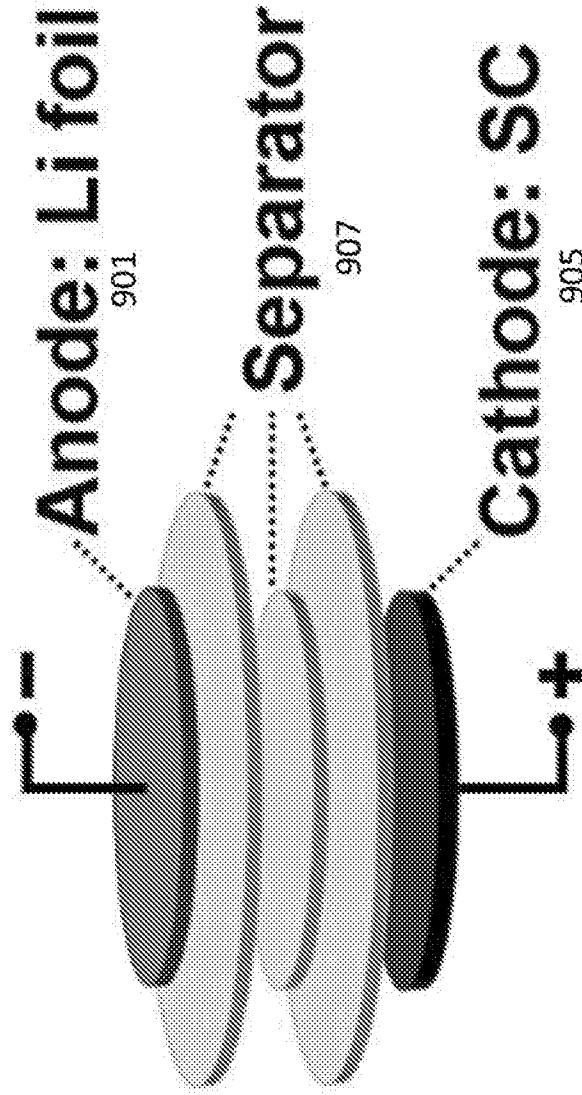
ctrl-3
906

FIG. 9C
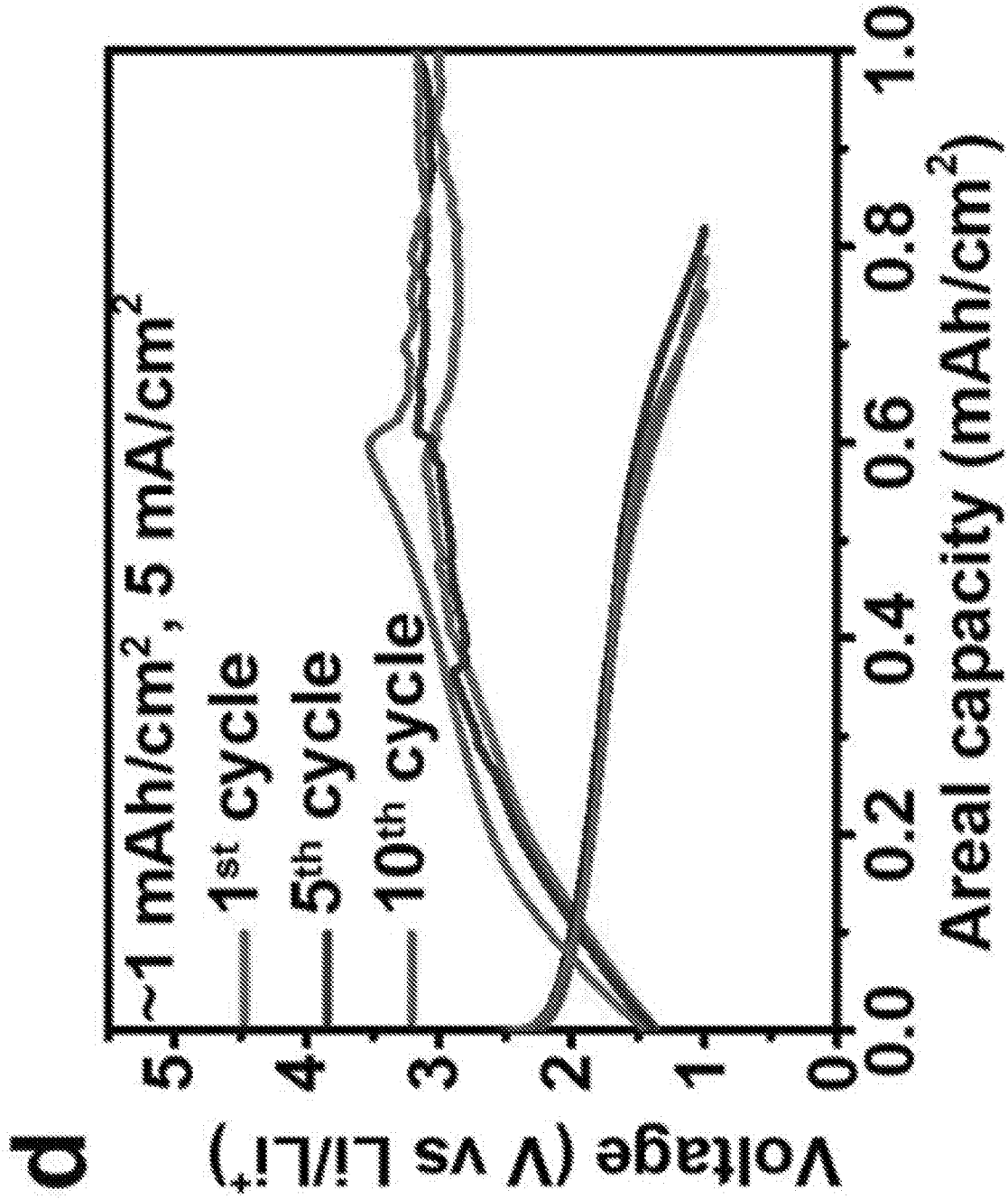
FIG. 9D
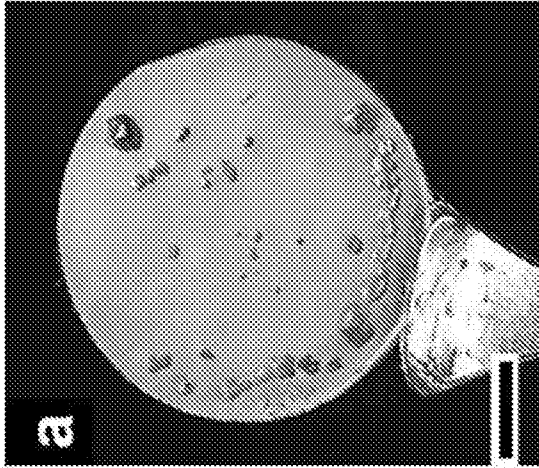
FIG. 10A
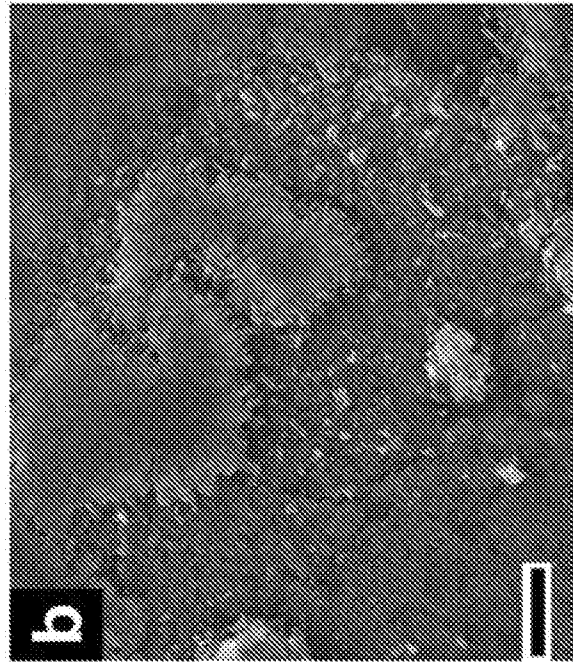
FIG. 10B

FIG. 10C

FIG. 11A

FIG. 11B

FIG. 11C

FIG. 11D

FIG. 11E

FIG. 11F

32/44
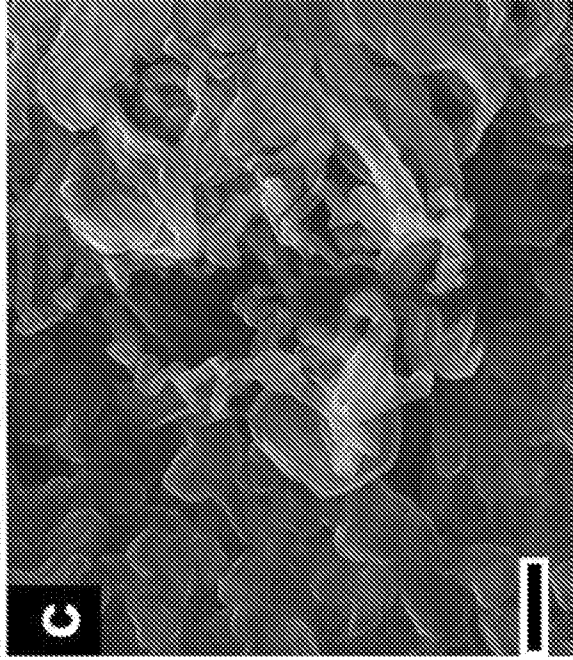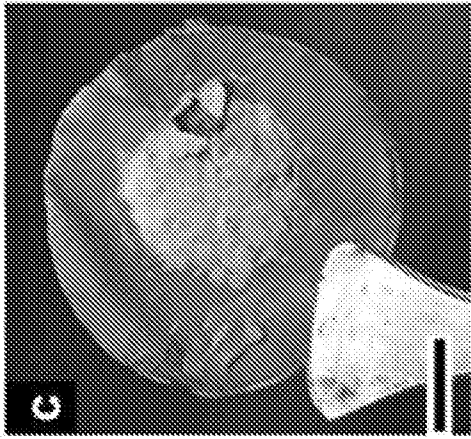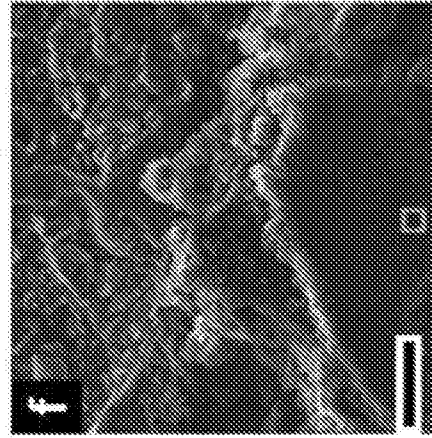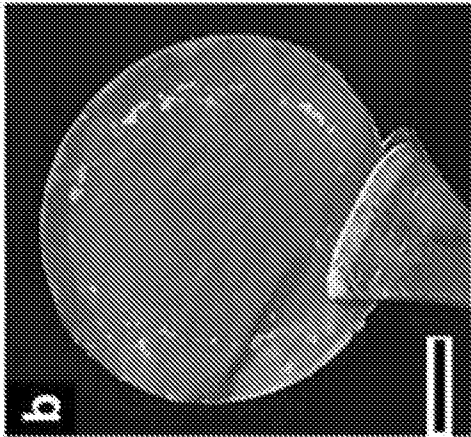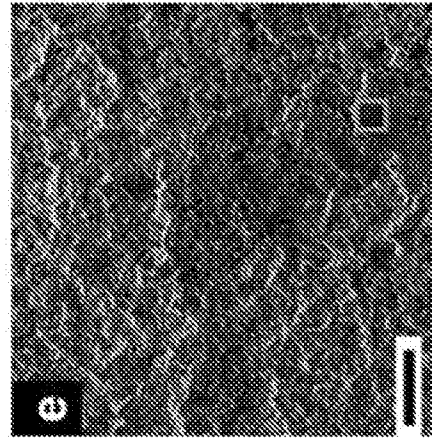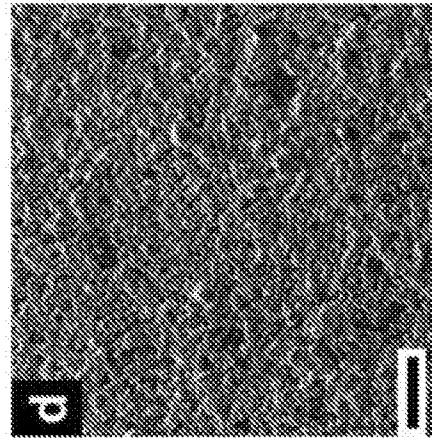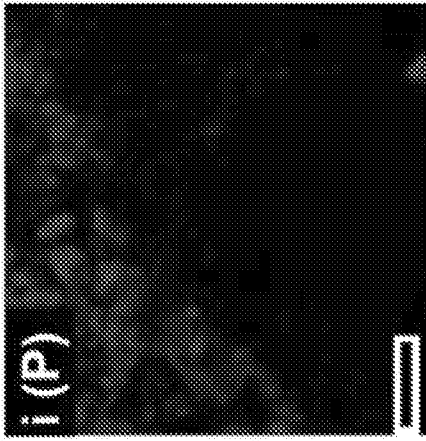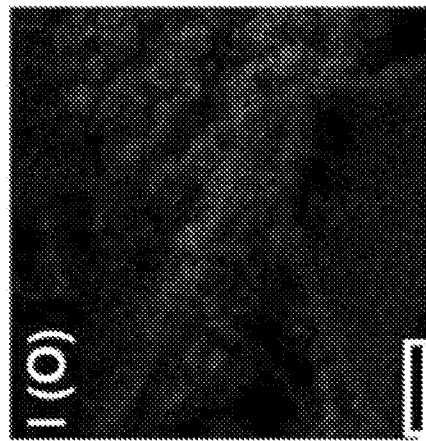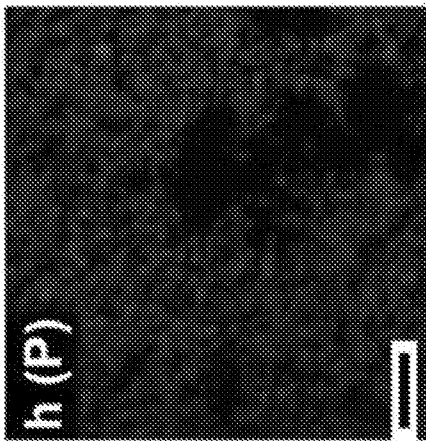
FIG. 11I

FIG. 11L

FIG. 11H
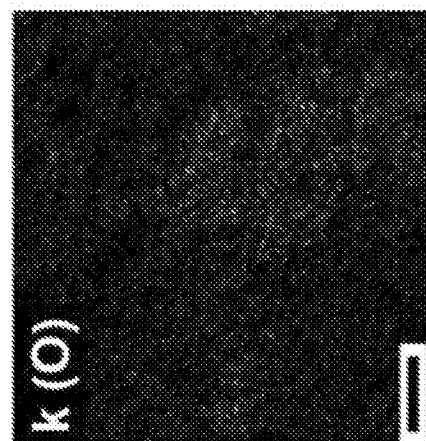
FIG. 11K
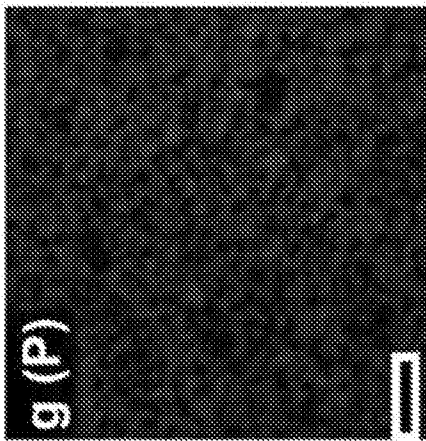
FIG. 11G
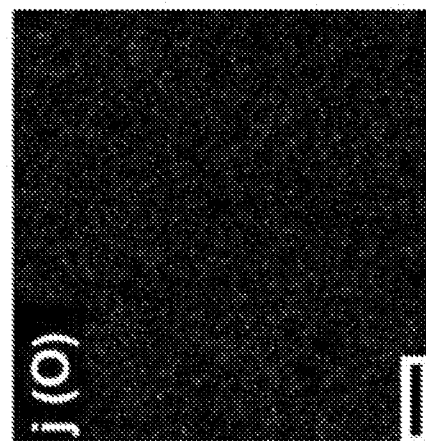
FIG. 11J
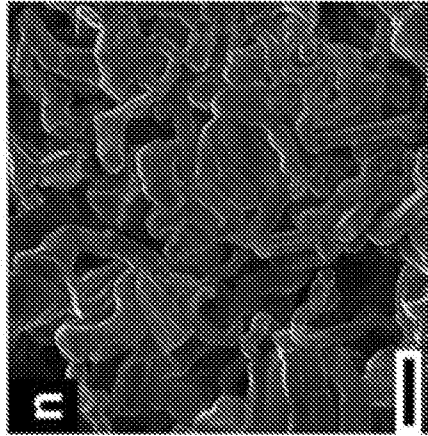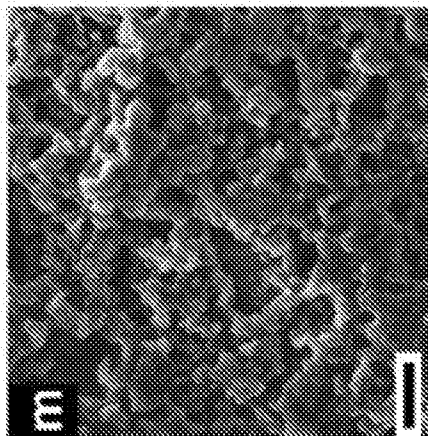
FIG. 11N

FIG. 11M

FIG. 12A

FIG. 12B

FIG. 12C

a

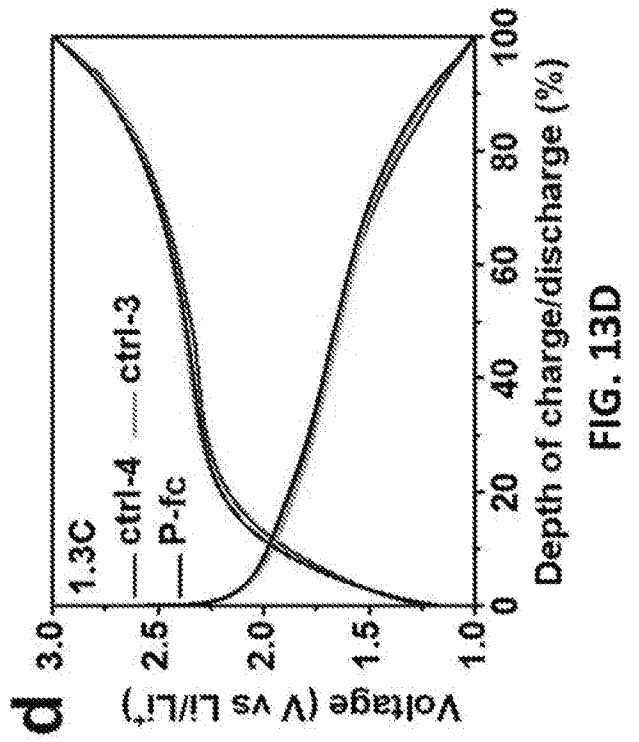Anode: Li foil
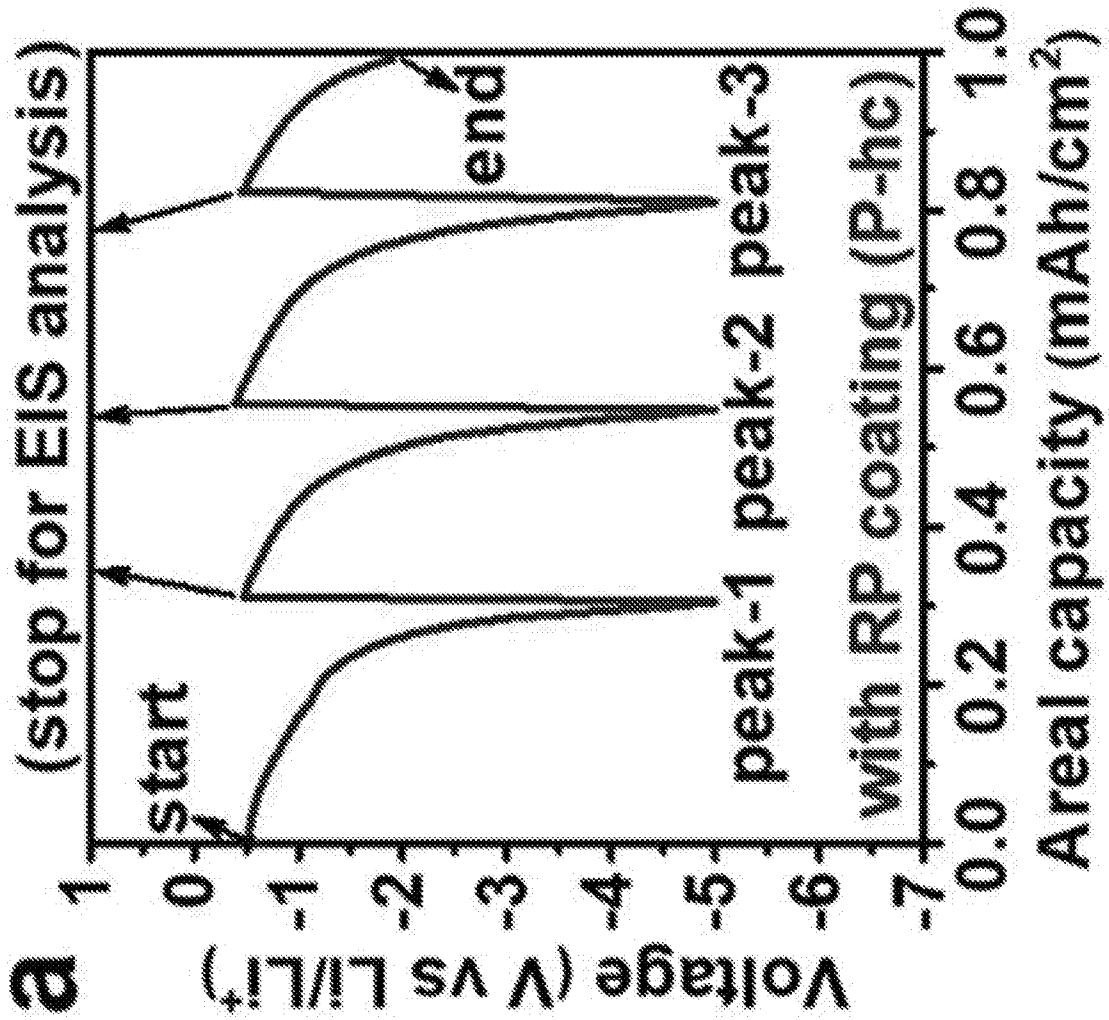301

Separator
307

Cathode: SC
305

ctrl-4
1300
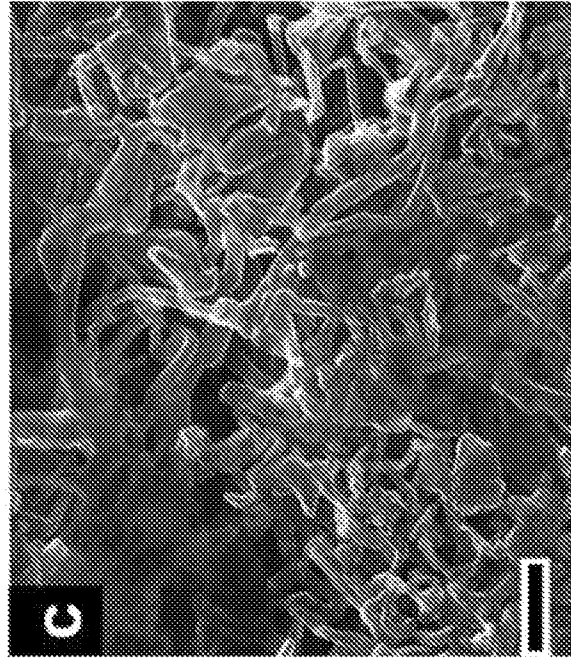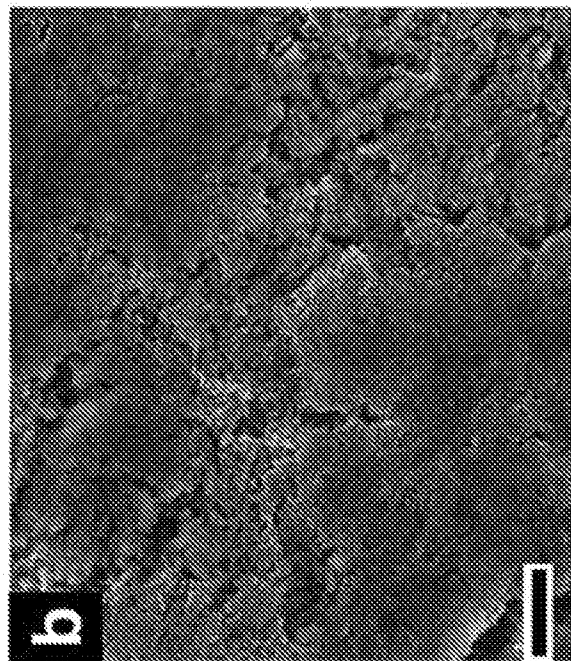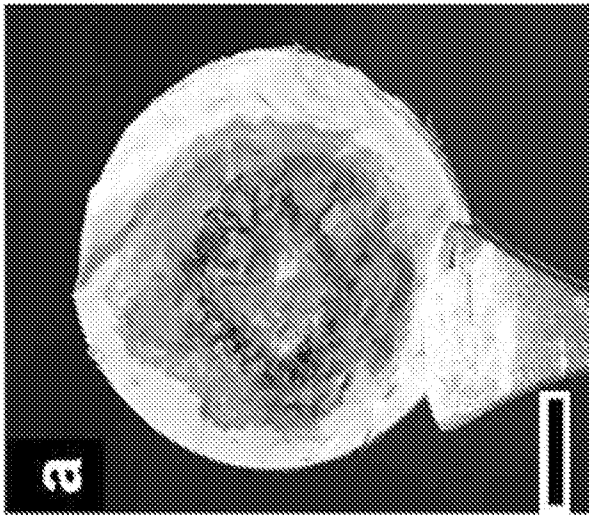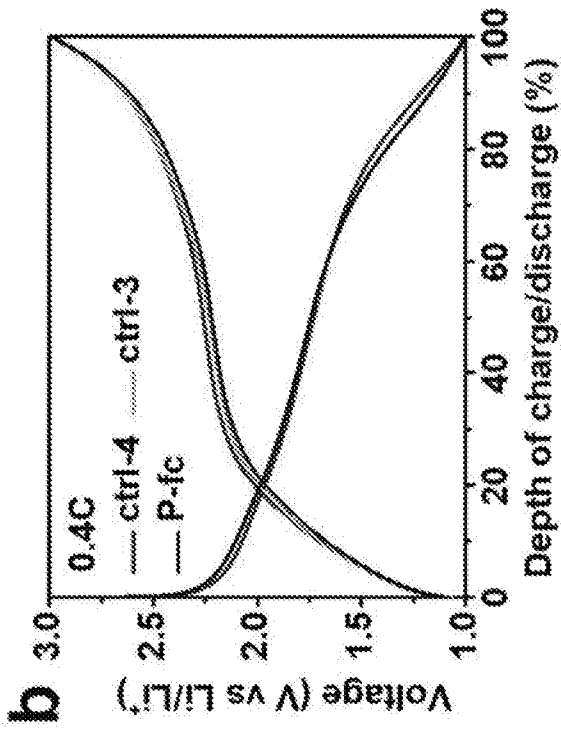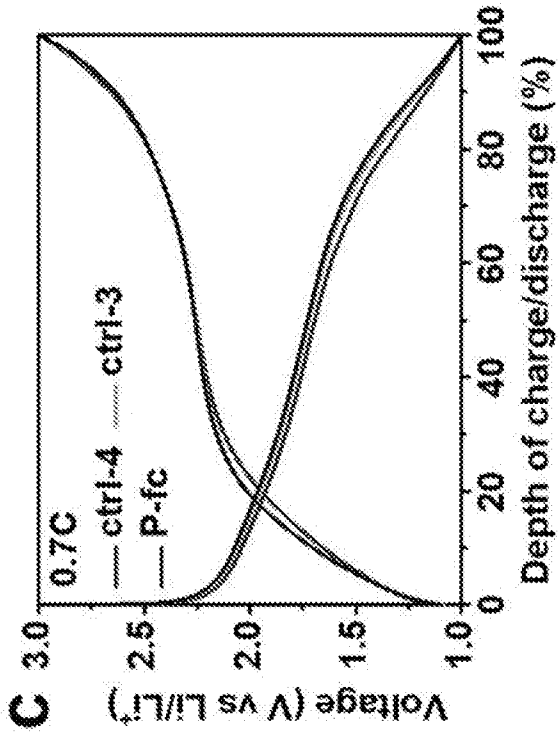
FIG. 13A

FIG. 13C

FIG. 13B

FIG. 13D
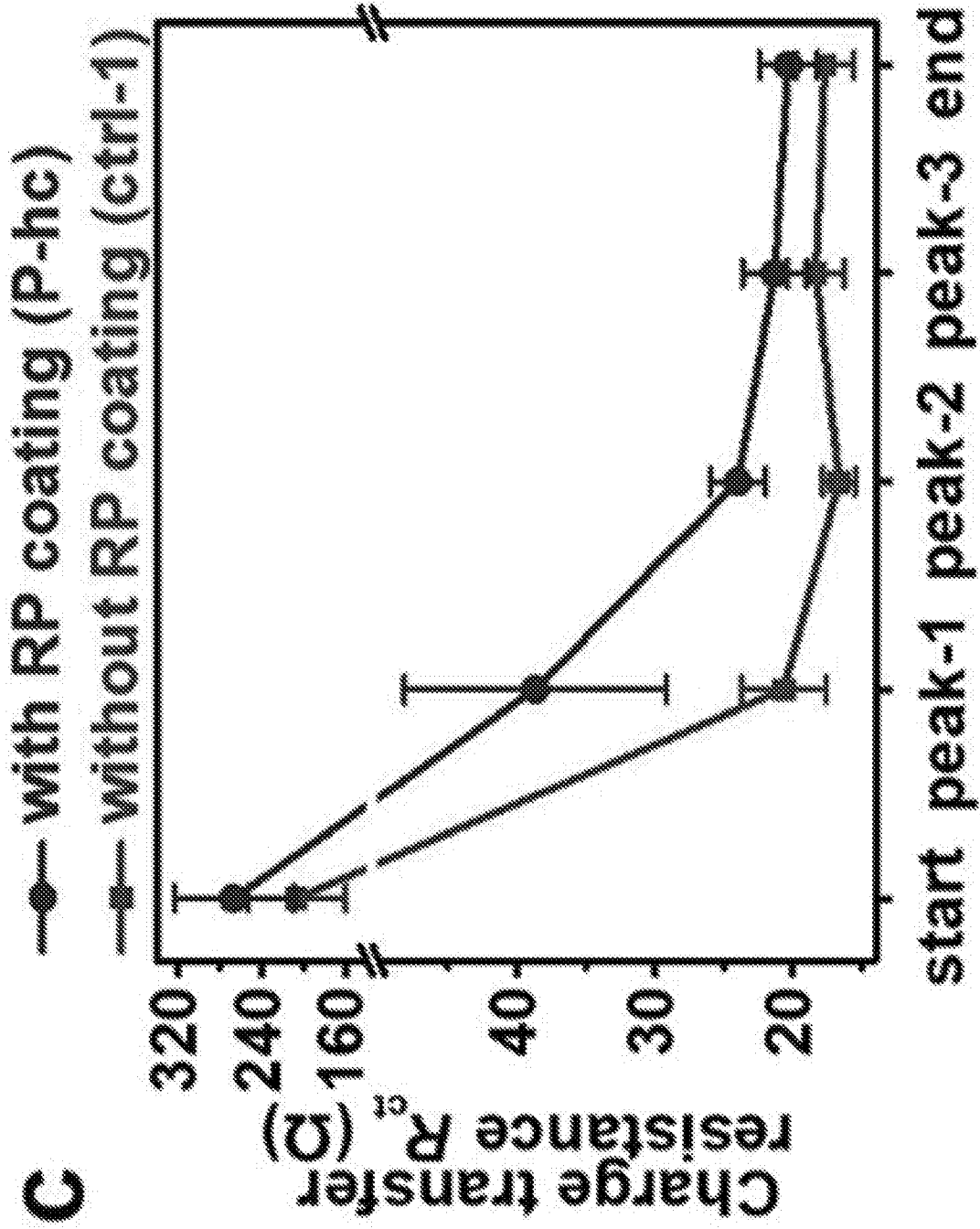
FIG. 14A

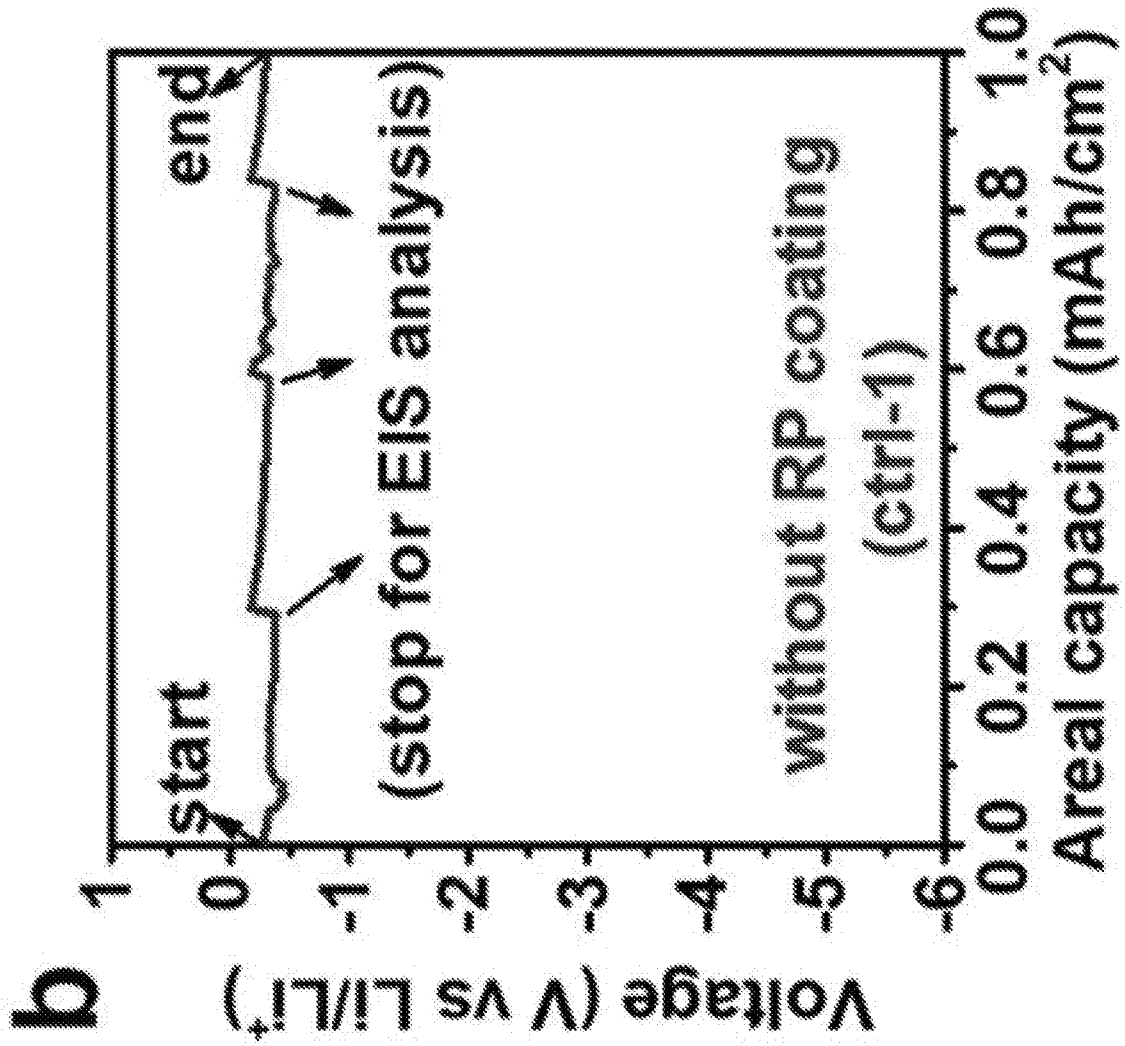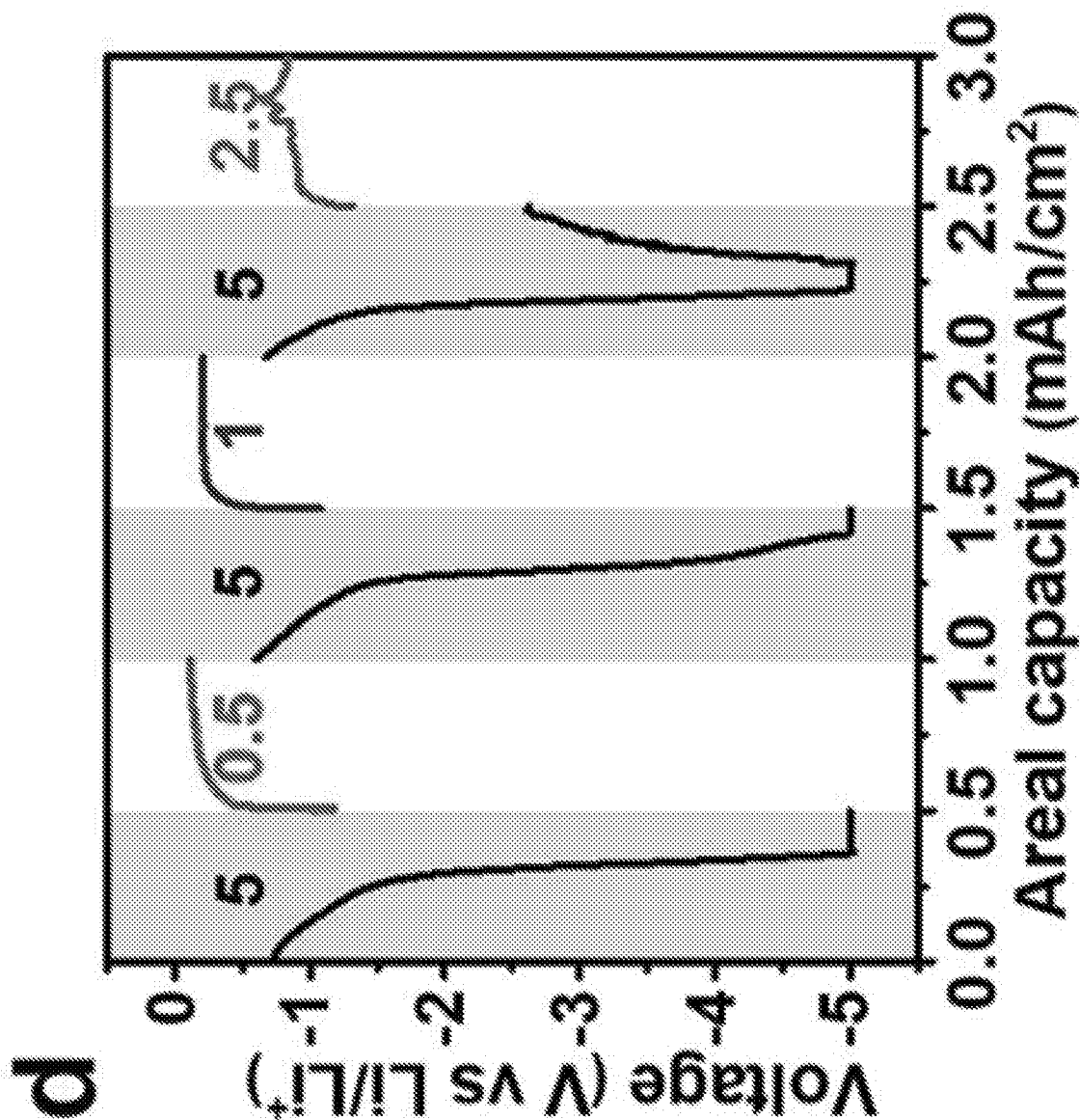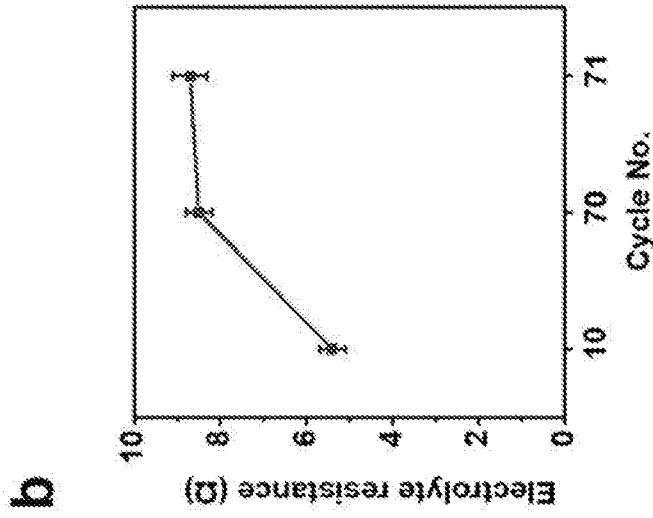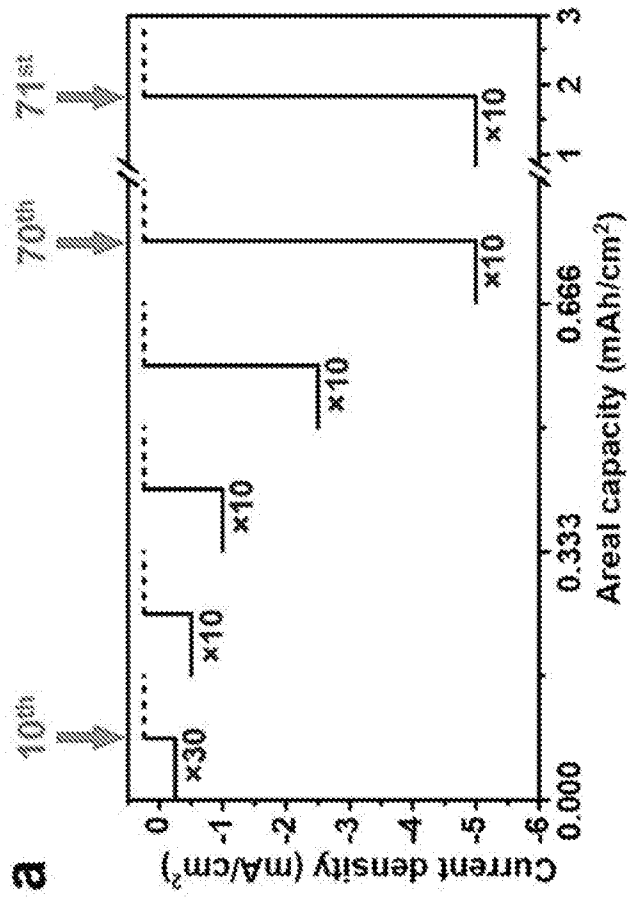FIG. 14B

FIG. 14C

FIG. 14D
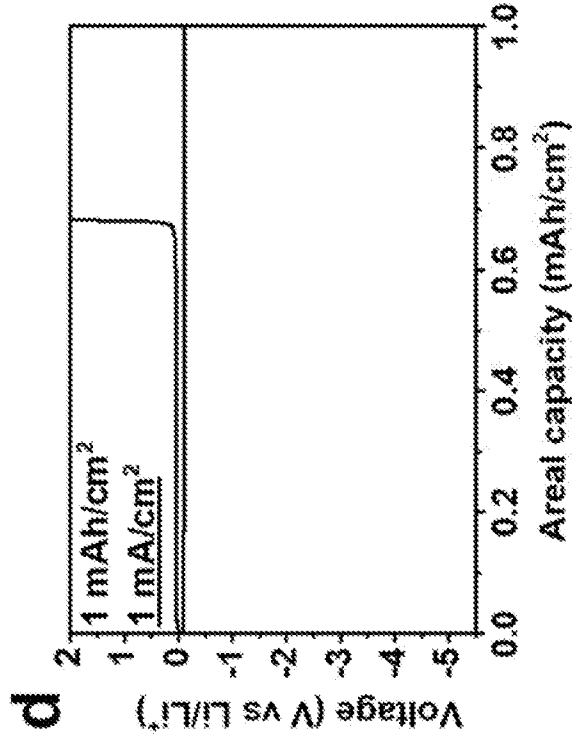
FIG. 14E

42/44

FIG. 15A
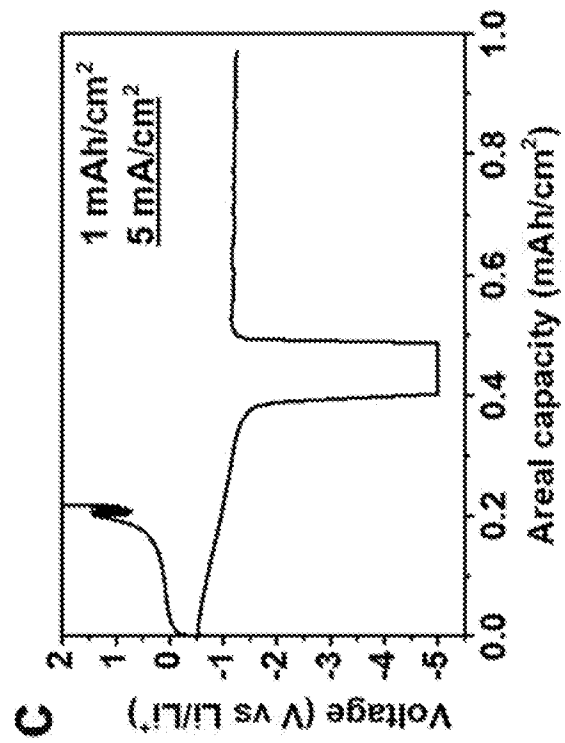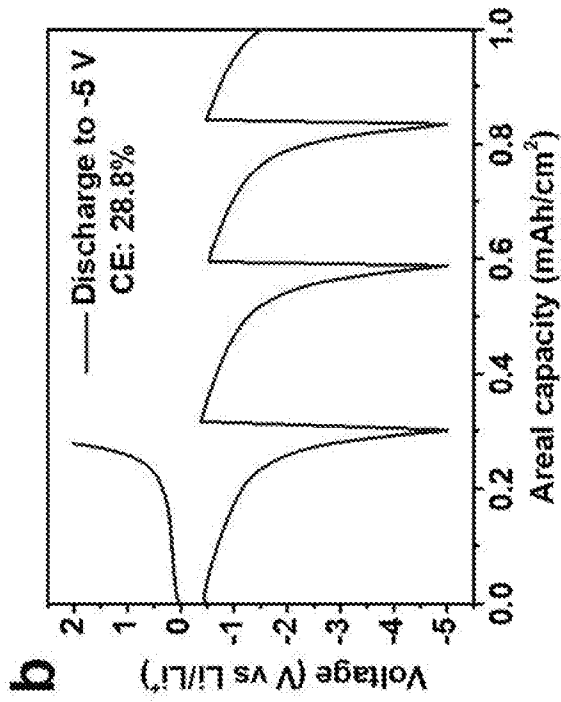
FIG. 15B

43/44

FIG. 15D

FIG. 15C

FIG. 16A
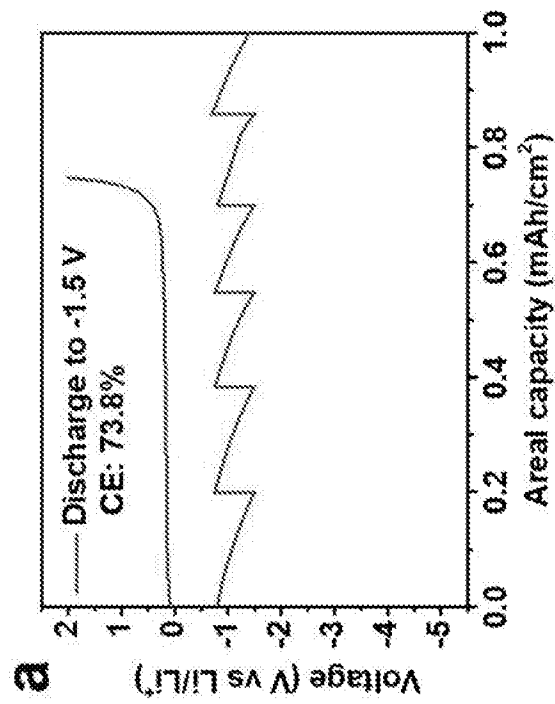
FIG. 16B

INTERNATIONAL SEARCH REPORT

A. CLASSIFICATION OF SUBJECT MATTER

INV. H01M2/16   H01M2/34   H01M4/38   H01M10/052   H01M10/42
H01M10/44   H01M10/48

ADD.

According to International Patent Classification (IPC) or to both national classification and IPC

B. FIELDS SEARCHED

Minimum documentation searched (classification system followed by classification symbols)

H01M

Documentation searched other than minimum documentation to the extent that such documents are included in the fields searched

Electronic data base consulted during the international search (name of data base and, where practicable, search terms used)

EPO-Internal, WPI Data

C. DOCUMENTS CONSIDERED TO BE RELEVANT

Category*	Citation of document, with indication, where appropriate, of the relevant passages	Relevant to claim No.
X	EP 3 151 328 A1 (W L GORE & ASS CO LTD [JP]) 5 April 2017 (2017-04-05) abstract paragraphs [0033] - [0039], [0094] -----	1-3
X	WO 2018/045226 A1 (UNIV RICE WILLIAM M [US]) 8 March 2018 (2018-03-08) abstract paragraphs [0005] - [0007], [0107], [0108], [0141], [0152] -----	1-3

☐ Further documents are listed in the continuation of Box C.   ☒ See patent family annex.

* Special categories of cited documents :

"A" document defining the general state of the art which is not considered to be of particular relevance

"E" earlier application or patent but published on or after the international filing date

"L" document which may throw doubts on priority claim(s) or which is cited to establish the publication date of another citation or other special reason (as specified)

"O" document referring to an oral disclosure, use, exhibition or other means

"P" document published prior to the international filing date but later than the priority date claimed

"T" later document published after the international filing date or priority date and not in conflict with the application but cited to understand the principle or theory underlying the invention

"X" document of particular relevance; the claimed invention cannot be considered novel or cannot be considered to involve an inventive step when the document is taken alone

"Y" document of particular relevance; the claimed invention cannot be considered to involve an inventive step when the document is combined with one or more other such documents, such combination being obvious to a person skilled in the art

"&" document member of the same patent family

Date of the actual completion of the international search	Date of mailing of the international search report
16 September 2019	15/11/2019

Name and mailing address of the ISA/	Authorized officer
European Patent Office, P.B. 5818 Patentlaan 2 NL - 2280 HV Rijswijk Tel. (+31-70) 340-2040, Fax: (+31-70) 340-3016	Lange, Ronny

1

Form PCT/ISA/210 (second sheet) (April 2005)

INTERNATIONAL SEARCH REPORT

Box No. II   Observations where certain claims were found unsearchable (Continuation of item 2 of first sheet)

This international search report has not been established in respect of certain claims under Article 17(2)(a) for the following reasons:

1. ☐ Claims Nos.:
because they relate to subject matter not required to be searched by this Authority, namely:

2. ☐ Claims Nos.:
because they relate to parts of the international application that do not comply with the prescribed requirements to such an extent that no meaningful international search can be carried out, specifically:

3. ☐ Claims Nos.:
because they are dependent claims and are not drafted in accordance with the second and third sentences of Rule 6.4(a).

Box No. III   Observations where unity of invention is lacking (Continuation of item 3 of first sheet)

This International Searching Authority found multiple inventions in this international application, as follows:

    see additional sheet

1. ☐ As all required additional search fees were timely paid by the applicant, this international search report covers all searchable claims.

2. ☐ As all searchable claims could be searched without effort justifying an additional fees, this Authority did not invite payment of additional fees.

3. ☐ As only some of the required additional search fees were timely paid by the applicant, this international search report covers only those claims for which fees were paid, specifically claims Nos.:

4. ☒ No required additional search fees were timely paid by the applicant. Consequently, this international search report is restricted to the invention first mentioned in the claims; it is covered by claims Nos.:

    2, 3(completely); 1(partially)

Remark on Protest   ☐ The additional search fees were accompanied by the applicant's protest and, where applicable, the payment of a protest fee.

☐ The additional search fees were accompanied by the applicant's protest but the applicable protest fee was not paid within the time limit specified in the invitation.

☐ No protest accompanied the payment of additional search fees.

Form PCT/ISA/210 (continuation of first sheet (2)) (April 2005)

FURTHER INFORMATION CONTINUED FROM   PCT/ISA/ 210

This International Searching Authority found multiple (groups of) inventions in this international application, as follows:

1. claims: 2, 3(completely); 1(partially)

>Inventive concept I concerns a structure in a metal-anode-based battery comprising:(a) an anode that comprises a metal; (b) a cathode; and (c) an electrodeless separator positioned between the anode and the cathode, wherein a detectable electrical response signal will result during a charging or discharging of the battery when the metal from the metal anode contacts the electrodeless separator, wherein the metal that contacts the electrodeless separator extends from the anode and/or wherein the metal is selected from a group consisting of lithium, sodium, potassium, magnesium, calcium, aluminum, zinc, cesium, mixtures thereof, and composites therefrom.
>
>---

2. claims: 4-9, 16-35(completely); 1(partially)

>Inventive concept II concerns a structure in a metal-anode-based battery comprising:(a) an anode that comprises a metal; (b) a cathode; and (c) an electrodeless separator positioned between the anode and the cathode, wherein a detectable electrical response signal will result during a charging or discharging of the battery when the metal from the metal anode contacts the electrodeless separator, wherein the electrodeless separator has a resistance of at most 10-5 S/cm and/or wherein the electrodeless separator comprises a material selected from a group consisting of red phosphorous, silicon, germanium, arsenic, metal oxides, metal halides, metal chalcogenides, chalcogenides, $LiM_xE_yO_z$ with M=metal, E=nonmetal, O=oxygen, x>0, y>0, and z>0, MXenes, 2D materials, polymers, organic polymers, inorganic polymers, and mixtures thereof or composites therefrom.
>
>---

3. claims: 10-15(completely); 1(partially)

>Inventive concept III concerns an electronic system with a structure in a metal-anode-based battery comprising: (a) an anode that comprises a metal; (b) a cathode; and (c) an electrodeless separator positioned between the anode and the cathode, wherein a detectable electrical response signal will result during a charging or discharging of the battery when the metal from the metal anode contacts the electrodeless separator, wherein the electronic system is operable to signal a turnoff or cessation of battery use in response to the detectable electrical response signal resulting from the metal from the metal anode contacting the electrodeless separator.
>Inventive concept III also concerns the respective method to prevent short circuits or fires in the metal-anode based

battery.

---

4. claims: 36-55

Inventive concept IV concerns a test method for dendrite detection in an energy-storage device having a first electrode and a second electrode, the test method comprising:(a) measuring charge timing of the energy-storage device;(b) storing a charging model of the measured charge timing of the energy-storage device, the charging model providing an expected charge timing;(c) charging the energy-storage device while monitoring a charging time and a charging voltage between the first electrode and the second electrode; and(d) issuing a dendrite-detection signal if the charging voltage reaches a threshold voltage before the expected charge timing and/or a test method for dendrite detection in an energy-storage device having a first electrode and a second electrode, the test method comprising:(a) storing a charging model of the energy-storage device, the charging model providing an expected charge voltage;(b) charging the energy-storage device while monitoring a charging voltage between the first electrode and the second electrode; and(c) issuing a dendrite-detection signal if the charging voltage exceeds the expected charge voltage.

Patent document cited in search report		Publication date	Patent family member(s)			Publication date
EP 3151328	A1	05-04-2017	CA	2950400	A1	03-12-2015
			CN	106415913	A	15-02-2017
			EP	3151328	A1	05-04-2017
			JP	6297145	B2	20-03-2018
			JP	WO2015182615	A1	20-04-2017
			KR	20170016881	A	14-02-2017
			US	2017155116	A1	01-06-2017
			WO	2015182615	A1	03-12-2015
WO 2018045226	A1	08-03-2018	CN	109923693	A	21-06-2019
			TW	201826592	A	16-07-2018
			US	2019181425	A1	13-06-2019
			WO	2018045226	A1	08-03-2018